GRAĐEVINSKI
MATERIJALI I KONSTRUKCIJE

BUILDING
MATERIALS AND STRUCTURES

Volume 69
June 2026
ISSN 2217-8139 (Print)
ISSN 2335-0229 (Online)
UDK: 06.055.2:62-03+620.1+624.001.5(497.1)=861

2

Society for Materials and Structures Testing of Serbia
University of Belgrade Faculty of Civil Engineering
Association of Structural Engineers of Serbia

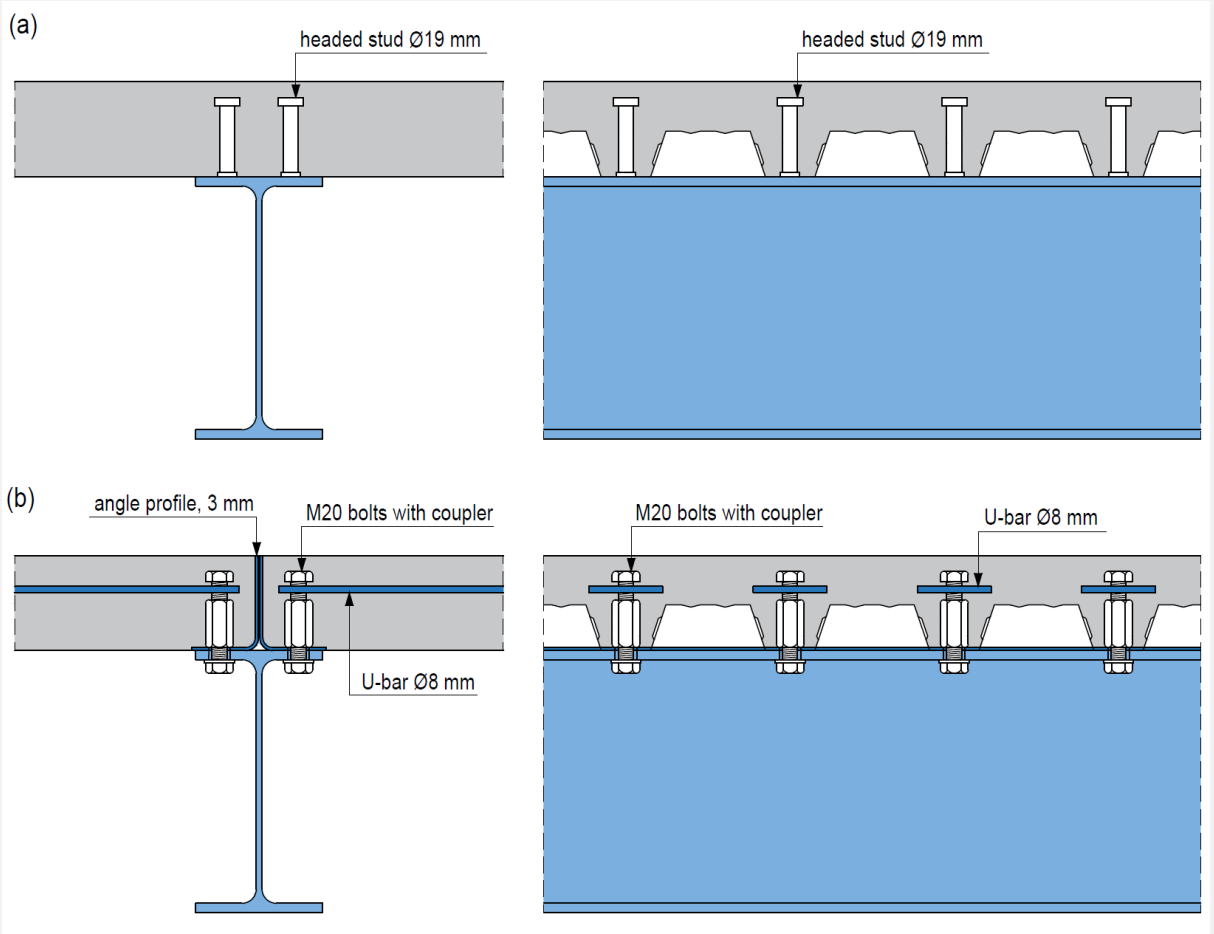

GRAĐEVINSKI MATERIJALI I KONSTRUKCIJE

BUILDING MATERIALS AND STRUCTURES

ISSN 2217-8139 (PRINT)
ISSN 2335-0229 (Online)

VOLUME 69(2)
June 2026

CONTENTS

GRAĐEVINSKI MATERIJALI I KONSTRUKCIJE

BUILDING MATERIALS AND STRUCTURES

ISSN 2217-8139 (PRINT)
ISSN 2335-0229 (Online)

VOLUME 69(2)
June 2026

EDITORIAL BOARD

Secretary: **Slavica Živković**, Master of Economics
Society for Materials and Structures Testing of Serbia, 11000 Belgrade, Kneza Milosa 9
Telephone: 381 11/3242-589; e-mail:office@dimk.rs, veb sajt: www.dimk.rs
English editing: Professor **Jelisaveta Šafranj**, University of Novi Sad, Faculty of Technical Sciences, Novi Sad, Serbia
Technical support: **Stoja Todorović**, e-mail: saska@imk.grf.bg.ac.rs

Aims and scope

Building Materials and Structures aims at providing an international forum for communication and dissemination of innovative research and application in the field of building materials and structures. Journal publishes papers on the characterization of building materials properties, their technologies and modeling. In the area of structural engineering Journal publishes papers dealing with new developments in application of structural mechanics principles and digital technologies for the analysis and design of structures, as well as on the application and skillful use of novel building materials and technologies.

The scope of Building Materials and Structures encompasses, but is not restricted to, the following areas: conventional and non-conventional building materials, recycled materials, smart materials such as nanomaterials and bio-inspired materials, infrastructure engineering, earthquake engineering, wind engineering, fire engineering, blast engineering, structural reliability and integrity, life cycle assessment, structural optimization, structural health monitoring, digital design methods, data-driven analysis methods, experimental methods, performance-based design, innovative construction technologies, and value engineering.

Publishers Society for Materials and Structures Testing of Serbia, Belgrade, Serbia, veb sajt: www.dimk.rs
University of Belgrade Faculty of Civil Engineering, Belgrade, Serbia, www.grf.bg.ac.rs
Association of Structural Engineers of Serbia, Belgrade, Serbia, dgks.grf.bg.ac.rs

Print Razvojno istraživački centar grafičkog inženjerstva, Belgrade, Serbia

Edition quarterly

Peer reviewed journal

Journal homepage www.buildingmaterialsstructures.com

Cover Shear connection: (a) non-demountable, (b) demountable, from *Comparative environmental assessment of conventional and designed for deconstruction steel-concrete composite floor structures* by Snežana Marinković, Isidora Jakovljević, Nina Gluhović, and Milan Spremić

Financial support Ministry of Education, Science and Technological Development of Republic of Serbia
University of Belgrade Faculty of Civil Engineering
Faculty of Technical Sciences, University of Novi Sad, Department of Civil Engineering
Serbian Chamber of Engineers

CIP - Каталогизација у публикацији
Народна библиотека Србије, Београд

620.1

GRAĐEVINSKI materijali i konstrukcije = Building materials and structures / editor-in-chief Snežana Marinković
. - God. 54, br. 3 (2011)- . - Belgrade : Society for Materials and Structures Testing of Serbia : University of Belgrade, Faculty of Civil Engineering : Association of Structural Engineers of Serbia, 2011- (Belgrade : Razvojno istraživački centar grafičkog inženjerstva). - 30 cm

Tromesečno. - Je nastavak: Materijali i konstrukcije = ISSN 0543-0798. - Drugo izdanje na drugom medijumu: Građevinski materijali i konstrukcije (Online) = ISSN 2335-0229
ISSN 2217-8139 = Građevinski materijali i konstrukcije
COBISS.SR-ID 188695820

Građevinski materijali i konstrukcije
Building Materials and Structures
journal homepage: www.buildingmaterialsstructures.com

https://doi.org/10.5937/GRMK2600015R UDK: 666.972.16
624.012.45

Original scientific paper

Accelerated and natural carbonation of high-volume limestone powder concrete: an experimental study

Andrija Radović[*1)], Vedran Carević[2)], Aleksandar Savić[2)]

[1)] *University of Priština in Kosovska Mitrovica, Faculty of Technical Sciences, Knjaza Miloša 7, 38220, Kosovska Mitrovica, Serbia*
[2)] *University of Belgrade, Faculty of Civil Engineering, Bulevar kralja Aleksandra 73, 11000, Belgrade, Serbia*

Article history
Received: 02 May 2026
Received in revised form: 12 May 2026
Accepted: 18 May 2026
Available online: 01 June 2026

Keywords
carbonation depth,
prediction model,
durability,
reinforced concrete structures

ABSTRACT

Carbonation-induced corrosion is a primary durability concern for reinforced concrete structures in continental climates. At the same time, efforts to mitigate the environmental impact of cement production have driven the development of low-clinker concrete, including those incorporating high volumes of limestone powder (HVLPC). Although these concretes offer significant sustainability benefits, their carbonation resistance, often compromised due to lower alkaline reserve, remains a critical challenge. In addition to a reference mixture, nine HVLPC mixtures were produced with cement mass replacement levels of 30%, 45%, and 55%, using three limestone powders of different fineness. All mixtures were designed to achieve similar workability and compressive strength. Carbonation was monitored under accelerated conditions for 56 days and under natural laboratory exposure for two years. The results indicate a pronounced reduction in carbonation resistance with increasing limestone powder content. While moderate replacement levels (up to 30%) caused relatively limited changes, mixtures with higher substitution levels (≥ 45%) led to a pronounced increase in carbonation depth. The effect of particle size was found to be secondary and inconsistent. Analysis confirmed that while the square-root-of-time relationship adequately describes carbonation kinetics under accelerated conditions, even for replacement levels exceeding 50%, direct extrapolation to natural exposure remains unreliable. Findings indicate that existing models correlating accelerated and natural carbonation depths are not directly applicable to HVLPC. To overcome this limitation, a modification of the *fib* Model Code 2010 was proposed by introducing empirical coefficients for different replacement ranges (0–30% and 45–55%). This modification ensured a more accurate and reliable prediction.

1 Introduction

It has been reported that carbonation is responsible for a significant proportion of damage in reinforced concrete structures, especially in urban, non-marine environments [1–3]. Some studies suggest that a large portion, around 65-70%, of reinforced concrete structures are at least partially affected by carbonation during their service life, although the extent strongly depends on environmental exposure and material properties [4–7]. Despite its importance, carbonation was historically underestimated compared to other deterioration mechanisms, particularly in earlier design practices that assumed sufficient durability through high cement content and low permeability. However, the traditionally high cement content used to mitigate durability issues is increasingly challenged due to its substantial environmental impact, with cement production contributing approximately 7–10% of global anthropogenic CO_2 emissions [8,9].

Carbonation is a physicochemical process in which atmospheric CO_2 penetrates the concrete pore system and reacts with calcium hydroxide ($Ca(OH)_2$) and other hydration products, leading to a reduction in pore solution alkalinity. Once the pH drops below a critical threshold (9–10), the passivation layer that protect embedded steel reinforcement is destabilized, making reinforcement susceptible to corrosion [10].

In the contemporary context of sustainable construction, the increased use of supplementary cementitious materials (SCM) and fillers, while beneficial in reducing CO_2 emissions, may have unintended consequences on durability performance. In particular, concretes with reduced clinker content generally exhibit lower calcium hydroxide content and altered pore structure, which can accelerate carbonation rates [11,12]. This has raised concerns

* Corresponding author:
E-mail address: andrija.radovic@pr.ac.rs

regarding the long-term performance of these concretes, especially in environments where carbonation is the dominant deterioration mechanism.

Over the past two decades, extensive research has been devoted to understanding the carbonation behavior of concrete containing SCMs and mineral fillers. It is well established that the incorporation of SCMs generally alters both the chemical buffering capacity and the pore structure of concrete, which are the two key parameters governing carbonation resistance [13,14]. While some pozzolanic materials tend to refine the pore structure over time, their lower calcium hydroxide content often results in increased carbonation depth, particularly at early ages [11,15]. However, the influence of limestone powder on carbonation resistance remains a subject of ongoing research and debate.

Several studies have reported an increased carbonation depth in concretes with high limestone content, primarily due to the dilution of clinker and reduced alkalinity [14,16–18]. On the other hand, improvements in microstructure due to filler effects and optimized particle packing may partially mitigate this negative impact, especially at lower replacement levels [19]. Bertolini et al. [20,21] also obtained different results in their works, especially at lower replacement percentages (up to 15%). The effect becomes even more complex in the case of high-volume limestone powder concrete (> 35%), where cement replacement levels significantly exceed those traditionally allowed in standards. However, at such high replacement levels, a distinctly negative trend is observed regarding the addition of limestone powder and its effect on the carbonation resistance of concrete [22–24].

Years of research have resulted in numerous recommendations and the development of new or by modifying existing models for predicting the carbonation resistance of concrete, incorporating different types of supplementary cementitious materials [25–27]. Meanwhile, Radović et al. [24] are refining the existing *fib* model [28], originally formulated for OPC concrete, extending its applicability to concretes with a high limestone powder content. Based on this modification, they proposed adjusted (higher) values for concrete cover depth compared to those prescribed for conventional OPC concretes [29]. These revised recommendations take into account the specificities related to the carbonation resistance of high-volume limestone powder concrete (HVLPC) and aim to ensure the required service life of 50 and 100 years.

2 Objectives

Despite the significant research, most available studies rely predominantly on accelerated carbonation testing, typically conducted under elevated CO_2 concentrations. While these methods enable rapid comparison between mixtures, their ability to accurately represent natural carbonation processes remains limited. Consequently, there is still a lack of comprehensive experimental studies that combine both accelerated and long-term natural carbonation data for HVLPC. This gap is especially critical in the context of modern sustainable concrete design, where high levels of clinker substitution are increasingly being considered. In this context, the present study aims to investigate the carbonation resistance of high-volume limestone powder concrete through a comprehensive experimental program. Both accelerated and natural carbonation exposures are considered in order to evaluate the influence of limestone powder content and fineness on carbonation kinetics.

3 Experimental research

3.1 Component materials and concrete mixture proportions

All concrete mixtures were produced using Ordinary Portland cement CEM I 42.5R in accordance with EN 197–1 [30], with the median particle size of approximately d_{50} = 11.1 µm and a particles density of about 3100 kg/m^3.

To investigate the influence of limestone powder fineness, three limestone powders with different particle size distributions were employed: L1 (d_{50} = 2.9 µm), L2 (d_{50} = 5.4 µm), and L3 (d_{50} = 11.7 µm). These limestones contain approximately 98% $CaCO_3$ [31] and meet the requirements of the EN 197-1 [30] in terms of chemical composition. The density of limestone powder particles was in the range of 2690±30 kg/m^3. Particle size distributions with the corresponding curves are shown in Figure 1.

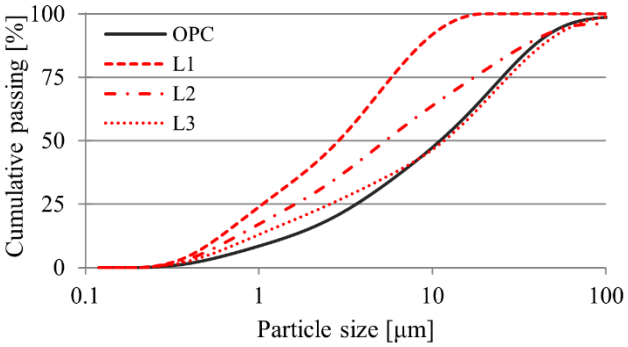

Figure 1. Particle size distribution of cement and limestone powders

Natural river aggregate originating from the Danube River was used, consisting of three fractions: 0–4 mm, 4–8 mm, and 8–16 mm. The oven-dried density of the aggregate grains varied in the range of 2594-2660 kg/m^3. After drying the aggregate, its particle size distribution was determined by dry sieving in accordance with EN 933-1 [32]. The grading curves of the tested aggregate fractions are presented in Figure 2. In the same figure, the reference curves, indicated by dashed lines, represent the limiting envelopes for the respective fractions SRPS B.B3.100 [33] and SRPS B.B2.01 [34]. The grading curves for all aggregate fractions showed slight deviations from the recommended ranges. Fraction I exhibited a somewhat lower amount of fine particles, with cumulative passing of approximately 5% on the 0.25 mm sieve and 1% on the 0.125 mm sieve, compared to the recommended values of 8% and 2%, respectively. Fraction II contained approximately 19% of undersized particles passing the 4 mm sieve, exceeding the recommended 15%. Fraction III exhibits a marginally increased proportion of oversized particles, around 2% retained on the 16 mm sieve and the intermediate 11.2 mm sieve. It can be concluded that these deviations are minor and do not hinder the practical use of the aggregate. It should also be noted that compliance with the reference grading envelopes is not strictly mandatory, as these limits are primarily intended as guidelines rather than strict acceptance criteria.

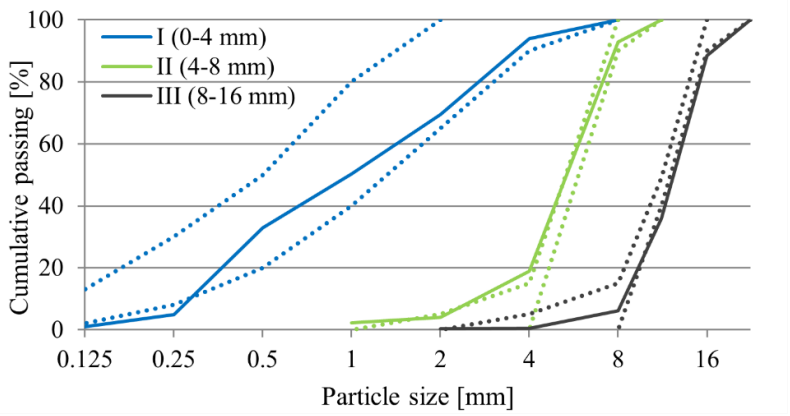

Figure 2. Particle size distribution of natural aggregate

The proportioning of individual aggregate fractions in the mixture was determined using the Funk–Dinger model [35,36], which was originally developed based on computer simulations assuming ideally spherical particles. The model can be expressed as follows:

$$Y_{(d)} = \frac{d^n - d_{min}^n}{d_{max}^n - d_{min}^n} \quad (1)$$

where:

$Y_{(d)}$ – Cumulative passing through a sieve with an opening d

d_{max} – nominal value of the maximum particle size [mm]

d_{min} – nominal value of the minimum particle size [mm]

n – exponent that governs the distribution between finer and coarser particles, i.e., it controls the packing density of the mixture

One limitation of this approach is that it does not consider the actual particle shape, which may significantly influence particle packing density. Furthermore, it can be questioned whether such a simple formulation can adequately describe a system in which particle sizes differ by several orders of magnitude (up to 10^4–10^5 times). Nevertheless, for the commonly adopted exponent value of $n = 0.37$, the model yields the maximum packing density, which has been confirmed by numerous experimental studies [35,37–39].

The recommended range of aggregate particle size distribution (curves A, B, and C) is defined by the SRPS U.M1.206 [40]. Figure 3 presents these reference curves, which delineate the optimal grading envelope for concrete, along with the Funk–Dinger curves corresponding to exponent values of 0.37 and 0.32. A lower exponent value results in a higher proportion of fine particles, which generally improves workability, although it may lead to a slight reduction in compressive strength.

It can be observed that the grading curves obtained using the Funk–Dinger model lie within the reference envelope bounded by curves A and C over nearly the entire particle size range from 0.25 to 16 mm. In practice, it is not necessary for the particle size distribution of a concrete mixture to exactly match a specific reference curve or to remain entirely within the prescribed grading envelope. If experimental results confirm that the designed mixture meets the required performance criteria, minor deviations from the recommended ranges can be considered acceptable [41].

The adopted total amount of aggregate was approximately 1850 kg/m3 (±1%) in all mixtures, and the shares of each fraction were 52%, 21%, and 27%, respectively. The particle size distribution curve of the OPC mixture, with minor local

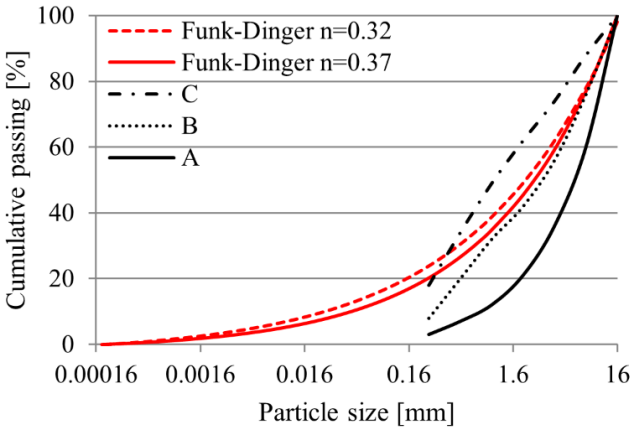

Figure 3. Comparison of different models for selecting aggregate particle size distribution

deviations, closely follows the region bounded by the Funk–Dinger curves corresponding to exponent values of 0.37 and 0.32. A similar trend can be observed for the other mixtures; however, due to the presence of limestone powder, these contain a higher proportion of very fine particles (< 0.1 mm), which results in more noticeable deviations in this size range.

A polycarboxylate-based superplasticizer was used to regulate the workability of fresh mixtures, with a target slump of at least 200 mm (consistency classes S4–S5 according to EN 206-1 [30]).

Final concrete mix compositions were determined using the absolute volume method. The reference mixture (OPC) was prepared with 330 kg/m³ of cement and a water-to-cement ratio (*w/c*) of 0.51. Cement was partially replaced by mass with 30%, 45% and 55% of limestone powders L1, L2 and L3, while *w/c* ratios ranged between 0.62 and 0.75. In mixtures containing limestone powder, lower effective *w/c* ratios were required to maintain the desired strength level and target compressive strength (approximately $f_{cm,cube}$ = 47 ± 6 MPa on 150 mm cubes) corresponding to commonly used structural concrete classes C25/30 and C30/37 [42]. This led to a reduction in cement paste volume, which was compensated by increasing the amount of limestone powder beyond the mass of the replaced cement. In this way, the overall particle packing and rheological properties of the mixtures were improved. The detailed mixture proportions and designations, defined by the type of limestone powder and percentage of cement replacement, are summarized in Table 1.

Table 1. Proportions of paste constituents in concrete mixtures

Concrete mix	Cement [kg/m^3]	Limestone [kg/m^3]	Water [kg/m^3]	w/c [–]	Superplast. [%]
OPC	330	0	169	0.51	1.0
L1-30%	230	200	143	0.62	1.5
L2-30%	230	200	143	0.62	1.5
L3-30%	230	200	143	0.62	1.5
L1-45%	180	250	126	0.70	2.0
L2-45%	180	250	126	0.70	2.0
L3-45%	180	250	127	0.70	2.0
L1-55%	150	280	112	0.75	2.0
L2-55%	150	280	112	0.75	2.0
L3-55%	150	280	112	0.75	2.0

3.2 Preparation, casting, curing, and testing of concrete

Each concrete mixture was mixed for a total duration of approximately five minutes. The consistency of fresh concrete was verified using the standard slump test in accordance with EN 12350-2 [43]. Immediately after testing, the mixtures were placed into moulds and compacted using vibrating table without delay. After removal from the moulds, all samples were subsequently cured in water at a temperature of 20 ± 2°C for 28 days. Compressive strength was determined at the age of 28 days on 150 mm cube specimens, following EN 12390-3 [44]. For each mixture, three specimens were tested and the average value was reported.

The resistance to carbonation was evaluated using prismatic specimens with dimensions of 120×120×360 mm, with two prisms prepared per mixture. After the initial 28-day curing period, all specimens were subjected to an additional conditioning phase lasting 14 days in a controlled climate chamber (20 ± 2°C and 65 ± 5% relative humidity) to achieve a uniform internal moisture state prior to CO_2 exposure. Following conditioning, each prism was split into two parts. One half was used for accelerated carbonation testing, while the other was reserved for natural carbonation exposure. Accelerated carbonation (ACC) was performed in a chamber under controlled conditions (2% CO_2 concentration, temperature of 20 ± 2°C, and relative humidity of 65 ± 5%), in line with *fib* recommendations [28,45]. The duration of exposure was 56 days, with intermediate measurements conducted after 7, 14, 21, 28, and 56 days.

Specimens designated for natural carbonation (NAC) were stored under ambient laboratory conditions for a period of 2 years. Environmental parameters that were continuously measured during this period included temperature, relative humidity, and CO_2 concentration and are shown, along with their mean values, in Figure 4.

Carbonation depth was determined using the phenolphthalein indicator method, in accordance with EN 14630 [46], Figure 5. For each specimen, measurements were taken at eight points on each exposed surface, and the reported values represent the mean carbonation depth for both accelerated and natural exposure conditions.

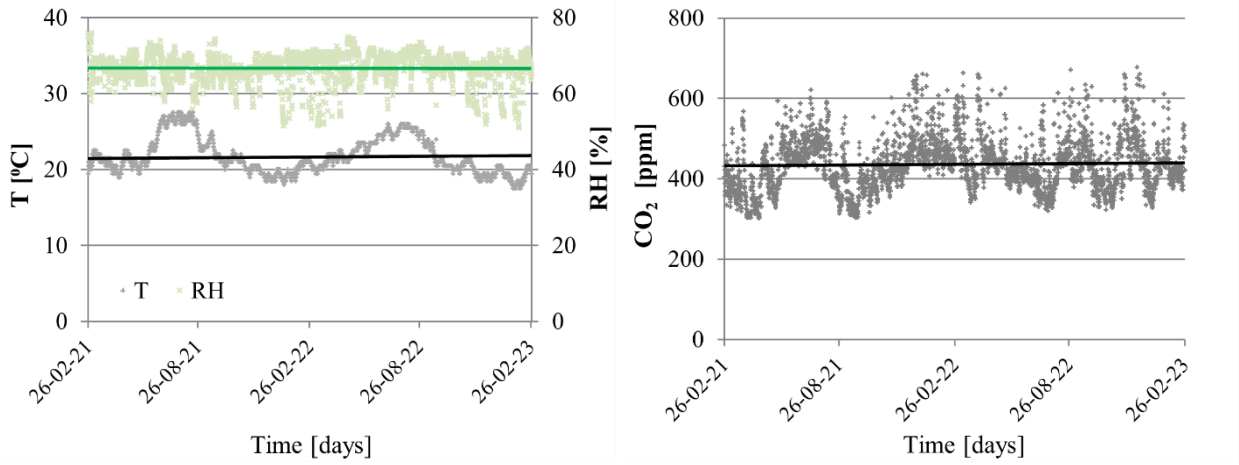

Figure 4. Environmental parameters during natural carbonation test

Figure 5. Appearance of a sample prepared for measuring carbonation depth after surface treatment with phenolphthalein solution

4 Results and discussion

4.1 Workability and compressive strength

All concrete mixtures achieved a high level of workability, corresponding to consistency classes S4 and S5 [47], with slump values between 200 and 250 mm, Figure 6. Such consistency indicates excellent flowability and confirms that all mixtures are well suited for applications such as pumped concrete. It was observed that mixtures with higher levels of cement replacement required increased dosages of superplasticizer to maintain the same workability. This behavior can be explained by the reduced absolute water content in these mixtures. Although the nominal *w/c* ratios were higher compared to the reference OPC mixture, the lower cement content resulted in a reduced volume of free water available for lubrication of the mix, thereby necessitating additional chemical admixture. It should also be noted that, if slightly lower workability is acceptable, the dosage of superplasticizer could be reduced. This would have a direct positive impact on the overall cost-effectiveness of the mixtures [48].

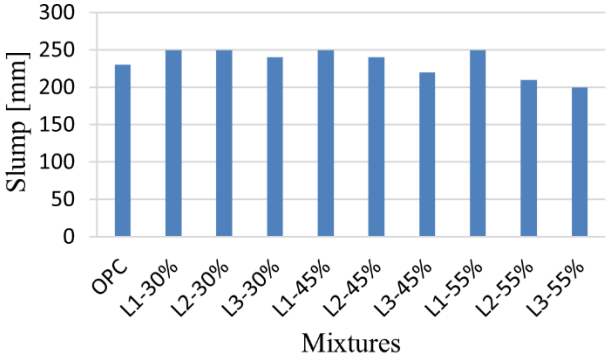

Figure 6. Measured slump values

The compressive strength of the tested concrete mixtures at the age of 28 days, determined on cube specimens, is presented in Figure 7. It can be observed that all mixtures satisfied the target strength requirements corresponding to concrete classes C25/30 and C30/37, with measured values ranging between 41 and 53 MPa. The highest compressive strength was recorded for mixture L1-30%, which exceeded the reference mixture by approximately 8%. This improvement can be attributed to the filler and packing effects of finely ground limestone powder. The presence of very fine particles enhances particle packing, reduces voids within the matrix, and leads to a denser microstructure, which positively affects strength development.

Mixtures L2-30% and L1-45% followed, exhibiting compressive strength values very close to OPC concrete. In contrast, the remaining mixtures generally showed slightly lower strengths, with most values being 1.5–8% below the OPC. The lowest compressive strengths were observed for mixtures L3-45% and L3-55%, which exhibited reductions of approximately 17% and 15%, respectively, compared to the OPC mixture. The coarser particle size of the limestone powder (L3) results in a less pronounced packing effect, which contributes to a decrease in strength. Nevertheless, all mixtures remained within the targeted strength range, confirming their suitability for structural applications.

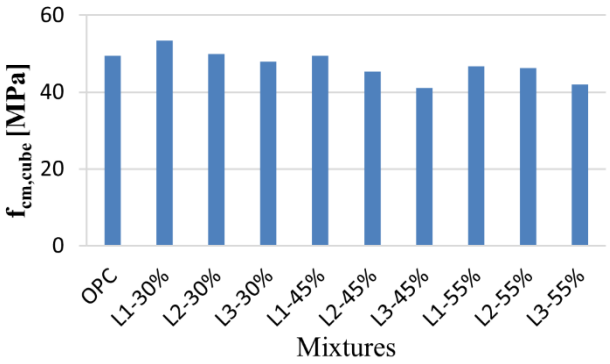

Figure 7. Compressive strength of concrete mixtures at 28 days

4.2 Accelerated and natural carbonation

The carbonation depths obtained from the accelerated test after 28 and 56 days of exposure are presented in Figure 8. A clear negative effect of increasing limestone powder content on the carbonation resistance of concrete can be observed. Mixtures with 30% cement replacement exhibited carbonation depths that were 9–28% higher than that OPC concrete after 28 days of exposure. With further increases in limestone powder content beyond 30%, the reduction of carbonation resistance becomes more pronounced, accompanied by greater scatter in the results. During the same exposure period, mixtures with 45% cement replacement showed carbonation depths that were 90–157% higher than the OPC mixture. Comparable values were also observed for mixtures with 55% cement replacement.

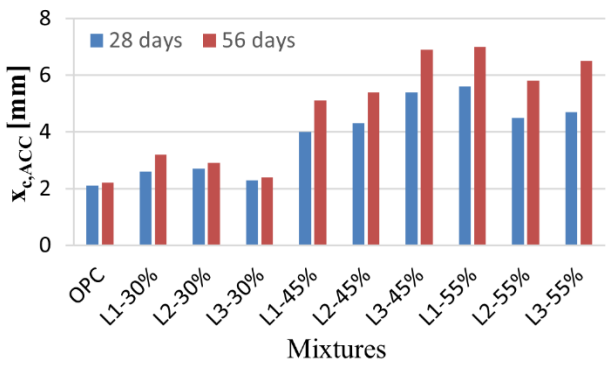

Figure 8. Measured carbonation depths after 28 and 56 days of exposure

Extending the exposure period to 56 days led to only a modest increase (approximately 5%) in carbonation depth for the reference concrete, whereas mixtures containing limestone powder exhibited significantly larger increases, ranging from 13% to 40%, depending on the replacement level. This indicates that the differences in carbonation resistance between conventional OPC concrete and HVLPC become more pronounced with prolonged exposure.

Based on the presented results, the influence of limestone powder fineness on accelerated carbonation resistance cannot be clearly established. For mixtures with 30% cement replacement, those incorporating the coarser powder (L3) performed slightly better, while at 45% replacement the best results were achieved with the finest powder (L1), and at 55% replacement with the intermediate powder (L2). Overall, these findings suggest that the particle size distribution of limestone powder does not have a decisive influence on carbonation resistance under accelerated conditions.

According to the square-root theory, the carbonation depth can be related to the exposure time in accordance with Fick's second law, as expressed by the following relationship (Tuutti, 1982):

$$x_c = k_c \cdot t^{0.5} \tag{2}$$

For given environmental conditions (e.g., CO_2 concentration, relative humidity, and temperature), a linear relationship is typically observed between the carbonation depth (x_c) and the square root of exposure time ($t^{0.5}$). This relationship is characterized by the carbonation coefficient (k_c), which serves as a useful parameter for comparing the carbonation resistance of different concrete mixtures. The same formulation has been adopted in the latest version of EN 12390-10 [49].

Figure 9 illustrates the evolution of carbonation depth under accelerated conditions as a function of exposure time (7, 14, 21, 28 and 56 days), together with the corresponding values of the carbonation coefficient obtained through regression analysis. Even under accelerated carbonation conditions, a strong linear correlation between carbonation depth and the square root of time is observed. This is confirmed by the very high coefficients of determination (R^2 = 0.97–1.00) obtained for all mixtures, indicating that the square-root model provides an excellent representation of the carbonation process within the investigated time frame. These observations confirm that the square-root model is still fully applicable even at very high limestone powder contents.

The obtained carbonation coefficients show a clear and consistent increase with the incorporation of limestone powder. The reference OPC mixture exhibited the lowest value, approximately 0.35 mm/day$^{0.5}$. At 30% cement replacement, the k_c values increase gradually to 0.39–0.46 mm/day$^{0.5}$, corresponding to a 11–31% increase compared to the OPC concrete. Within this group, the best performance was achieved with the coarsest limestone powder (L3), while the finest powder (L1) resulted in the highest carbonation rate. This indicates that, at moderate replacement levels, the beneficial effect of improved packing is not sufficient to compensate for the reduced alkaline reserve.

At 45% replacement, carbonation resistance is further reduced, these values increase significantly to about 0.75 mm/day$^{0.5}$ (L1-45%), 0.79 mm/day$^{0.5}$ (L2-45%), and 0.98 mm/day$^{0.5}$ (L3-45%), corresponding to an increase of about 114–180% compared to OPC concrete. In this case, the influence of particle size becomes less systematic, suggesting that the dominant factor is no longer packing density but the reduced cement content and increased porosity associated with high cement substitution. These results indicate a transitional behavior where dilution effects begin to govern carbonation performance.

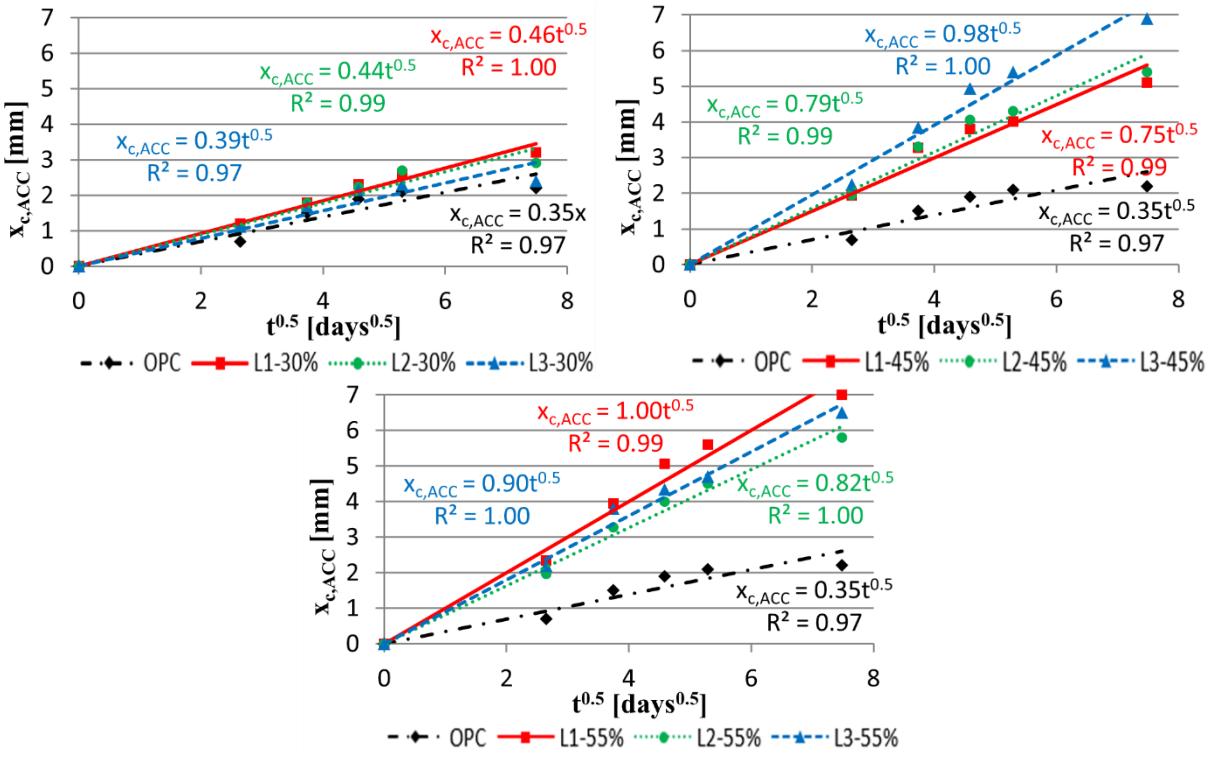

Figure 9. Development of accelerated carbonation over time for mixtures with different cement replacements

Finally, increased cement replacement level up to 55% does not lead to a drastic further increase in the carbonation coefficient. The k_c values remain within almost identical limits as the previous ones 0.82–1.0 mm/day$^{0.5}$, with a minor change. Within this group, mixtures with coarser limestone powder again show slightly better resistance, while the finest powder exhibits the highest carbonation rate. Overall, the results confirm that high levels of cement replacement significantly impair carbonation resistance, with particle size effects becoming secondary to the dominant influence of cement dilution.

This behavior can primarily be attributed to the reduced alkaline reserve of such systems [14], which lowers their buffering capacity against CO_2 ingress. In addition, the dilution effect, resulting from reduced clinker content, leads to a lower amount of hydration products, while changes in pore structure and potential increases in porosity associated with calcium carbonate formation [50] further contribute to the reduced carbonation resistance. Although finer particles may improve packing density, their beneficial effect is insufficient to counterbalance these dominant mechanisms at high replacement levels.

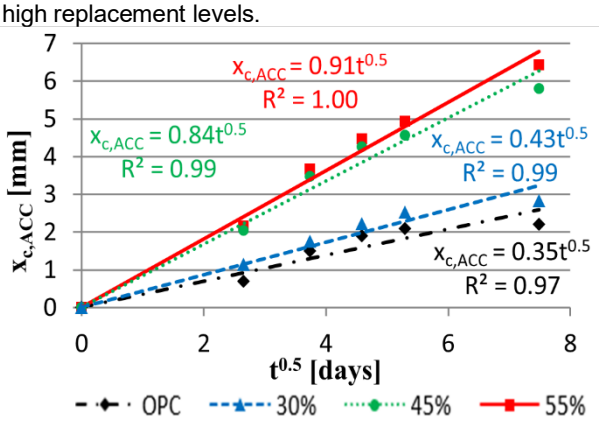

Figure 10. Development of accelerated carbonation over time - averaged for different cement replacement percentages

A comparison of the average carbonation coefficients across all mixture groups further confirms the dominant role of cement replacement level, Figure 10. While the increase at 30% remains moderate (≈ 23%), a sharp increase occurs between 30% and 45%, where the carbonation rate nearly doubles. These results suggest the existence of a critical threshold at approximately 40–45% cement replacement, beyond which carbonation resistance deteriorates rapidly. Below this level, the negative effects of clinker reduction can still be partially mitigated through improved particle packing and microstructural densification. Although limestone powder fineness influences results within individual groups, its overall effect is secondary compared to the replacement level. However, at higher replacement levels, the loss of alkaline reserve becomes the governing factor controlling carbonation behavior.

Figure 11 presents the measured carbonation depths under natural exposure conditions after two years. A comparison of the results clearly indicates significantly higher carbonation depths in mixtures containing limestone powder compared to the reference OPC concrete. Among all mixtures, L1-30% showed the smallest deviation, with a carbonation depth approximately 8% higher than that of the reference. Mixtures L2-30%, L3-30%, and L1-45% exhibited increases of around 25%. In contrast, the remaining mixtures showed substantially higher carbonation depths, ranging from 67% to 82% above the OPC mixture, despite relatively modest reductions in compressive strength (only 6–15%). These findings highlight that, even when comparable compressive strength is achieved, concrete with limestone powder remains more susceptible to carbonation.

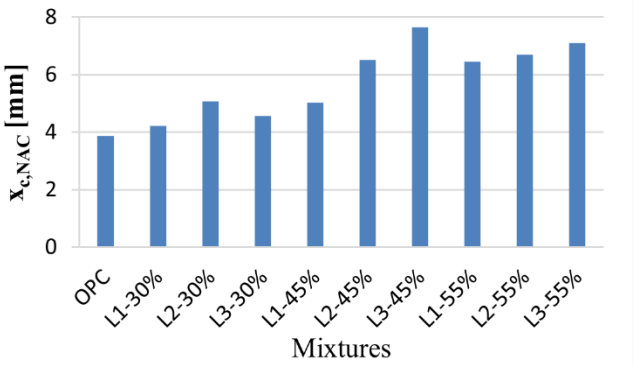

Figure 11. Measured carbonation depths after 2 years

It is also noteworthy that the differences in carbonation depth between the OPC and limestone-containing mixtures were more pronounced in the accelerated tests. This may indicate that carbonation kinetics in limestone powder concrete differ under elevated CO_2 concentrations, suggesting that accelerated testing conditions may amplify these differences.

Unlike the accelerated tests, the influence of limestone powder fineness is more evident under natural exposure conditions. Mixtures incorporating the coarser powder (L3) exhibited carbonation depths that were 10% to 54% higher than those prepared with the finest powder (L1). Similar trends have been reported by other researchers [51,52], confirming the beneficial role of finer particles in improving the microstructure and, consequently, the resistance to carbonation. However, contradictory results have also been documented in the literature, even under natural carbonation conditions [23].

Measured carbonation depths under accelerated conditions (56 days) and natural exposure (2 years), together with their relationships with *w/c* ratio and cement content, are presented in Figure 12 (left and right, respectively). Carbonation depth increases significantly with increasing *w/c* ratio and decreasing cement content under both exposure conditions. In both cases, this effect is more pronounced for accelerated carbonation. These trends reflect the combined influence of increased porosity at higher *w/c* ratios and reduced alkaline reserve at lower cement contents, noting that mixtures with lower cement content also had higher *w/c* ratios.

The steeper trends observed under accelerated conditions indicate differences in carbonation kinetics, suggesting that accelerated testing amplifies the sensitivity of carbonation depth to mixture parameters. Moreover, the differing slopes of the curves confirm that the relationship between natural and accelerated carbonation is not uniform across all mixtures. The largest discrepancy between natural and accelerated carbonation was observed for the OPC mixture (approximately 76%), while this difference gradually decreased with increasing *w/c* ratio (i.e., decreasing cement content). For mixtures with the highest *w/c* ratio, carbonation depths under natural and accelerated conditions became nearly equal (average difference of about 5%), with the curves almost intersecting at this point. Finally, slightly higher coefficients of determination for accelerated carbonation (R^2 = 0.81–0.84) compared to natural conditions (R^2 = 0.68–0.69)

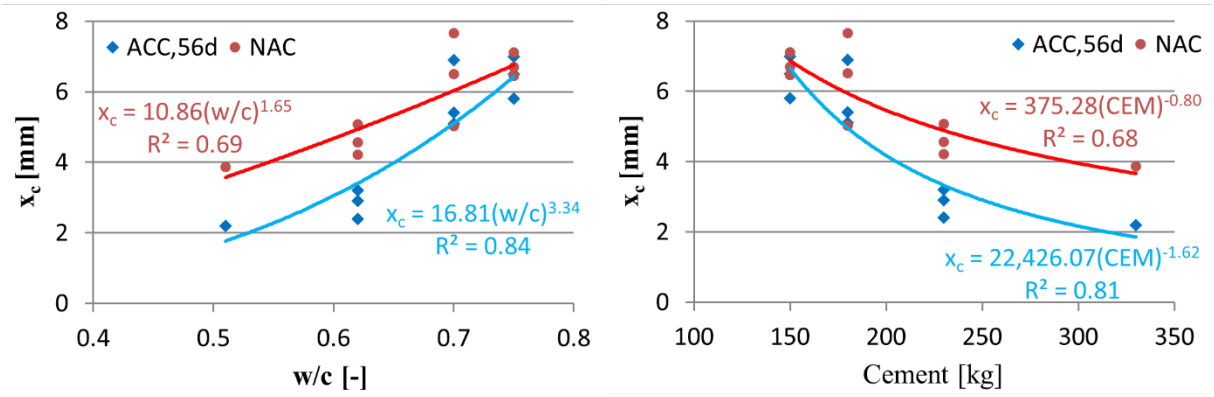

Figure 12. Accelerated (56 days) and natural (2 years) carbonation regarding to water-to-cement ratio (left) and cement content (right)

indicate a more consistent relationship between mixture parameters and carbonation depth under accelerated testing. The cause of this phenomenon may be an increase in the internal humidity of the concrete due to water generated in the carbonation reaction [53,54]. The higher the CO_2 concentration, the greater the amount of water produced, which slows down the process. At low CO_2 concentrations, the internal humidity cannot reach a level higher than the external humidity, so the process is unlikely to change.

5 Prediction of carbonation depth based on accelerated tests and exposure time

The carbonation depth relationship, Eq. (2), can be expressed in terms of carbon-dioxide concentration as:

$$x_c = K \cdot \sqrt{CO_2} \cdot t^{0.5} \tag{3}$$

where the coefficient *K* depends on concrete properties, relative humidity, and ambient temperature, but is independent of CO_2 concentration, which appears as an explicit variable in the equation.

Standards for carbonation depth assessment specify different reference CO_2 concentrations. To compare carbonation depths at different conditions, the following relationship can be derived for the same concrete type [15,27]:

$$\frac{x_{c,1}}{x_{c,2}} = \sqrt{\frac{|CO_2|_1}{|CO_2|_2}} \cdot \left(\frac{t_1}{t_2}\right)^{0.5} \tag{4}$$

The determination of carbonation coefficients under natural exposure conditions typically requires several years, which makes this approach impractical for direct use in structural design. For this reason, accelerated carbonation testing is widely used, reducing the testing period from years to days or weeks. However, carbonation depths under natural conditions remain the primary input for durability design of reinforced concrete structures, as they directly govern concrete cover requirements and service life predictions.

Since the environmental conditions in this research are comparable between natural and accelerated tests, and the coefficient K is independent of CO_2 concentration, the carbonation depth under natural exposure can be estimated from accelerated test results using:

$$x_{c,NAC}(t) = x_{c,ACC} \sqrt{\frac{|CO_2|_{NAC}}{|CO_2|_{ACC}}} \cdot \left(\frac{t_{NAC}}{t_{ACC}}\right)^n \tag{5}$$

where n is the time exponent that accounts for differences in carbonation kinetics between natural and accelerated exposure conditions.

A commonly adopted value of the time exponent is *n = 0.5*, consistent with the classical square-root-of-time relationship for carbonation depth [1]. However, alternative values have been proposed to account for deviations from ideal diffusion-controlled behavior. For example, *n = 0.4* was suggested by Sisomphon and Franke [15] to incorporate pore refinement effects during carbonation, while Carević et al. [27] reported *n = 0.78* for concretes with high fly ash content.

Based on the previously defined relationship, the value of exponent can be determined for known quantities as:

$$n = \frac{log\left(\frac{\frac{x_{c,NAC}}{x_{c,ACC}}}{\sqrt{\frac{|CO_2|_{NAC}}{|CO_2|_{ACC}}}}\right)}{log\left(\frac{t_{NAC}}{t_{ACC}}\right)} = \frac{log\left(\frac{x_{c,NAC}}{x_{c,ACC}} \cdot \sqrt{\frac{|CO_2|_{ACC}}{|CO_2|_{NAC}}}\right)}{log\left(\frac{t_{NAC}}{t_{ACC}}\right)} \tag{6}$$

Using this expression and the experimental results, the exponent *n* was evaluated for each mixture and exposure period. The obtained values, summarized in Figure 13, show

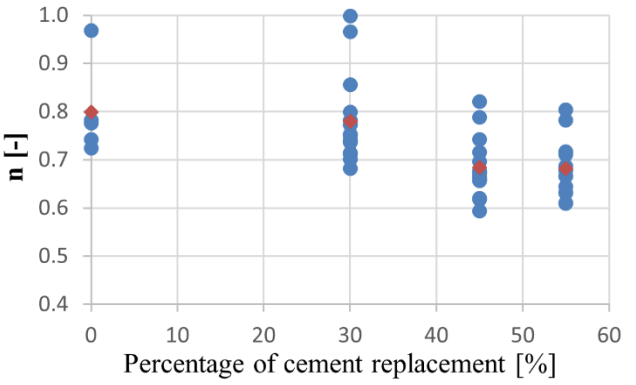

Figure 13. Exponent values as a function of cement replacement percentage with mean values for each group

notable scatter within individual mixture groups. Nevertheless, the average values reveal a clear trend: OPC and mixtures with 30% cement replacement exhibit similar behavior (n = *0.78*), while mixtures with 45% and 55% replacement yield lower values (n = *0.68*).

This observation supports grouping the mixtures into two categories: (I) 0–30% and (II) 45–55% cement replacement. To preserve the classical square-root formulation (n = *0.5*) and avoid introducing a variable exponent, the data were reformulated by analyzing the relationship between $\frac{x_{c,NAC}}{x_{c,ACC}\cdot\sqrt{|CO_2|_{NAC}/|CO_2|_{ACC}}}$ and $\frac{t_{NAC}}{t_{ACC}}$ for both groups (Figure 14). The high coefficients of determination (R^2 = 0.80 and 0.89) confirm the validity of this approach.

Based on these results, modified expressions for carbonation depth under natural conditions are proposed:

- For 0–30% replacement:

$$x_{c,NAC}(t) = 2.65 \cdot x_{c,ACC}(t)\sqrt{\frac{|CO_2|_{NAC}}{|CO_2|_{ACC}}}\cdot\left(\frac{t_{NAC}}{t_{ACC}}\right)^{0.5} \quad (7)$$

- For 45–55% replacement:

$$x_{c,NAC}(t) = 1.85 \cdot x_{c,ACC}(t)\sqrt{\frac{|CO_2|_{NAC}}{|CO_2|_{ACC}}}\cdot\left(\frac{t_{NAC}}{t_{ACC}}\right)^{0.5} \quad (8)$$

The higher coefficients (as well as the higher exponent) obtained for the 0–30% group do not indicate greater carbonation depths, but rather reflect differences in carbonation kinetics between natural and accelerated conditions, as previously discussed. The differences between natural and accelerated carbonation are captured through empirically derived coefficients.

Overall, the results demonstrate that a single conversion factor between accelerated and natural carbonation is not sufficient, and that the effect of cement replacement level must be explicitly accounted for. The proposed modification of the model preserves its physical basis while significantly improving its predictive capability for HVLPC.

Figures 15–19 present the predicted carbonation depths under natural conditions after 2 years, calculated based on accelerated carbonation results obtained after 7, 14, 28, and 56 days of exposure, together with the corresponding measured values for each mixture. The predictions were carried out using the proposed modified expressions (Eq. 7 and Eq. 8) for the groups with 0–30% and 45–55% cement replacement, respectively. For comparison, results obtained using modified values of the time exponent (n = *0.78* for 0–30% and n = *0.68* for 45–55% replacement) as well as the commonly adopted value n = *0.5* according to the square-root-of-time theory are also shown.

A clear trend can be observed from these figures: the classical formulation with n = *0.5* provided the least accurate predictions, systematically underestimating carbonation depths under natural conditions. For mixtures with 45–55% cement replacement, the predicted values were approximately 50% lower than the measured ones ($x_{c,calc}$ / $x_{c,exp}$ = *0.54*), while for the 0–30% group the underestimation is even more pronounced ($x_{c,calc}$ / $x_{c,exp}$ = *0.38*). The corresponding coefficients of variation remained relatively low (13–15%), indicating consistent but biased predictions. The use of modified time exponents (n = *0.78* and n = *0.68*) significantly improved prediction accuracy. The average ratios between predicted and measured values were 1.07 (CoV ≈ 25%) for the 0–30% group and 1.03 (CoV = 17.7%) for the 45–55% group, indicating good agreement, although with increased scatter.

The highest level of accuracy is achieved with the proposed approach that introduces empirical coefficients while preserving the classical square-root formulation (Eq. 7 and Eq. 8). In this case, the predicted and measured values were in excellent agreement, with average ratios of 1.01 and 0.99 for the two groups, respectively. At the same time, the coefficients of variation remained low (13–15%), confirming both the accuracy and robustness of the proposed model.

In the previous paragraph, the accuracy of the three considered approaches was evaluated in general terms. However, their performance shows noticeable deviations depending on the duration of accelerated carbonation exposure. The smallest deviations were obtained with the proposed approach. For mixtures with 0–30% cement replacement, the largest discrepancies were observed for exposure durations of 7 and 56 days, with coefficients of variation of 19.3% and 17.1%, and corresponding ratios $x_{c,calc}$ / $x_{c,exp}$ of 0.92 and 0.85, respectively. For intermediate exposure periods (14 and 28 days), the predictions are more consistent, with ratios in the range of 1.08–1.11 and lower scatter (CoV = 8.3–9.2%). Higher prediction accuracy is observed for mixtures with 45–55% cement replacement. In this case, both the ratios and scatter remain relatively stable across different exposure durations. For 7 and 56 days, the ratios are 0.90 and 0.92, indicating slightly non-conservative

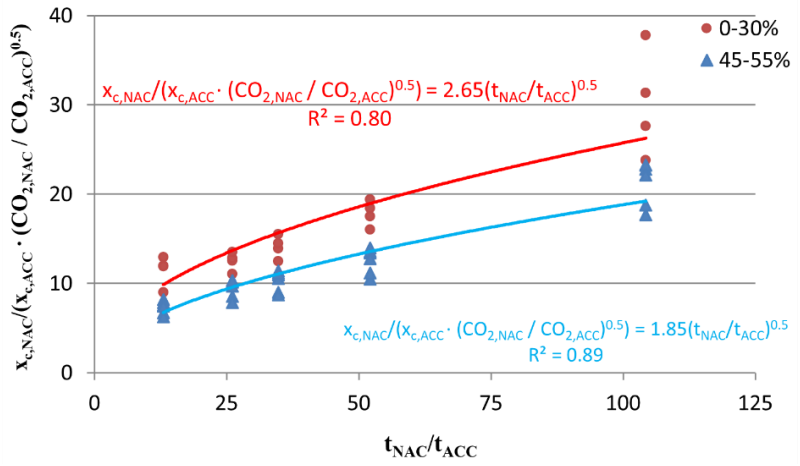

Figure 14. Relationship between $\frac{x_{c,NAC}}{x_{c,ACC}\cdot\sqrt{|CO_2|_{NAC}/|CO_2|_{ACC}}}$ *and* $\frac{t_{NAC}}{t_{ACC}}$ *for 0–30% and 45–55% cement replacement*

estimates, while for intermediate durations the results are generally on the safe side, with ratios between 0.99 and 1.08. The coefficients of variation are consistently low, ranging from 10% to 13%.

These results indicate that the duration of accelerated carbonation exposure has a non-negligible influence on prediction accuracy. Very short exposure periods (e.g., 7 days) may not sufficiently capture the carbonation kinetics, while prolonged exposure (e.g., 56 days) may alter the governing mechanisms due to sustained high CO_2 concentrations. Therefore, an optimal exposure duration should be adopted to ensure reliable correlation with natural carbonation behavior. Overall, the proposed approach shows strong potential for practical implementation in carbonation depth predictions and service life design, particularly by enhancing the reliability of carbonation-based durability predictions and supporting a more rational determination of concrete cover thickness in structures incorporating high volumes of limestone powder.

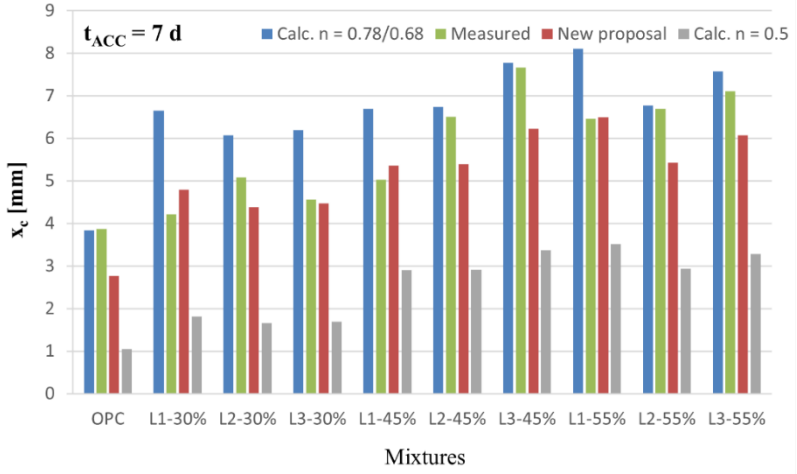

Figure 15. Calculated natural carbonation depths after 2 years based on accelerated carbonation over 7 days

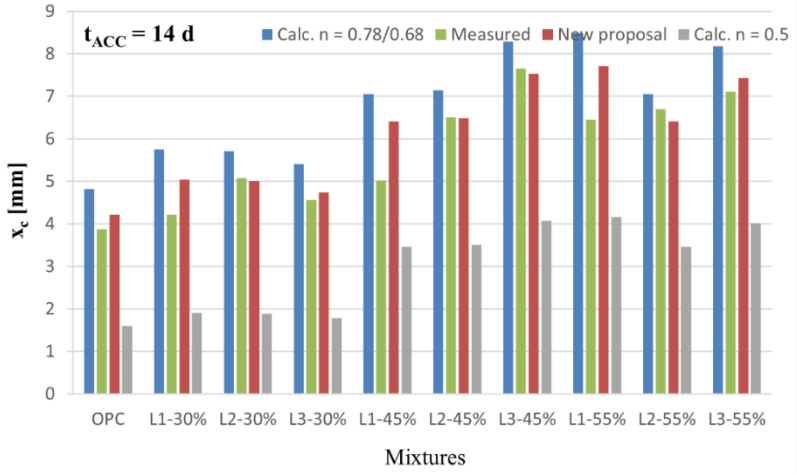

Figure 16. Calculated natural carbonation depths after 2 years based on accelerated carbonation over 14 days

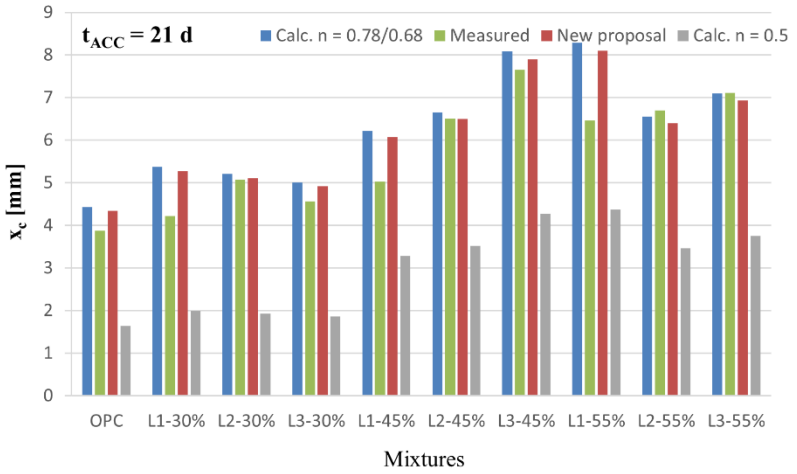

Figure 17. Calculated natural carbonation depths after 2 years based on accelerated carbonation over 21 days

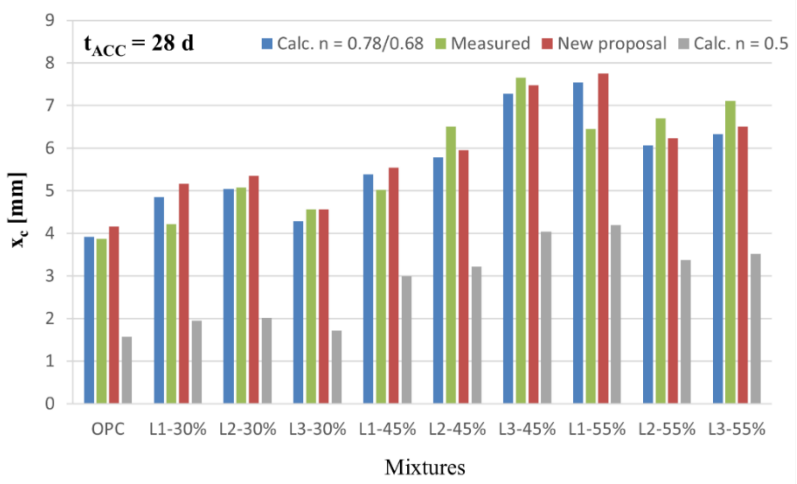

Figure 18. Calculated natural carbonation depths after 2 years based on accelerated carbonation over 28 days

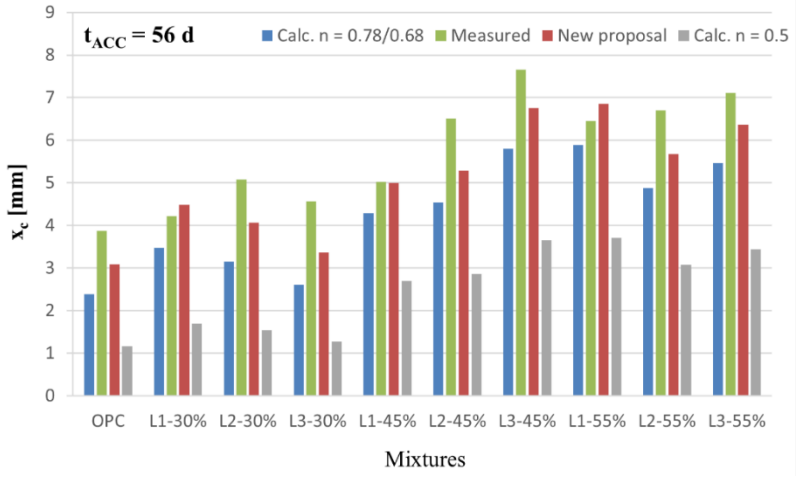

Figure 19. Calculated natural carbonation depths after 2 years based on accelerated carbonation over 56 days

For the sake of clarity, Figure 20 summarizes the ratios between calculated and measured carbonation depths as a function of accelerated exposure duration for all three approaches. Based on the proposed model (Eq. 7 and Eq. 8), the mean values and corresponding coefficients of variation were used to define the 5% and 95% fractiles, forming the confidence interval. Accordingly, no more than 10% of the results are expected to fall outside this range. Using the proposed approach, the predicted carbonation depths deviate from the measured values by up to ±26% for mixtures with 0–30% cement replacement and ±22% for those with 45–55% replacement. Only two data points per group fall outside the confidence bounds. In general, these observations are consistent with the previous discussion, with the largest deviations associated with the shortest (7 days) and longest (56 days) exposure periods.

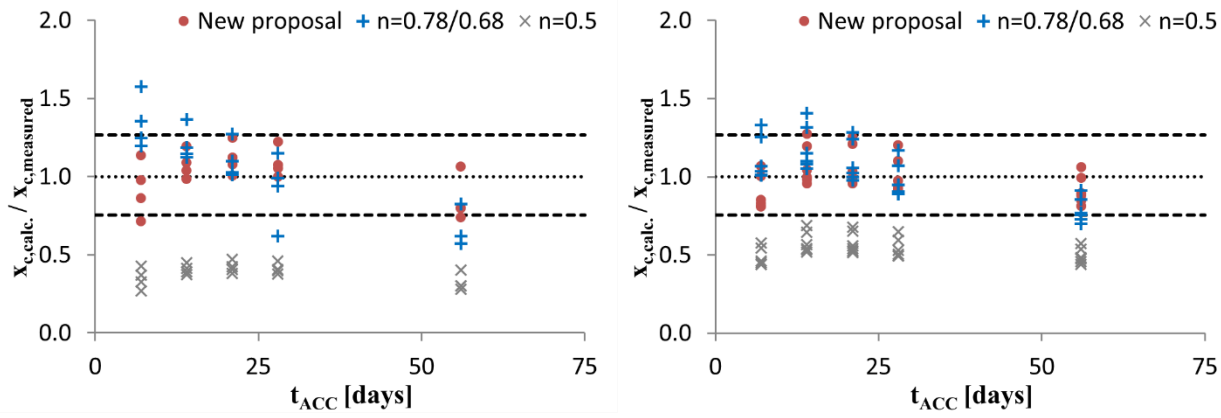

Figure 20. Ratio of calculated and measured carbonation depth for percentage cement replacement 0-30% (left) and 45-55% (right)

The classical formulation with $n = 0.5$ exhibits a similar distribution pattern with respect to exposure duration, but consistently underestimates carbonation depth. In contrast, the approach based on fixed modified exponents ($n = 0.78$ and 0.68) shows the largest scatter and less stable predictions. Together with a noticeable systematic trend with exposure duration, indicating that this formulation introduces a time-dependent bias rather than a stable improvement in prediction accuracy.

6 Conclusions

In this study, an experimental program was conducted to evaluate the influence of limestone powder content and its fineness on the carbonation resistance of concrete. In addition, workability and compressive strength were examined, as these properties are essential for practical structural applications. A total of ten concrete mixtures were produced and tested, including one reference mixture and nine mixtures with cement replaced by limestone powder at levels of 30%, 45%, and 55% by mass. Three limestone powders of the same mineralogical origin but different particle sizes were used.

Based on the experimental results and the performed analysis, the following conclusions can be drawn:

- All mixtures achieved high workability (slump above 200 mm) and met the target compressive strength requirements, with values ranging from 41 to 53 MPa. The highest strength was recorded for mixture L1-30%, exceeding the reference by approximately 8%, while the lowest strengths were observed for L3-45% and L3-55%, with reductions of about 17% and 15%, respectively. The mixtures containing the finest powder exhibiting on average about 6% and 15% higher strengths compared to those with medium and coarse limestone powders.
- Accelerated carbonation results indicate a significant reduction in carbonation resistance with increasing limestone powder content. Mixtures with 30% replacement showed carbonation depths 9–28% higher than the reference after 28 days, while mixtures with 45% and 55% replacement exhibited substantially higher values, in the range of 90–157%. Extending the exposure period from 28 to 56 days had a minor effect on OPC (5% increase), but a much more pronounced effect on HVLPC mixtures (13-40%).
- Development of accelerated carbonation depth over time follows linear trend for all mixtures, indicating that the square-root model remains applicable even at high limestone powder contents. The reference OPC mixture exhibited the lowest k_c value (0.35 mm/day$^{0.5}$), while mixtures with 30% replacement showed moderate increases of 11–31%. At higher replacement levels, a significant rise in k_c was observed, reaching approximately 0.75–0.98 mm/day$^{0.5}$ for 45% and up to 1.00 mm/day$^{0.5}$ for 55% replacement.
- Natural carbonation results after 2 years followed similar trends. The smallest deviation was observed for mixture L1-30% (about 8% higher than OPC), while mixtures L2-30%, L3-30%, and L1-45% showed increases of around 25%. The remaining mixtures exhibited significantly higher carbonation depths, ranging from 67% to 82% above the reference.
- The analysis showed that existing approaches for correlating accelerated and natural carbonation are not directly applicable to HVLPC, significantly underestimating carbonation depth (average calculated-to-measured ratio was 0.47, CoV ≈ 21%). Therefore, a modification of the *fib* Model Code 2010 formulation was proposed. By introducing empirical coefficients (2.65 for 0–30% and 1.85 for 45–55% cement replacement), while retaining the square-root-of-time relationship, a substantial improvement in prediction accuracy was achieved (average calculated-to-measured ratio was 1.00, CoV ≈ 14%).

The presented findings highlight the need for adjusted predictive models when dealing with HVLPC. However, it should be noted that the proposed modification is based only on the experimental results obtained within this study. Keeping this in mind, the conclusions should be interpreted within the limitations of the present study, which considered one cement type (CEM I 42.5R), one aggregate type (river), a specific w/c range (0.51–0.75), accelerated and laboratory natural exposure conditions. Therefore, application to different concrete compositions or in-situ exposure conditions requires additional experimental validation.

Future studies involving: a wider range of materials, concrete strength classes, and environmental conditions (including longer-term natural exposure investigations as well as accelerated carbonation tests under higher CO_2 concentrations) are needed to further assess the robustness and applicability of the proposed approach. Finally, these and similar studies should contribute to the development of broader experimental databases covering a wider range of input parameters. Such databases would enable more reliable calibration and refinement of existing code-based prediction models, thereby supporting the gradual inclusion of HVLPC into future standards provisions.

CRediT authorship contribution statement

A. Radović: Data curation, Investigation, Methodology, Formal analysis, Writing - original draft.

V. Carević: Conceptualization, Methodology, Formal analysis, Writing - review & editing.

A. Savić: Supervision, Resources, Writing - review & editing.

Declaration of competing interest

The authors declare no conflict of interest.

Acknowledgments

This research was funded by the Ministry of Education, Science and Technological Development of the Republic of Serbia [Grant No. 2000920].

The authors would like to express their sincere gratitude to Lafarge Srbija BFC d.o.o., Omya Venčac d.o.o., ELITA-COP d.o.o., TKK d.o.o., and Sika Srbija d.o.o. for their valuable support of this research.

References

[1] K. Tuutti, Corrosion of steel in concrete, Swedish Cem. Concr. Res. Institute, Stock. (1982) 474, Doctoral dissertation.

[2] C. Pade, M. Guimaraes, The CO2 uptake of concrete in a 100 year perspective, Cem. Concr. Res. 37 (2007) 1348–1356. https://doi.org/10.1016/j.cemconres.2007.06.009

[3] V.G. Papadakis, C.G. Vayenas, M.N. Fardis, Fundamental Modeling and Experimental Investigation of Concrete Carbonation, ACI Mater. J. 88 (1991) 363–373. https://doi.org/10.14359/1863

[4] L.J. Parrott, A review of carbonation in reinforced concrete, Cem. Concr. Assoc. UK (1987).

[5] A. Köliö, T.A. Pakkala, J. Lahdensivu, M. Kiviste, Durability demands related to carbonation induced corrosion for Finnish concrete buildings in changing

climate, Eng. Struct. 63–63 (2014) 42–52. https://doi.org/10.1016/j.engstruct.2014.01.032
[6] R. Jones, R.K. Dhir, M.D. Newlands, A.M.O. Abbas, A study of the CEN test method for measurement of the carbonation depth of hardened concrete, Mater. Struct. 33 (2000) 135–142. https://doi.org/10.1007/BF02484168
[7] R. Neves, F.A. Branco, J. de Brito, A method for the use of accelerated carbonation tests in durability design, Constr. Build. Mater. 36 (2012) 585–591. https://doi.org/10.1016/j.conbuildmat.2012.06.028
[8] S.A. Miller, A. Horvath, P.J.M. Monteiro, Readily implementable techniques can cut annual CO2 emissions from the production of concrete by over 20%, Environ. Res. Lett. 11 (2016). https://doi.org/10.1088/1748-9326/11/7/074029
[9] P. Friedlingstein et. al., Global Carbon Budget 2023, Earth Syst. Sci. Data 15 (2023) 5301–5369. https://doi.org/https://doi.org/10.5194/essd-15-5301-2023
[10] V.G. Papadakis, C.G. Vayenas, M.N. Fardis, A reaction engineering approach to the problem of concrete carbonation, AIChE J. 35 (1989) 1639–1650. https://doi.org/https://doi.org/10.1002/aic.690351008
[11] V.G. Papadakis, C.G. Vayenas, M.N. Fardis, Physical , and Chemical Characteristics Affecting the Durability of Concrete, ACI Mater. J. 89 (1992) 186–196.
[12] M. Marinković, A. Radović, V. Carević, Carbonation of limestone powder concrete: State-of-the-art overview, Build. Mater. Struct. 66 (2023) 127–139. https://doi.org/10.5937/grmk2300005m
[13] K.L. Scrivener, V.M. John, E.M. Gartner, Eco-efficient cements: Potential economically viable solutions for a low-CO2 cement-based materials industry, Cem. Concr. Res. 114 (2018) 2–26. https://doi.org/10.1016/j.cemconres.2018.03.015
[14] V.M. John, B.L. Damineli, M. Quattrone, R.G. Pileggi, Fillers in cementitious materials — Experience, recent advances and future potential, Cem. Concr. Res. 114 (2018) 65–78. https://doi.org/10.1016/j.cemconres.2017.09.013
[15] K. Sisomphon, L. Franke, Carbonation rates of concretes containing high volume of pozzolanic materials, Cem. Concr. Res. 37 (2007) 1647–1653. https://doi.org/10.1016/j.cemconres.2007.08.014
[16] R.K. Dhir, M.C. Limbachiya, M.J. McCarthy, A. Chaipanich, Evaluation of Portland limestone cements for use in concrete construction, Mater. Struct. 40 (2007) 459–473. https://doi.org/10.1617/s11527-006-9143-7
[17] A.A. Elgalhud, R.K. Dhir, G.S. Ghataora, Carbonation resistance of concrete: Limestone addition effect, Mag. Concr. Res. 69 (2017) 84–106. https://doi.org/10.1680/jmacr.16.00371
[18] M.S. Meddah, M.C. Lmbachiya, R.K. Dhir, Potential use of binary and composite limestone cements in concrete production, Constr. Build. Mater. 58 (2014) 193–205. https://doi.org/10.1016/j.conbuildmat.2013.12.012
[19] T. Matschei, B. Lothenbach, F.P. Glasser, The role of calcium carbonate in cement hydration, Cem. Concr. Res. 37 (2007) 551–558. https://doi.org/10.1016/j.cemconres.2006.10.013
[20] L. Bertolini, F. Lollini, E. Redaelli, M. Dipartimento, I. Chimica, Influence of concrete composition on parameters related to the durability of reinforced concrete structures, Int. RILEM Work. Integr. Serv. Life Model. Concr. Struct. (2013) 71–78.
[21] L. Bertolini, F. Lollini, E. Redaelli, The Effect of Ground Limestone Addition on Carbonation and Chloride Resistance of Concrete, XII DBMC Int. Conf. Durab. Build. Mater. Components (2011) 1–8.
[22] F. Lollini, E. Redaelli, L. Bertolini, Effects of portland cement replacement with limestone on the properties of hardened concrete, Cem. Concr. Compos. 46 (2014) 32–40. https://doi.org/10.1016/j.cemconcomp.2013.10.016
[23] A. Radović, V. Carević, S. Marinković, Impact of the water-curing time on the carbonation initiation period of high-volume limestone powder concrete, Build. Mater. Struct. 68 (2025) 73–81. https://doi.org/10.5937/GRMK2500004R
[24] A. Radović, V. Carević, S. Marinković, J. Plavšić, K. Tešić, Prediction model for calculation of the limestone powder concrete carbonation depth, J. Build. Eng. 86 (2024) 108776. https://doi.org/10.1016/j.jobe.2024.108776
[25] X.Y. Wang, Optimal mix design of low-CO2 blended concrete with limestone powder, Constr. Build. Mater. 263 (2020) 121006. https://doi.org/10.1016/j.conbuildmat.2020.121006
[26] A. Marani, T. Oyinkanola, D.K. Panesar, Probabilistic deep learning prediction of natural carbonation of low-carbon concrete incorporating SCMs, Cem. Concr. Compos. 152 (2024) 105635. https://doi.org/10.1016/j.cemconcomp.2024.105635
[27] V. Carević, I. Ignjatović, J. Dragaš, Model for practical carbonation depth prediction for high volume fly ash concrete and recycled aggregate concrete, Constr. Build. Mater. 213 (2019) 194–208. https://doi.org/10.1016/j.conbuildmat.2019.03.267
[28] *fib*, Model Code for Concrete Structures 2010. International Federation for Structural Concrete (*fib*), Lausanne., 2013.
[29] V. Carević, S. Marinković, J. Plavšić, A. Radović, Service Life Design of Concrete Structures Made of High-Volume Limestone Powder Concrete—Case of the Carbonation-Induced Corrosion, Build. 13 (2023) 3112. https://doi.org/10.3390/buildings13123112
[30] EN 197-1, Cement - Part 1: Composition, specifications and conformity criteria for common cements, Eur. Comm. Stand. Brussels (2013).
[31] A. Radović, V. Carević, A. Radević, B. Stupar, D. Veličkov, Influence of curing period on some mechanical and durability-related properties of limestone powder concrete, Build. Mater. Struct. 67 (2024) 111–121. https://doi.org/10.5937/GRMK2400007R
[32] EN 933-1, Tests for geometrical properties of aggregates - Part 1: Determination of particle size distribution — Sieving method, Eur. Comm. Stand. Brussels (2009).
[33] SRPS B.B3.100, Kameni agregat - Frakcionisani kameni agregat za beton i asfalt - Osnovni uslov kvaliteta, Inst. Za Stand. Srb. (1983). (In Serbian)
[34] SRPS B.B2.01, Separisani agregat (granulat) za beton - Tehnički uslovi, Inst. Za Stand. Srb. (1986). (In Serbian)
[35] C. Vogt, Ultrafine particles in concrete - Influence of ultrafine particles on concrete properties and application to concrete mix design, Sch. Archit. Built Environ. Div. Concr. Struct. (2010) 177, Doctoral dissertation.

[36] H.S. Müller, M. Haist, M. Vogel, Assessment of the sustainability potential of concrete and concrete structures considering their environmental impact, performance and lifetime, Constr. Build. Mater. 67 (2014) 321–337. https://doi.org/10.1016/j.conbuildmat.2014.01.039

[37] M.T. de Grazia, L.F.M. Sanchez, R.C.O. Romano, R.G. Pileggi, Investigation of the use of continuous particle packing models (PPMs) on the fresh and hardened properties of low-cement concrete (LCC) systems, Constr. Build. Mater. 195 (2019) 524–536. https://doi.org/10.1016/j.conbuildmat.2018.11.051

[38] K. Tešić, S. Marinković, A. Savić, Influence of cement replacement with limestone filler on the properties of concrete, Build. Mater. Struct. 64 (2021) 165–170. https://doi.org/10.5937/grmk2103165t

[39] S. Yousuf, L.F.M. Sanchez, S.A. Shammeh, The use of particle packing models (PPMs) to design structural low cement concrete as an alternative for construction industry, J. Build. Eng. 25 (2019) 100815. https://doi.org/10.1016/j.jobe.2019.100815

[40] SRPS U.M1.206, Guidance and rules for national technical requirements for production of concrete applied in concrete, reinforced concrete and prestressed concrete structures, Inst. Stand. Serbia (2023).

[41] M. Muravljov, D. Zakić, A. Radević, Tehnologija betona: teorija i praksa, Građevinski Fak. Univ. u Beogradu (2022). (In Serbian)

[42] EN 1992-1-1, Eurocode 2: Design of concrete structures - Part 1-1, General rules and rules for buildings, Eur. Comm. Stand. Brussels (2015).

[43] EN 12350-2, Testing fresh concrete – Part 2: Slump test, Eur. Comm. Stand. Brussels (2019).

[44] EN 12390-3, Testing hardened concrete - Part 3: Compressive strength of test specimens, Eur. Comm. Stand. Brussels (2019).

[45] *fib* bulletin 34, Model code for service life design. International Federation for Structural Concrete (*fib*), Lausanne., 2006.

[46] EN 14630, Products and systems for the protection and repair of concrete structures - Test methods - Determination of carbonation depth in hardened concrete by the phenolphthalein method, Eur. Comm. Stand. Brussels (2006).

[47] EN 206, Concrete - Specification, performance, production and conformity, Eur. Comm. Stand. Brussels (2021).

[48] A. Radović, H. Hafez, N. Tošić, S. Marinković, A. de la Fuente, ECO2 framework assessment of limestone powder concrete slabs and columns, J. Build. Eng. 57 (2022) 104928. https://doi.org/10.1016/j.jobe.2022.104928

[49] EN 12390-10, Testing hardened concrete - Part 10: Determination of the carbonation resistance of concrete at atmospheric levels of carbon dioxide, Eur. Comm. Stand. Brussels (2018).

[50] M. Thiery, G. Villain, P. Dangla, G. Platret, Investigation of the carbonation front shape on cementitious materials: Effects of the chemical kinetics, Cem. Concr. Res. 37 (2007) 1047–1058. https://doi.org/10.1016/j.cemconres.2007.04.002

[51] T. Proske, S. Hainer, M. Rezvani, C.A. Graubner, Eco-friendly concretes with reduced water and cement contents - Mix design principles and laboratory tests, Cem. Concr. Res. 51 (2013) 38–46. https://doi.org/10.1016/j.cemconres.2013.04.011

[52] S. Palm, T. Proske, M. Rezvani, S. Hainer, C. Müller, C.A. Graubner, Cements with a high limestone content - Mechanical properties, durability and ecological characteristics of the concrete, Constr. Build. Mater. 119 (2016) 308–318. https://doi.org/10.1016/j.conbuildmat.2016.05.009

[53] A. V Saetta, B.A. Schrefler, R. V Vitaliani, The Carbonation of concrete and mechanism of moisture, heat and carbon dioxide flow through porous materials, Cem. Concr. Res. 23 (1993) 761–772. https://doi.org/https://doi.org/10.1016/0008-8846(93)90030-D

[54] J.H.M. Visser, Influence of the carbon dioxide concentration on the resistance to carbonation of concrete, Constr. Build. Mater. 67 (2014) 8–13. https://doi.org/10.1016/j.conbuildmat.2013.11.005

Građevinski materijali i konstrukcije
Building Materials and Structures
journal homepage: www.buildingmaterialsstructures.com

https://doi.org/10.5937/GRMK2600018M UDK: 624.016:69.059.62]:502.131.1
69.059.62:502.174.1

Original scientific paper

Comparative environmental assessment of conventional and designed for deconstruction steel-concrete composite floor structures

Snežana Marinković[1)], Isidora Jakovljević[*1)], Nina Gluhović[1)], Milan Spremić[1)]

[1)] *Faculty of Civil Engineering, University of Belgrade, Bulevar kralja Aleksandra 73, Belgrade, Serbia*

Article history
Received: 29 April 2026
Received in revised form: 23 May 2026
Accepted: 01 June 2026
Available online: 18 June 2026

Keywords
steel-concrete composite floor,
design for deconstruction,
reuse,
environmental impact,
LCA

ABSTRACT

Design for deconstruction and reuse is a design strategy that can effectively contribute to circular economy goals in the building sector. However, its potential to reduce the environmental impact of steel and concrete building structures has to be assessed using scientific-based methods, like life cycle assessment (LCA). In this study, the environmental impacts of two steel-concrete composite floor structural solutions of a typical office building were assessed and compared: conventional (not demountable) and designed for deconstruction (DfD) solution. Both solutions were designed to provide two subsequent 50-years life spans of the building with the same spatial layout, where second building was built at different location. Composite floor in the relocated building in the conventional case was made of new materials, while in DfD alternative it was made of reused elements from the first use cycle. Chosen impact category indicators were calculated for both cycles together using LCA system expansion. The assessment was performed for two scenarios that differed in the anticipated steel production route for the second building structure. In scenario S1, current average European steel production technology mix (combined BF-BOF and scrap-EAF) was assumed, while in scenario S2 it was 100% scrap-EAF route for all structural steel. The results showed that material production (steel and concrete) phase was by far the largest contributor to overall indicator values, ranging between 85% and 95% for both solutions and both scenarios. Environmental benefits of DfD solution depended significantly on the assumed steel production technology. Low energy- and emission- intensive scrap-EAF route assumed for the second building in the scenario S2 led to decrease of DfD indicators reduction (compared to conventional solution): from around 37% in the scenario S1 to 16% - 24% in the scenario S2, which proved the importance of including future technology development in LCA.

1 Introduction

The construction industry's activities, especially in the buildings sector, generate significant impact on the environmental, economic and social aspects of sustainability. According to [1,2], buildings are responsible for 40% of all waste generated (by volume), 40% of all material resource use (by volume) and 33% of all human-induced emissions globally. As much as 11% of global greenhouse gas (GHG) emissions originate globally from the manufacturing of construction materials [3]. Within the linear economy concept (take-make-use-dispose) it can only be expected those figures to rise due to the population and urbanization growth. Based on the trends of global migration from land to cities it is forecasted that by 2050 almost 75% of the world's population will be urbanized [4]. This can potentially lead to increase of the demand for global construction (expected 70% increase over the next 10 years [4]) which puts a tremendous pressure on the already depleted world's resources.

Historically, the use phase of buildings has been shown to be the highest contributor to the environmental impacts [5] due to large consumption of energy during the building operation. In the recent decade, many policies were put in action with a goal of improving the energy performance of buildings and decarbonizing their energy consumption [6]. However, as buildings become more energy efficient and electricity grids more decarbonized, the embodied environmental impacts (from production, construction, maintenance and disposal of building materials) represent an increasing share of buildings total environmental burden [7]. For instance, it is estimated that 25% of global buildings GHG emissions are embodied carbon [8] but that their share will rise from the current 25% to nearly half by 2050 [9].

Structural components are major contributors to embodied environmental impacts of buildings [10–12].

* Corresponding author:
E-mail address: isidora@imk.grf.bg.ac.rs

Although non-structural elements have shorter service lives and generally need to be repaired/replaced within the building's life span, structures are the most material- and energy-intensive parts of the buildings. Therefore, with constantly reducing the impacts of operational energy, design and construction of buildings load-bearing systems become important target in achieving the sustainable goals of this sector.

In order to reduce the environmental burdens, preserve natural resources and minimize the waste generation, circular economy (CE) agenda in buildings sector has been intensively promoted recently [13,14]. The basic CE principles include slowing loops (prolonging the service lives), closing loops (recycling and reuse) and narrowing loops (reducing resource use) of products and processes [15]. Reuse of construction products is much more effective in retaining the product's value compared to recycling, if additional processing can be kept at minimal level. For instance, it is estimated that the value of the reinforced concrete (RC) wall element is some 50 times higher per ton than the value of the aggregates into which it is recycled when building is demolished [4].

1.1 Design for deconstruction (disassembly) of steel-concrete composite floor structures

Design for deconstruction (DfD) is a design strategy that can efficiently contribute to CE, and more broadly, sustainability goals in the building sector. DfD enables downstream reuse, i.e. the building (structural) elements are designed to be reused in future with minimal transformation, over multiple life cycles of the building. To accomplish this goal, structural elements should be ideally prefabricated (even better if they are modular) and connected with dry joints, which enable easy dismantling without damage to connected structural elements. Therefore, instead of welded and chemical connections (in the case of RC structures cast-in-place concrete with additional reinforcement), easy assessable mechanical connections are required.

Steel-concrete composite floor structures are characterized by high structural efficiency, as composite action reduces the required quantities of both concrete and steel, resulting in lighter structures. Furthermore, compared to non-composite systems, longer spans can be achieved. However, conventional steel-concrete composite structures, in which shear connections between steel beams and solid or composite concrete slabs are typically realized using welded headed studs, do not allow for demountability. Consequently, significant research efforts over recent decades have focused on the development of effective demountable shear connections, which are the crucial detail in the design of reusable steel-concrete composite floor structures [16,17]. The majority of proposed demountable shear connections include the application of various types of bolts, with the most common being bolts with embedded nuts [18,19], friction-grip bolts [18,20–22] and bolts with a coupler system [22,23]. Nevertheless, some solutions with headed studs were proposed as well, such as threaded studs [24,25] and a connection combining welded studs and bolts [26].

The primary requirement for demountable connectors is to provide high stiffness and shear resistance while ensuring rapid, straightforward disassembly and reassembly. Connectors should be designed to leave both the steel profile and the concrete slab undamaged, facilitating their reuse in subsequent life cycles. Furthermore, the ability to secure connectors within the slab or remove them entirely is advantageous, since it minimizes the risk of connector damage during structural transport and on-site handling.

While existing connector designs often exhibit high load-bearing capacities, the critical challenge lies in preventing initial slip within the bolt holes of the steel flange [27]. If left unaddressed, this slip increases beam deflections, as composite action is only achieved once the bolt-to-hole clearances are closed. The issue is compounded by the fact that standard bolt-to-hole clearances of 1-3 mm are insufficient for application along the entire beam length, as they do not provide adequate execution tolerances for simple and rapid floor structure assembly [27,28]. To balance assembly efficiency and structural stiffness, two approaches are used: bolt preloading to provide slip resistance or injecting epoxy resin to eliminate clearances [22,29]. The epoxy resin should effectively fill bolt-to-hole gaps while remaining easily removable, therefore enabling the connector to be withdrawn without causing damage to the steel or concrete components, and facilitating their reuse in next life cycles.

Design provisions for reusable steel–concrete composite structures are still not included in current standards, although certain directions could be found in guidance publications [29]. As previously noted, connector stiffness should be considered when assessing serviceability limit states and beam deflections. Another important aspect of composite beam design with demountable connectors is their limited ductility. Although such connectors often exhibit slip at failure exceeding 6 mm [17,29], they are not considered ductile, and this characteristic should be explicitly accounted for in design. Furthermore, to prevent plastic deformation of the shear connectors and to ensure their successful reuse at the end of the first life cycle, the slab-to-beam end slip should be appropriately limited for serviceability loads.

1.2 Scope and objectives

In order to explore the environmental benefits of DfD reuse, two composite floor structural solutions of a typical office building were assessed with LCA: conventional, not demountable and DfD solution. Both solutions for the composite floor were designed to provide two subsequent 50-years life spans of the building with the same spatial layout, but at different locations. The system expansion LCA method was applied, i.e. chosen impact category indicators were calculated for both use cycles together. Comparison between alternatives showed the potential of DfD solution to reduce the conventional solution's environmental impacts in this specific case study.

2 State-of-knowledge

LCA is standardized [30] and well recognized method for calculating the environmental impacts of products and services during their whole life cycle. However, LCA faces several challenges when applied to modelling of DfD structures. Firstly, more than one cycle should be included in the assessment, which poses the question on the allocation of impacts between them. Secondly, there is a large uncertainty about the distant future technologies. The future processes avoided by reuse of structural elements will probably be more environmentally sustainable compared to the current once.

Generally, the universal consensus on the LCA modelling approach in the reuse case (multiple use cycles) is lacking. There are two possible approaches in LCA: the expansion of

system boundaries to include all use cycles, and partitioning into separate use cycles in which case some type of allocation between them is required. In the former case, results are obtained for all cycles together and there is no need for allocation. In the latter case, results are obtained for each cycle but are sensitive to the chosen allocation type. As shown by De Wolf et al. [31] and Eberhardt et al. [32] the allocation method can have a significant impact and therefore introduce a bias into results and conclusions and inconsistencies between different studies.

As for LCA of steel-concrete composite floor structures, several studies compared conventional with novel DfD solutions [33–35]. None of them included the future technology development in the assessment.

Eckelman et al. [33] compared the DfD floor system consisting of precast concrete planks and steel beams connected using clamping connectors with traditional composite floor made of cast-in-place RC slabs on steel deck connected to steel beams via headed shear studs. The authors investigated three scenarios assuming 0-3 reuses. In DfD cases, environmental impacts were calculated as an average of the original building and subsequent buildings incorporating reused components impacts. This means that the higher the number of reuses, the lower impacts of a building are. For three reuse cycles, the impacts per building were reduced by on average 60–70% compared to traditional design. Authors also showed that, if not reused, DfD structural solutions could lead to increased environmental impacts compared to traditional design of a building with the same configuration, because of the higher production impacts in DfD case.

Brambilla et al. [34] compared demountable steel-concrete floor made of precast concrete slabs and steel beams connected using pretensioned High-Strength Friction-Grip bolts with several conventional composite floor designs. Unlike Eckelman et al. [33], for LCA modelling authors applied EN 15978 [36] which enables including several use cycles in the system boundaries by adopting the reference study period equal to duration of all included use cycles. In the specific case study of an office building, the authors adopted the reference study period equal to two design service lives of structural elements (typically 50 years for office building). The system boundaries therefore included the first building and the relocated one, i.e. the first and second use of structural elements in the demountable case. A 100% reuse rate was adopted as a best-case scenario. In the conventional case, the relocated building (second 50 years) was assumed to be completely built with new materials. Authors reported savings of at least 80 kg CO_2-eq/m^2 in GHG emissions and at least 800 MJ/m^2 of primary energy resources compared to the conventional structural systems.

3 Methods

3.1 Conventional (reference) and DfD composite floor structural solution

The analysis included two steel-concrete composite floor structural solutions of a typical office building designed and constructed using two approaches: (i) a conventional, non-demountable, composite floor structure, and (ii) a reusable and demountable composite floor structure designed according to the DfD principles. The overall geometry of the analyzed composite floor structures, as shown in Figure 1, with inter-column spans of 7.5 and 10 m, ensures adaptability to different future uses across life cycles, accommodates diverse functional requirements and enhances reuse potential. Figure 1 presents a symmetrical view of the building layout. The left side shows a traditional non-demountable design featuring a monolithic composite slab with profiled steel sheeting that spans the whole floor. The right side illustrates the alternative demountable system,

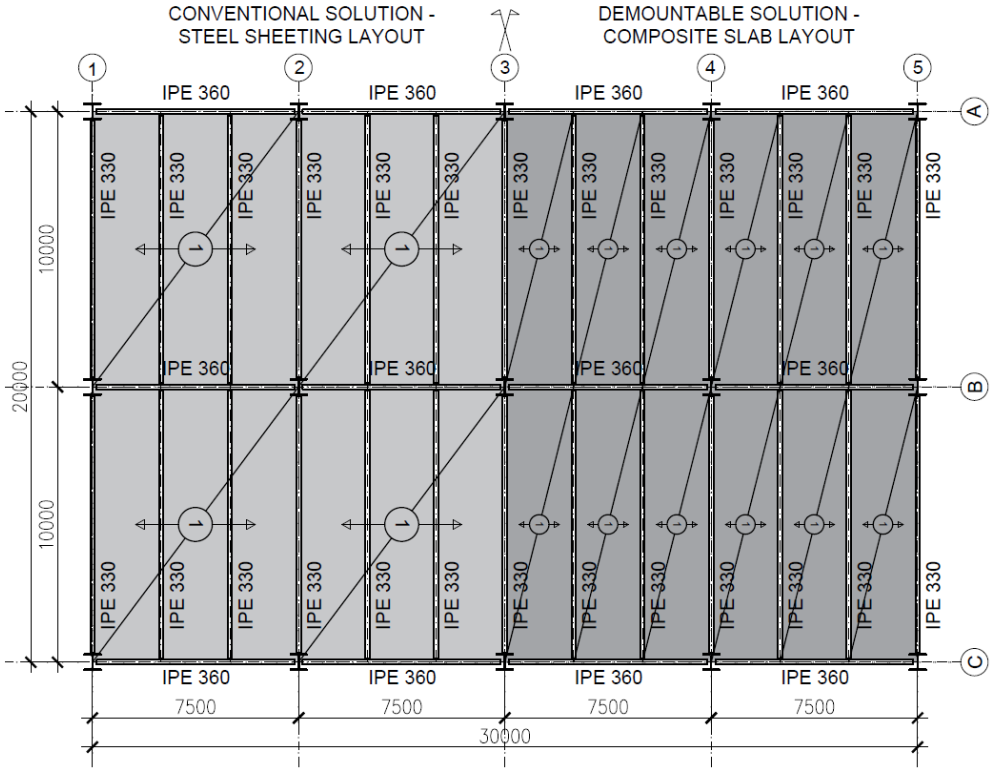

Figure 1. Composite floor structure layout

using 2.5 x 10 m slab segments. These segments are supported individually by the steel beam grid, and there are no connections linking the adjacent slabs to one another. The building's vertical load-bearing elements, which support the analyzed composite floors, comprise a system of steel columns and vertical steel bracing elements designed to maintain structural integrity and facilitate horizontal load distribution. The vertical supporting structure of the building was not part of the subject LCA analysis, but only the horizontal supporting structure, i.e. steel-concrete composite floor structure. The floor structure was designed according to the provisions of standards EN 1994-1-1 [37], EN 1993-1-1 [38], EN 1992-1-1 [39], and EN 1993-1-8 [40], to meet all requirements regarding ultimate and serviceability limit state conditions.

To design two comparable structural solutions for conventional and reusable floor structures, the following criteria were established: (i) the analyzed steel-concrete composite floor structure has overall surface of 600 m^2; (ii) a system of steel-concrete composite elements, consisting of a steel-concrete composite slab and primary and secondary steel-concrete composite beams, provides the structural spanning for the floor area; (iii) the span of composite slab is 2.5 m; (iv) the span of all secondary composite floor beams is 10.0 m, and the span of all primary composite floor beams is 7.5 m; (v) temporary propping is not used during the construction of the composite slab and beams; (vi) composite slab and beam elements are designed as simply supported; (vii) the vertical loads on the composite floor structure are adopted according to standard EN 1991-1-1 [41], for surface category B (characteristic live load value of 2.5 kN/m^2 and concentrated load of 4.5 kN).

The composite floor slab spans 2.5 m, corresponding to the spacing between the secondary floor beams that provide its support. In the conventional, non-demountable solution, the slab is cast continuously over the secondary beams across the entire floor area. In contrast, in the reusable solution, the slab is discontinuous over the supporting beams, and it is constructed from segments of a width of 2.5 m. Despite these structural differences, both options are treated as simply supported slabs in the design calculations. This complies with EN 1994-1-1 [37], which permits this approach even for continuous slabs as long as the minimum required reinforcement is provided. Overall depth of the composite floor slab is 120 mm for both structural solutions, conventional and reusable. Slabs are constructed using 58 mm deep trapezoidal profiled steel sheeting Cofraplus® 60 (thickness 1.25 mm) [42] with a 62 mm thick concrete layer above the sheeting. Concrete is adopted as a three-fraction concrete mixture with class C30/37. Both reusable and conventional solutions require the same amount of mesh reinforcement, as the governing criterion for the adoption of slab reinforcement is the control of longitudinal shear in the concrete slabs. Steel reinforcement B500 with an area of 503 mm^2/m (ϕ8/100 mm) in both directions is placed above the profiled steel sheeting.

Secondary floor beams are constructed as steel-concrete composite beams with a span of 10.0 m, built from steel hot-rolled section IPE 330 and constructional steel grade S355. Beams are simply supported by primary floor beams in the inner spans (between axes 1-2, 2-3, 3-4 and 4-5) and by columns in axes 1, 2, 3, 4 and 5, as shown in Figure 1. The secondary floor beams are designed as steel-concrete composite members supporting a composite slab with profiled steel sheeting on their upper flanges. Primary floor beams with a span of 7.5 m are also designed as steel-concrete composite floor beams, with a composite slab on their upper flanges. Those beams are built from hot-rolled steel cross-section IPE 360 with constructional steel grade S355 and simply supported by steel columns in axes A, B and C, as shown in Figure 1. They represent a support structure for the secondary floor beams at every 2.5 m.

Nominally pinned joints are provided between all steel-concrete composite floor beams, as well as between floor beams and columns, as shown in Figure 2. These joints are designed with a connecting plate (fin plate) of overall dimensions 110x10x250 mm, and four M16 bolts, grade 8.8. The same joint design is applied in both conventional and reusable structural solutions.

The key difference between the two analyzed design solutions, conventional and reusable, lies in the floor structure demountability and the design of the longitudinal shear connection. In a conventional floor structure, longitudinal shear transfer between the steel-concrete composite slab and primary and secondary steel beams is accomplished using a common solution of welded headed studs with a diameter of 19 mm and a height of 100 mm. For secondary floor beams, where the trapezoidal sheeting ribs are oriented transversely to the beam axis, two welded headed studs are provided in each rib within the width of the beam flange. In contrast, for primary beams, which are oriented orthogonally to the secondary beams, the sheeting ribs run longitudinally to the beam axis. In this case, welded headed studs are arranged at 200 mm spacing along the beam length, with two studs provided in each cross-section. The adopted connection is illustrated in Figure 3.a.

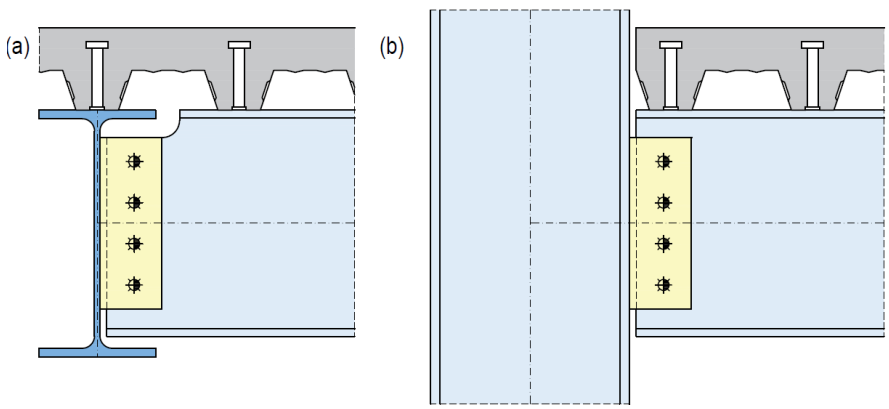

Figure 2. Nominally pinned joints: (a) between steel-concrete composite floor beams, (b) between secondary floor beams and columns

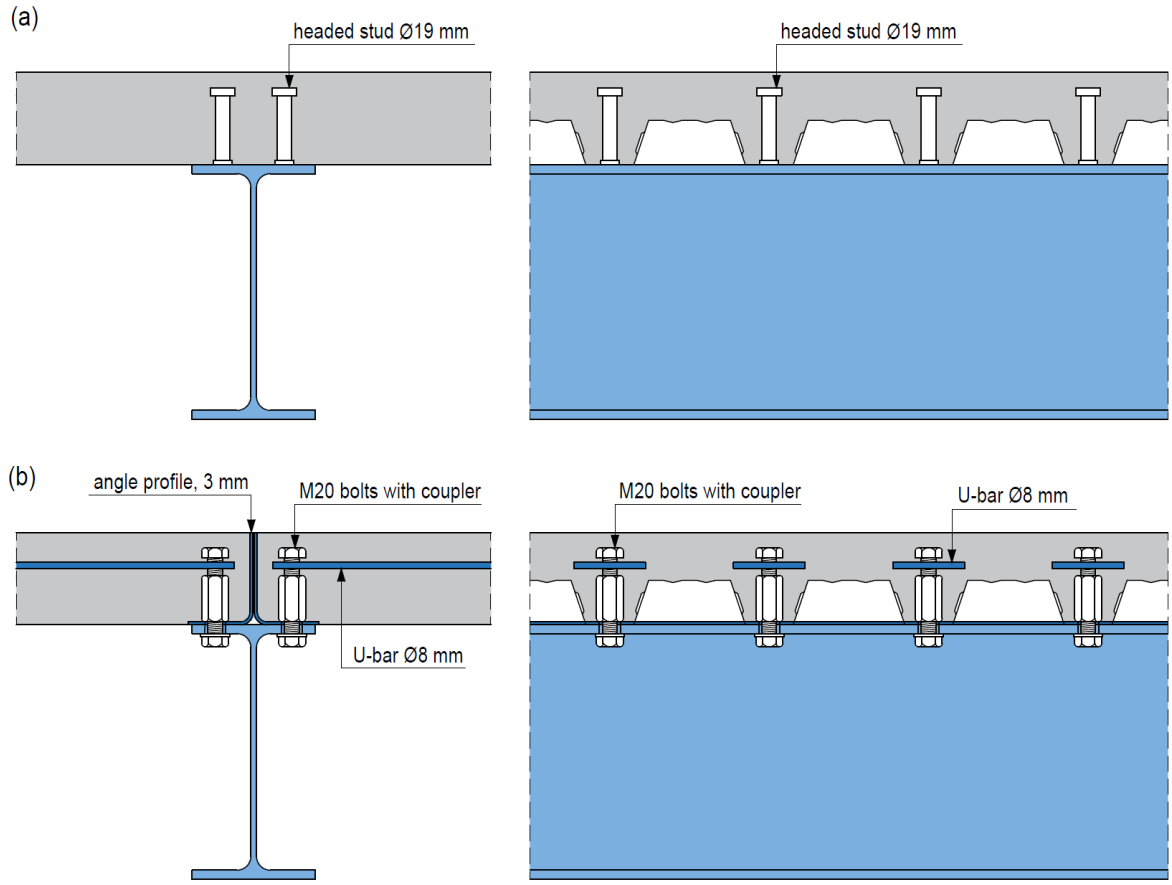

Figure 3. Shear connection: (a) non-demountable, (b) demountable

Demountability of the floor structure is achieved through a demountable longitudinal shear connection between the composite floor slab and steel beams. The adopted connection design is based on the solution proposed and investigated by Kozma et al. [22], consisting of two bolts connected by a coupler. This configuration enables demountability by unbolting the lower steel bolt from the coupler at the underside of the steel beam flange, while the coupler and the upper bolt remain embedded within the composite slab. Such an arrangement is convenient for on-site handling and transport during structure relocation, as parts of the connectors are either embedded or completely removed, thereby reducing their susceptibility to damage. To prevent the bolt slip within the holes in the beam flange and the associated reduction in shear connection stiffness, the lower bolts are pretensioned during installation. The adopted solution, presented in Figure 3.b, utilizes M20 bolts and couplers of grade 10.9. In addition, a 3 mm thick cold-formed angle profile is provided at the slab edge, along its full depth. This profile acts as permanent formwork during concrete casting and remains integrated within the composite cross-section. It also protects slab edges during disassembly and contributes to increased connector resistance, while reducing the risk of concrete splitting failure [26]. Furthermore, U-bars with a diameter of ϕ8 mm are arranged around the embedded bolts and couplers to strengthen the connection zone and the slab edge additionally.

Total material consumption for the conventional and reusable steel-concrete composite floor solutions is presented in Tables 1 and 2, respectively. While concrete consumption remains identical in both analyzed cases, steel consumption is higher in the demountable solution due to the more complex longitudinal shear connection between the steel profile and the composite slab. Consequently, reinforcement consumption increases by nearly 17%, while the total steel consumption (including connectors, sheeting and profiles, but excluding reinforcement) is higher by 14% in the reusable solution compared to the conventional one.

Table 1. Material consumption for the conventional steel-concrete composite structure

Concrete		[m^3/m^2]	0.085
Reinforcement		[kg/m^2]	8.68
Profiled steel sheeting		[kg/m^2]	14.22
Steel profiles		[kg/m^2]	29.85
Beam-to-beam and beam-to-column pinned joints	Bolts, nuts and washers	[kg/m^2]	0.09
	Fin plates	[kg/m^2]	0.27
Beam-to-slab longitudinal shear connection	Headed studs	[kg/m^2]	1.28

Table 2. Material consumption for the reusable steel-concrete composite structure

Concrete		[m^3/m^2]	0.085
Reinforcement		[kg/m^2]	10.15
Profiled steel sheeting		[kg/m^2]	14.22
Steel profiles		[kg/m^2]	29.85
Beam-to-beam and beam-to-column pinned joints	Bolts, nuts and washers	[kg/m^2]	0.09
	Fin plates	[kg/m^2]	0.27
Beam-to-slab longitudinal shear connection	Bolts, couplers and washers	[kg/m^2]	3.00
	Angle profiles	[kg/m^2]	4.71

3.2 LCA model

3.2.1 Goal, scope and system boundaries

The goal of this study was to compare environmental impact of conventional (REF) and DfD structural solution of steel-concrete composite floor described in Chapter 3.1. The functional unit (FU) was one square meter of the floor's area that can provide two 50-years use cycles of the office building with the same configuration and loads, but at different locations. Since conventional floor cannot be disassembled, the floor in the relocated building (in the second life span) was made of new materials, while in DfD alternative floor was made of reused elements from the first use cycle, where 90% reuse rate was assumed (10% of elements were damaged and not reused).

The LCA system expansion was adopted as modelling approach to avoid allocation between assumed two use cycles. The use phase was excluded from the assessment for two reasons. Firstly, type of structure doesn't influence the operational energy consumption. Secondly, structures are commonly designed to have working life equal to a life span of a building and therefore no replacement of the structure is anticipated in the use phase.

LCA was performed for two scenarios, which differed in the first building's End-of-Life (EoL) phase and steel production route for the second building. In both scenarios, concrete was produced with cement from conventional kilns and mix design was taken from previous work [43], Table 3. The production of plasticizer was neglected as its mass was lower than 2% of the concrete mass (0.3%).

- Scenario S1 - at the EoL of the first use cycle (first building) structural elements of the composite floor were disposed of in a landfill. All of them in the reference case, and 10% of them in the DfD case. The average European production technology route, a combined BF-BOF (63%) and scrap-EAF (37%) was adopted for the structural steel and reinforcement production in both buildings [44]. In the reference case, all floor structural elements for the second building were produced from new materials, while in the DfD case only 10% were newly produced. At the EoL of the second building disposal of all elements was assumed in both cases.

System boundaries in the scenario S1, for REF and DfD composite floor, are presented in Figures 4 and 5, respectively.

Table 3. Concrete mix proportion and compressive strength

Mixture components [kg/m^3]				Compressive strength f_{ck}
Cement CEM II/A	Water	River aggregate	Plasticizer	at 28 days [MPa]
320	162	1911	8.3	35

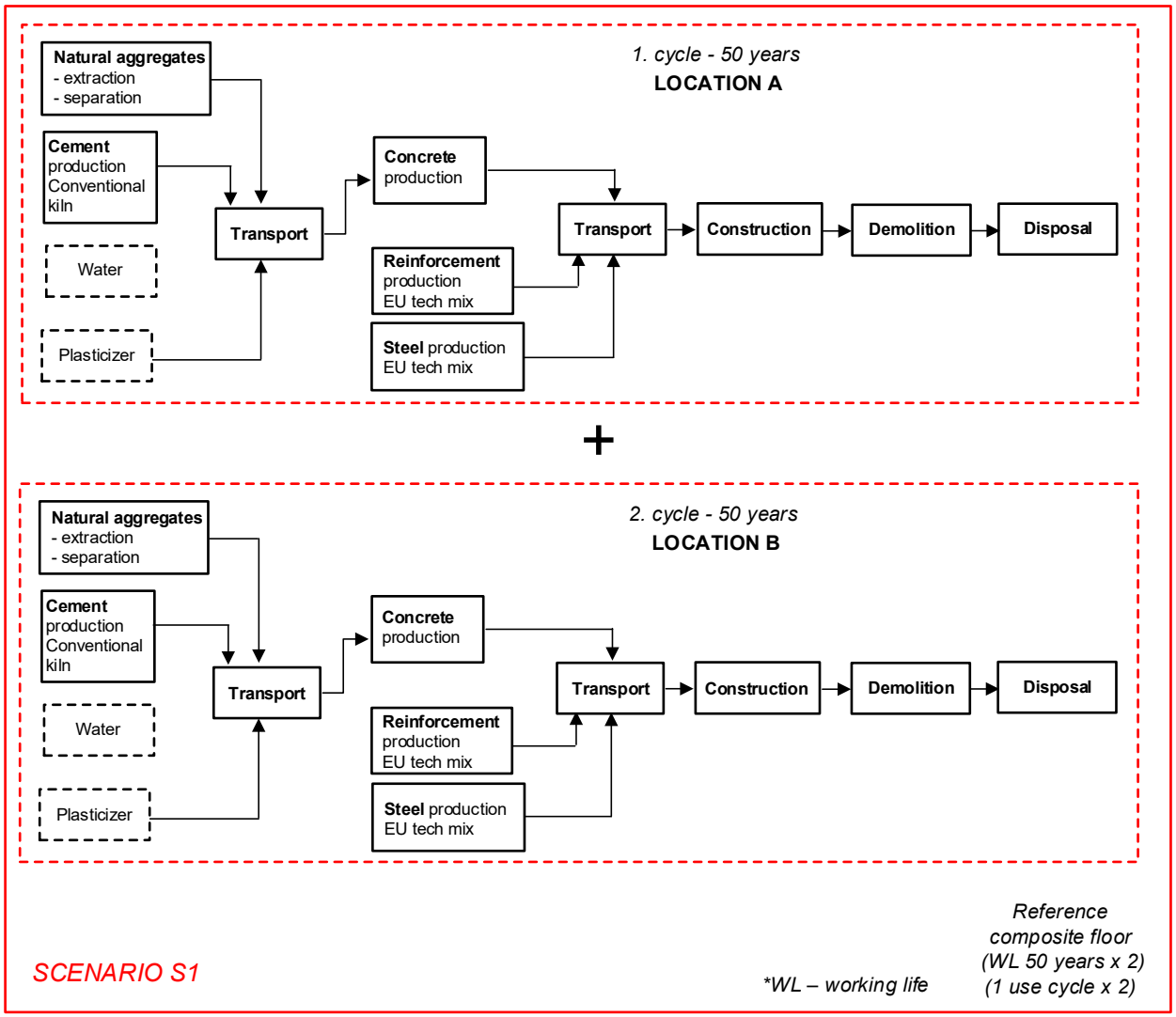

Figure 4. Reference composite floor, scenario S1

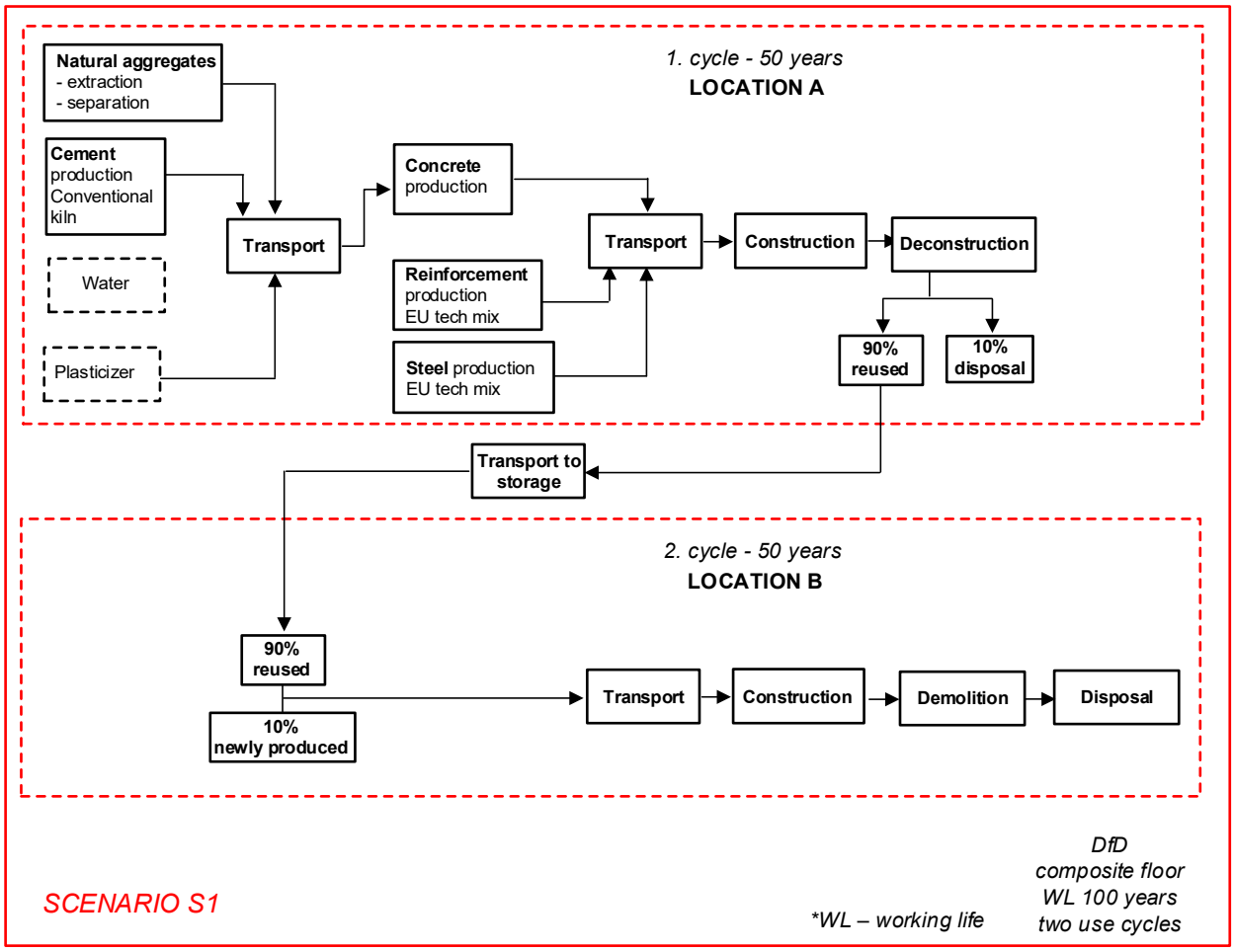

Figure 5. DfD composite floor, scenario S1

- Scenario S2 - at the EoL of the first use cycle (first building) structural steel of the composite floor was recycled, while reinforced concrete was disposed of in a landfill (the contribution of the eventual concrete recycling was neglected). In the REF case, 90% of the structural steel was recycled and 10% disposed of, while in the DfD case, all non-reusable steel (10%) was assumed to be recycled. Scrap obtained in that way was used for the structural steel production in the second building (with added amounts of scrap required for the production). This made a major difference to scenario S1 since scrap-EAF route was the only production route for new structural steel in the second building. At the EoL of the second building, similar to scenario S1, disposal of all elements was assumed in both cases.

System boundaries in the scenario S2, for REF and DfD composite floor, are presented in Figures 6 and 7, respectively.

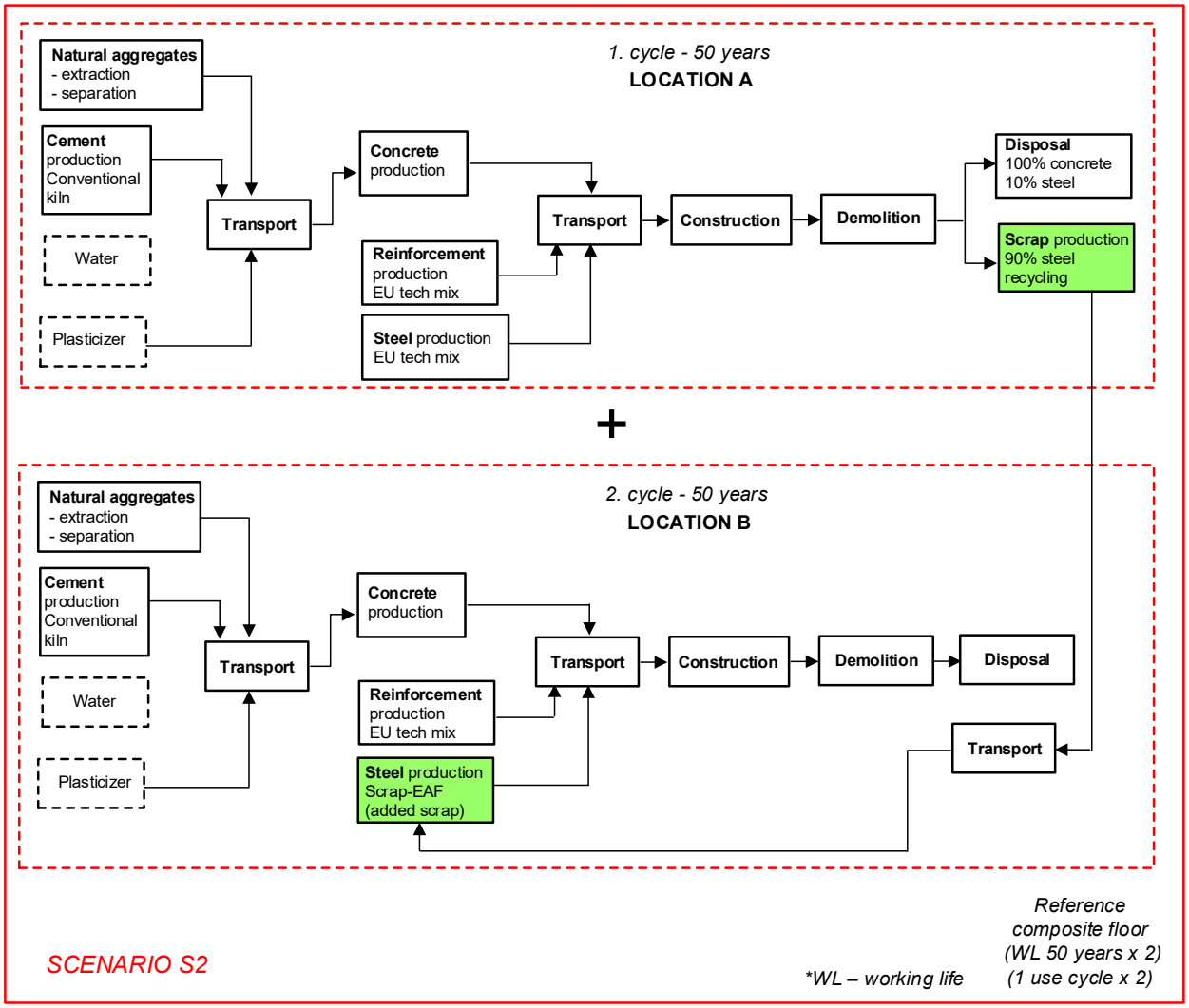

Figure 6. Reference composite floor, scenario S2

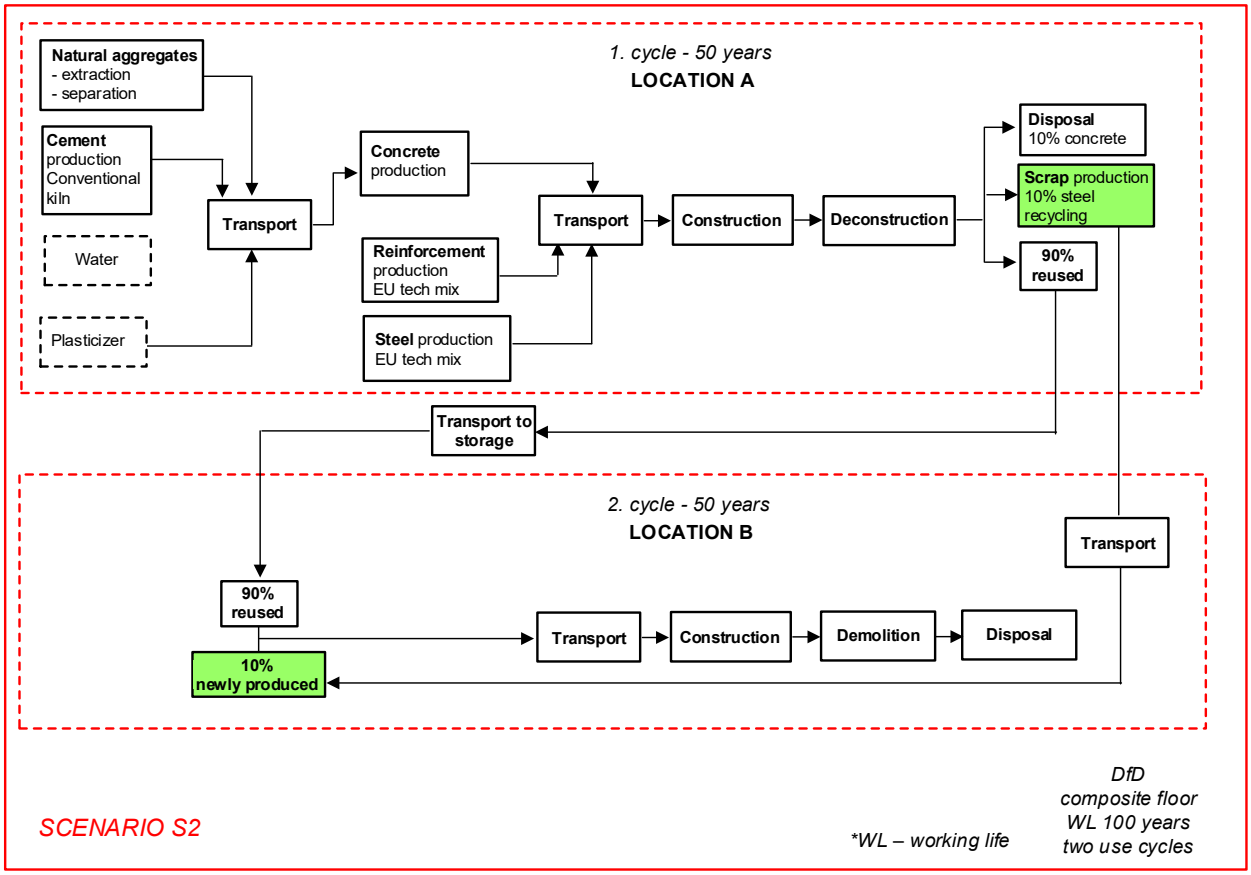

Figure 7. DfD composite floor, scenario S2

3.2.2 Life cycle inventory (LCI)

Required LCI data were taken from ecoinvent v2.1 database [45] as EU average data wherever possible, Table 4.

In both scenarios, transport distances and types were adopted as typical for the construction site located in Belgrade, capital of Serbia, Table 5. Transport distances were doubled to account for the return route of transport vehicles.

Table 4. Sources of LCI data

Type of data	Source (file name in ecoinvent v2.1)	Geography
Energy		
Coal mining and distribution	ecoinvent (hard coal, at regional storage/kg/EEU)	EU average
Diesel production, distribution, and usage	ecoinvent (diesel, at regional storage/kg/RER) (diesel, burned in building machine/MJ/GLO)	EU average
Natural gas production, distribution, and usage	ecoinvent (natural gas, high pressure, at consumer/MJ/RER) (natural gas, burned in industrial furnace >100kW/MJ/RER)	EU average
Electricity	ecoinvent (electricity, medium voltage, production RER, at grid/kWh/RER)	EU average
Concrete		
Cement production	Industry	Serbia
River aggregate production	ecoinvent (gravel, round, at mine /kg/CH)	estimated as EU average
Concrete production	(Kellenberger et al. [46])	estimated as EU average
Reinforcement		
Reinforcement production	ecoinvent (reinforcing steel, at plant/kg/RER)	EU average

Steel		
63% BF-BOF route 37% scrap-EAF	ecoinvent (steel, low-alloyed, at plant/kg/RER)	EU average
Scrap-EAF route	ecoinvent (steel, electric, un- and low-alloyed, at plant/kg/RER)	EU average
	ecoinvent (iron scrap, at plant/kg/RER)	
Construction/deconstruction	Ökobaudat [47]	estimated as EU average
Demolition	ecoinvent (disposal, building, reinforced concrete, to recycling/kg/CH)	estimated as EU average
Transport		
Road and river	ecoinvent (transport, lorry 7.5-16t, EURO5/tkm/RER) (transport, lorry 16–32t, EURO5/tkm/RER) (transport, barge/tkm/RER)	EU average

Table 5. Transport distances and types

Material	Route		Transport distance (km)	Transport type
	From	To		
River aggregate	Place of extraction	Concrete plant	100 x 2	Barge 10000 t
Cement	Cement factory	Concrete plant	100 x 2	Truck 16–32 t
Concrete	Concrete plant	Construction site	15 x 2	Truck 7.5–16 t
Reinforcement	Reinforcement plant	Construction site	100 x 2	Truck 16–32 t
Structural steel	Steel plant	Construction site	100 x 2	Truck 16–32 t
Waste	Demolition/deconstruction site	Landfill	15 x2	Truck 16–32 t
Scrap	Demolition/deconstruction site	Steel plant	50 x 2	Truck 16–32 t
Reused elements	Deconstruction site	Storage	15 x 2	Truck 16–32 t
Reused elements	Storage	Construction site	15 x 2	Truck 16–32 t

3.2.3 Life cycle impact assessment (LCIA)

The impact category indicators were calculated using the well-established CML (The Institute of Environmental Sciences of the Faculty of Sciences of Leiden University) baseline methodology [48]. In this work, Global warming potential (GWP), Eutrophication potential (EP), Acidification potential (AP), Photochemical oxidant creation potential (POCP), and Abiotic depletion of fossil fuels potential (ADPFF) were presented. The ADPFF was calculated using the following heating values of fossil fuels: 19.1 MJ/kg of hard coal, 8.8 MJ/kg of soft coal, 42.0 MJ/kg of diesel, and 39.0 MJ/m^3 of natural gas. An original Excel-based software was used for the life cycle inventory and the life cycle impact calculations.

4 Results and discussion

Impact category indicators for both floor structural solutions, REF and DfD, in scenarios S1 and S2 are presented in Figure 8. The environmental benefits from DfD solution and 90% reuse rate in scenario S1 are clearly displayed across all indicators. Brambilla et al. [34] obtained similar reductions, although for different DfD floor solution and different LCI data (based on Environmental Product Declarations).

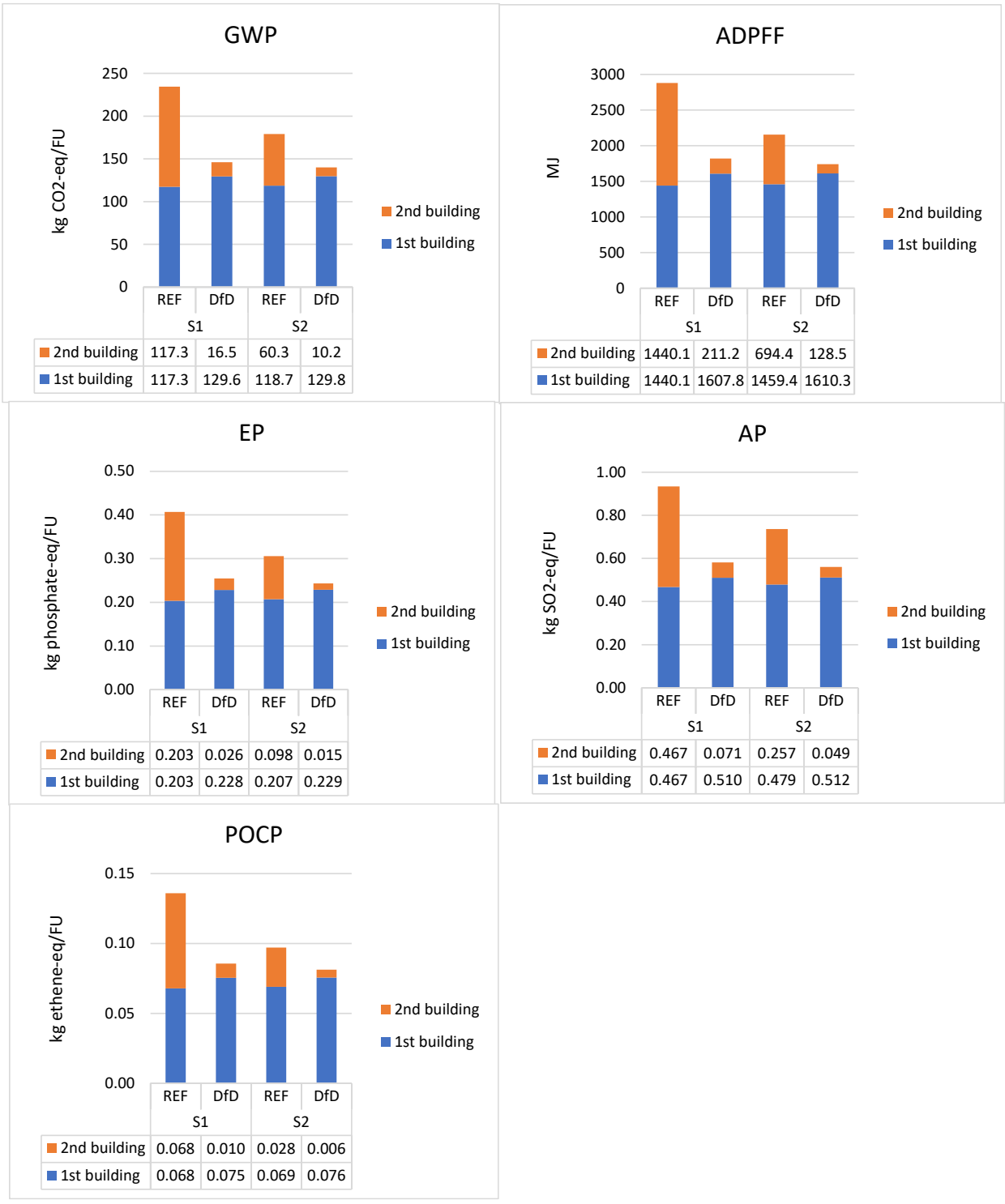

Figure 8. Impact category indicators in the 100 hundred years life cycle of the REF and DfD composite floor in scenarios S1 and S2

In scenario S2 however, benefits from DfD floor solution are lower. Figure 9 shows the reduction of DfD floor indicators compared to REF floor indicators for both scenarios. In the scenario S1, DfD floor indicators present about 63% of the REF's (reduction about 37%). In scenario S2, DfD floor indicators range from 76% to 84% of the REF's, i.e. reductions range from 16% to 24%, depending on the indicator.

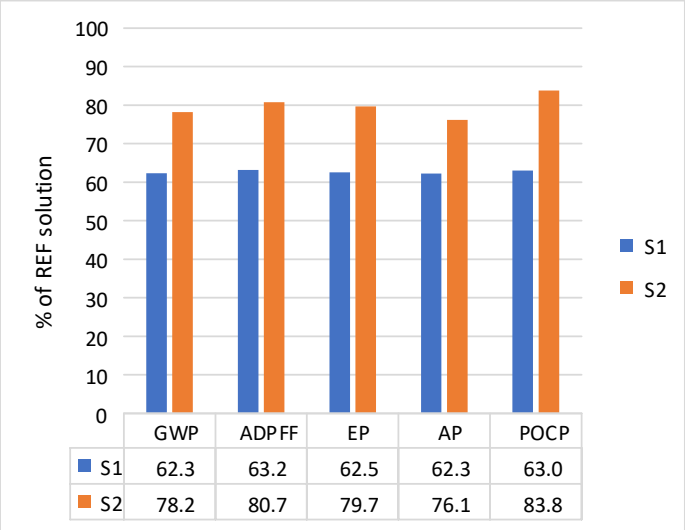

Figure 9. DfD composite floor impact category indicators reductions in scenarios S1 and S2

The main reason for decrease of the DfD floor environmental benefits in scenario S2 is the structural steel production route. In scenario S1, same combined production route was assumed in both use cycles, i.e. both buildings. In scenario S2, structural steel was produced only via scrap-EAF route in the second use cycle (second building). This caused a significant difference in the second building indicators in the REF case, while difference was much smaller in the DfD case since only 10% of structural elements were newly produced in the second building.

The BF-BOF and scrap-EAF steel production routes differ a lot regarding the emissions intensity according to required energy and type of fuels used. While the BF-BOF route is highly energy intensive and reliant on coked coal, the scrap-EAF route is fully reliant on electricity. For instance, BF-BOF emits an average of 2.1 tons of CO_2 per ton of crude steel [49]. On the other hand, CO_2 emissions in the scrap-EAF route are highly dependent on the carbon intensity of the electricity supply but are on average 0.5 t CO_2/t crude steel [49]. It should be kept in mind however that the scrap utilization is limited by its availability. The scrap availability is currently significantly lower compared to demand for the new steel: contribution of scrap in the total steel charge is currently at 34% globally, and could eventually grow to 45% in 2050 if scaled strategies to drive more efficient production, use, and recycling of steel are introduced [49]. Therefore, scenarios S1 and S2 present in fact the worst- and best-case scenarios for the REF floor solution if current steel production technologies were anticipated in the future. The assessment results that would fit the current real practices lie within these limits. The impact of the EoL treatment and more importantly, structural steel production route is low in DfD case because only 10% of the structural elements were newly produced in the second building.

Contribution analysis showed that by far the largest contributor to all indicators was steel production, in both scenarios and for both REF and DfD floor solution, Figure 10. The structural steel production contribution to overall indicator values ranged from 65% to 77%, depending on the indicator. The reinforced concrete production (concrete + reinforcement) contributed to the overall indicator values with approximately 19% to 27%, depending on the indicator. Therefore, 90%-95% of the impact category indicators originated from the material production phase, regardless of the floor structural solution. Within the rest 5%-10% (apart from the material production phase), transport had the highest contribution, ranging from 3% to 7%, depending on the scenario and floor structural solution. Only in the scenario S2 and REF floor solution, the material production contribution was slightly lower due to lower contribution of steel production in the second building, equal to approximately 85%-90%.

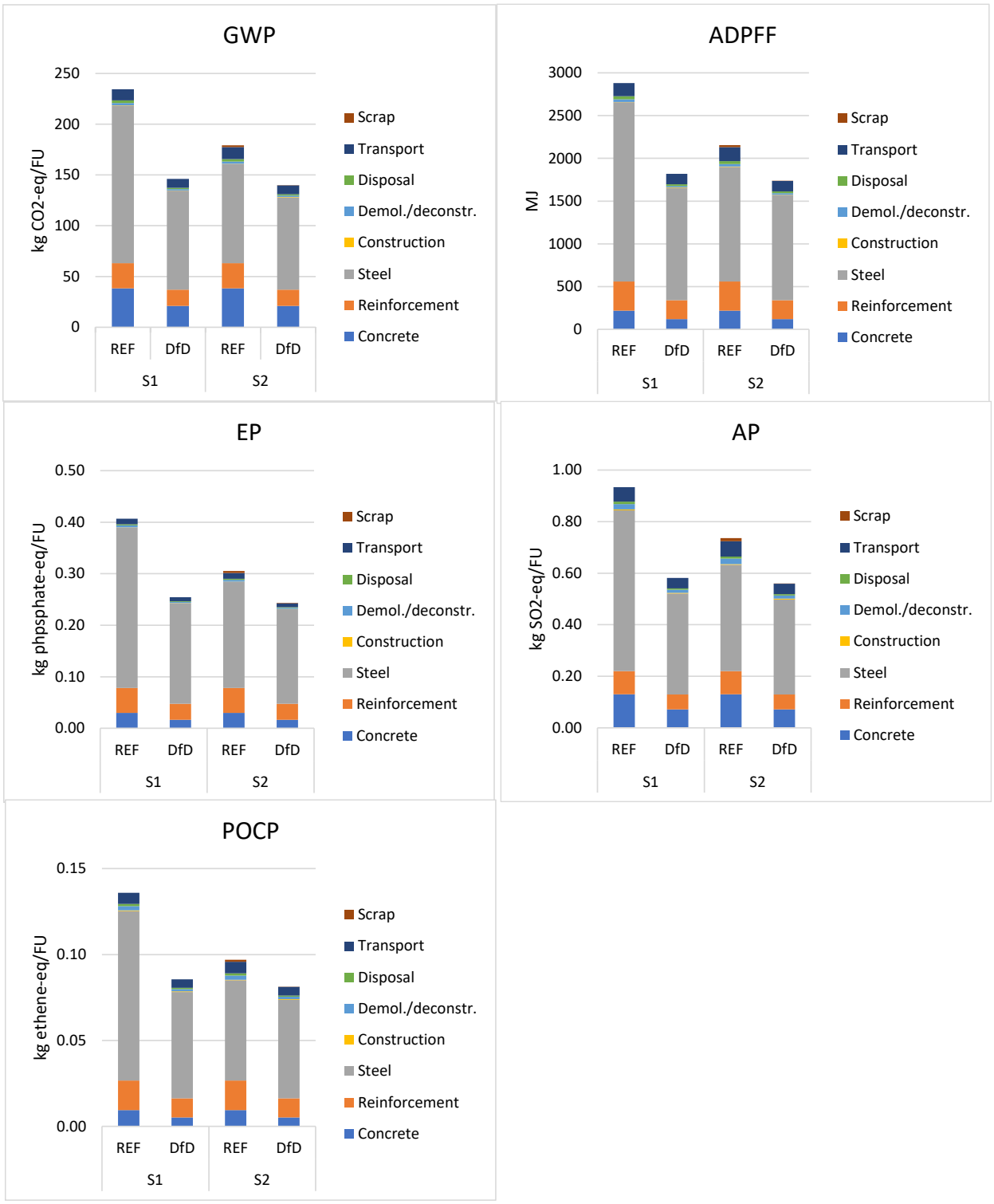

Figure 10. Contribution of various phases in the 100 years life cycle of the REF and DfD composite floor in scenarios S1 and S2

As already mentioned, it was assumed that all structural steel for the second building was produced via scrap-EAF route in Scenario 2. This assumption was used only as an upper limit to obtain the range of possible values, not as a prediction of future. Currently around 45% of European steel is manufactured using the scrap-EAF route, but at the same time, Europe exports 20% of its collected scrap [50]. The rise of this technology deployment can certainly be expected in Europe, especially with growing efforts to decarbonize the electricity production in which case it becomes a near-zero technology. According to some estimates, the contribution of scrap-EAF in Europe is projected to increase to roughly 57% of the total steel charge by 2050 [51], but further in future it will probably be limited by the steel scrap availability. The year of interest in this study is 2076 - predictions on

technologies' development so far in the future are highly uncertain.

Figure 11 shows the ratio between the reduction of the DfD solution's GWP (compared to REF's) and the scrap-EAF participation in the steel production. It can be seen that for estimated 60% participation in 2050, DfD's GWP is 69% of the REF's GWP, i.e. reduction is about 30%. However, it should be noted here that the current average European scrap-EAF route inventory was employed. In the case of fully decarbonized electricity production which is one of the European Union net-zero emissions targets, the GHG emissions from this route would be significantly lower and therefore GWP savings from the DfD enabled reuse would be lower as well.

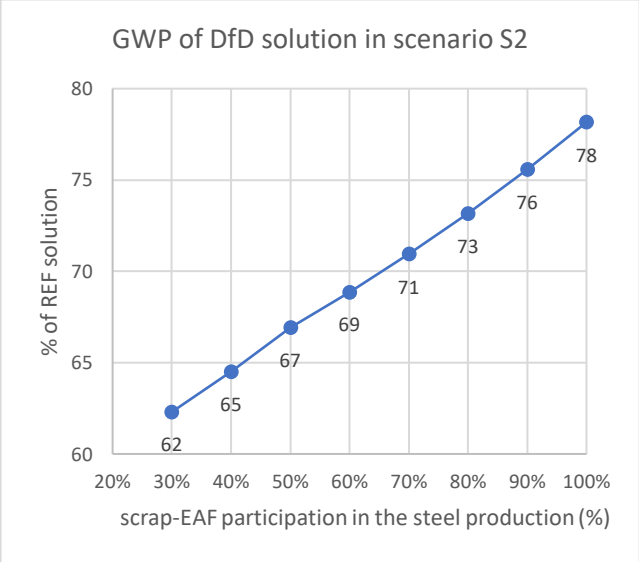

Figure 11. GWP of DfD solution compared to REF solution versus scrap-EAF route participation in the steel production

5 Limitations

As with any case study, results should not be generalized into definitive conclusions on the subject. The results are valid for the assumptions made in the whole process, which are many as we commonly face in each LCA. In this case, the results are most sensitive to the chosen steel production routes, and therefore for the assumptions different from those in scenarios S1 and S2, results would be different. The important parameter is the reuse rate as well. 90% was assumed in this work, but the benefits of DfD enabled reuse would be smaller for the lower reuse rates. Sensitivity analysis on the reuse rate should be performed to assess the impact of this parameter on the overall indicators results. The limitation factor is the assumption that current production technologies will be used 50 years in the future, which is not likely to happen. Transport distances and types are uncertain parameters that do not change significantly the results and conclusions in this case study – there contribution to overall indicators is less than 7%. Under different assumptions however, their contribution may be higher and therefore more significant.

6 Conclusions

In this study, comparative environmental assessment of two different floor structural solutions in a typical office building was performed: conventional, non-demountable, and designed for deconstruction solution, intended for reuse in one more use cycle (second relocated building). It was assumed that 90% of the floor structural elements were reused in DfD case, while the second building's floor structure in the conventional case was completely built with new materials (steel and concrete). The assessment was performed for two scenarios, which differed in the second building, therefore future, steel production route. In scenario S1, it was the current average European technology mix (37% scrap-EAF and 63% BF-BOF). In scenario S2, steel was produced solely by scrap-EAF route using scrap obtained from steel recycling at the EoL of the first building.

The assessment results of this case study showed:

- DfD floor solution showed clear environmental advantage across all calculated impact category indicators in both scenarios.
- The material production phase was the largest contributor, ranging from 85% to 95% of the overall indicator values, depending on the solution and scenario. Steel production made about 70% of the material production phase' impacts.
- Environmental benefits of DfD floor solution however depended on the assumed future steel production technology. The reductions of DfD floor's indicators were significantly lower in scenario S2, 16% - 24% compared to about 37% in scenario S1. It was the result of less energy- and emission - intensive steel production technology assumed for the second building in the REF case.

The results of this study are valid only for the assumptions made regarding several parameters. Regardless of that, study showed that material production technologies anticipated in future had significant impact on the results and therefore on the estimates of the DfD solution potential to reduce the structures' environmental impact. In order to attain broader understanding and support for decision-making, this aspect of future technology development should be taken into account in the prospective LCA – environmental benefits of designed for deconstruction and reuse structures are not guaranteed per se.

CRediT authorship contribution statement

Snežana Marinković: Conceptualization; Methodology; Data curation; Formal analysis; Writing. Isidora Jakovljević: Formal analysis; Visualization; Writing. Nina Gluhović: Formal analysis; Visualization; Writing. Milan Spremić: Supervision; Writing – Review & Editing.

Declaration of competing interest

Authors declare no conflict of interest.

Acknowledgments

Research was not supported by other persons or institutions.

References

[1] R. Becqué, E. Mackres, J. Layke, N. Aden, S. Liu, K. Managan, C. Nesler, S. Mazur-Stommen, K. Petrichenko, P. Graham, Accelerating building efficiency: eight actions for urban leaders, 2016. https://www.wri.org/research/accelerating-building-efficiency

[2] United Nations Environment Programme, Sustainable, resource efficient cities – making it happen!, Paris, 2012.

[3] IEA, Global Status Report for Buildings and Construction 2019, IEA, 2019. https://www.iea.org/reports/global-status-report-for-buildings-and-construction-2019

[4] K.G. Jensen, J. Sommer, Building a Circular Future, 3rd edition - 2018, 2018. https://gxn.3xn.com/wp-content/uploads/sites/4/2018/09/Building-a-Circular-Future_3rd-Edition_Compressed_V2-1.pdf

[5] A. Mastrucci, A. Marvuglia, U. Leopold, E. Benetto, Life Cycle Assessment of building stocks from urban to transnational scales: A review, Renewable and Sustainable Energy Reviews 74 (2017) 316–332. https://doi.org/10.1016/j.rser.2017.02.060

[6] G. Pristerà, D. Tonini, M. Lamperti Tornaghi, D. Caro, S. Sala, Taxonomy of design for deconstruction options to enable circular economy in buildings, Resources, Environment and Sustainability 15 (2024) 100153. https://doi.org/10.1016/j.resenv.2024.100153

[7] M. Röck, M.R.M. Saade, M. Balouktsi, F.N. Rasmussen, H. Birgisdottir, R. Frischknecht, G. Habert, T. Lützkendorf, A. Passer, Embodied GHG emissions of buildings – The hidden challenge for effective climate change mitigation, Applied Energy 258 (2020) 114107. https://doi.org/10.1016/j.apenergy.2019.114107

[8] Building Materials & The Climate, Chapter 1.1: The Built Environment's Impact on Global Carbon Emissions, (n.d.). https://globalabc.org/buildingmaterialsandclimate/chapter-1/1-1-the-built-environments.html

[9] Building Materials & The Climate, Chapter 2.1: Embodied versus Operational Carbon Emissions in Buildings, (n.d.). https://globalabc.org/buildingmaterialsandclimate/chapte-2-life-cycle-thinking/2-1-embodied-versus-operational-carbon-emissions-in-buildings.html

[10] M. Roberts, S. Allen, J. Clarke, J. Searle, D. Coley, Understanding the global warming potential of circular design strategies: Life cycle assessment of a design-for-disassembly building, Sustainable Production and Consumption 37 (2023) 331–343. https://doi.org/10.1016/j.spc.2023.03.001

[11] L.C.M. Eberhardt, H. Birgisdóttir, M. Birkved, Life cycle assessment of a Danish office building designed for disassembly, Building Research & Information 47 (2019) 666–80. https://doi.org/10.1080/09613218.2018.1517458

[12] C. Cavalliere, G. Habert, G.R. Dell'Osso, A. Hollberg, Continuous BIM-based assessment of embodied environmental impacts throughout the design process, Journal of Cleaner Production 211 (2019) 941–952. https://doi.org/10.1016/j.jclepro.2018.11.247

[13] European Commission, A New Circular Economy Action Plan: For a Cleaner and More Competitive Europe, European Commission, Brussels, 2020. https://eur-lex.europa.eu/legal-content/EN/TXT/?qid=1583933814386&uri=COM:2020:98:FIN#footnote37

[14] European Commission, Circular Economy Principles for Building Design, European Commission, Brussels, 2020. https://ec.europa.eu/docsroom/documents/39984

[15] M. Geissdoerfer, P. Savaget, N.M.P. Bocken, E.J. Hultink, The Circular Economy – A new sustainability paradigm?, Journal of Cleaner Production 143 (2017) 757–768. https://doi.org/10.1016/j.jclepro.2016.12.048

[16] I. Jakovljević, M. Spremić, Z. Marković, Towards circular construction: The second life cycle of steel-concrete composite structures, in: Society of Civil Engineers of Novi Sad, 2024: pp. 160–175.

[17] I. Jakovljević, M. Spremić, Z. Marković, Demountable composite steel-concrete floors: A state-of-the-art review, Journal of the Croatian Association of Civil Engineers 73 (2021) 249–263. https://doi.org/10.14256/JCE.2932.2020

[18] G. Kwon, M.D. Engelhardt, R.E. Klingner, Behavior of post-installed shear connectors under static and fatigue loading, Journal of Constructional Steel Research 66 (2010) 532–541. https://doi.org/10.1016/J.JCSR.2009.09.012

[19] M. Pavlović, Z. Marković, M. Veljković, D. Buđevac, Bolted shear connectors vs. headed studs behaviour in push-out tests, Journal of Constructional Steel Research 88 (2013) 134–149. https://doi.org/10.1016/j.jcsr.2013.05.003

[20] Y.-T. Chen, Y. Zhao, J.S. West, S. Walbridge, Behaviour of steel–precast composite girders with through-bolt shear connectors under static loading, Journal of Constructional Steel Research 103 (2014) 168–178. https://doi.org/10.1016/J.JCSR.2014.09.001

[21] X. Liu, M.A. Bradford, M.S.S. Lee, Behavior of High-Strength Friction-Grip Bolted Shear Connectors in Sustainable Composite Beams, Journal of Structural Engineering 141 (2015) 04014149. https://doi.org/10.1061/(ASCE)ST.1943-541X.0001090

[22] A. Kozma, C. Odenbreit, M.V. Braun, M. Veljkovic, M.P. Nijgh, Push-out tests on demountable shear connectors of steel-concrete composite structures, Structures 21 (2019) 0–1. https://doi.org/10.1016/j.istruc.2019.05.011

[23] F. Yang, Y. Liu, Z. Jiang, H. Xin, Shear performance of a novel demountable steel-concrete bolted connector under static push-out tests, Engineering Structures 160 (2018) 133–146. https://doi.org/10.1016/j.engstruct.2018.01.005

[24] X.H. Dai, D. Lam, E. Saveri, Effect of Concrete Strength and Stud Collar Size to Shear Capacity of Demountable Shear Connectors, Journal of Structural Engineering 141 (2015) 04015025. https://doi.org/10.1061/(asce)st.1943-541x.0001267

[25] N. Rehman, D. Lam, X. Dai, A.F. Ashour, Experimental study on demountable shear connectors in composite slabs with profiled decking, Journal of Constructional Steel Research 122 (2016) 178–189. https://doi.org/10.1016/j.jcsr.2016.03.021

[26] I. Jakovljević, M. Spremić, Z. Marković, Shear behaviour of demountable connections with bolts and headed studs, Advanced Steel Construction 19 (2023) 341–352. https://doi.org/10.18057/IJASC.2023.19.4.3

[27] I. Jakovljević, M. Spremić, N. Fric, Z. Marković, Behaviour of demountable steel-concrete composite beams with bolts and headed studs, in: Eurosteel 2023,

Amsterdam, 12-15 September 2023, 2023: pp. 84–89. https://doi.org/10.1002/cepa.2399
[28] M.P. Nijgh, A multi-scale approach towards reusable steel-concrete composite floor systems, TU Delft, 2021.
[29] A.M. Girão Coelho, M. Lawson, D. Lam, J. Yang, R.M. Lawson, D. Lam, J. Yang, Guidance on demountable composite construction systems for UK practice, SCI, Ascot, 2020.
[30] ISO 14044, Environmental management - Life cycle assessment-Requirements and guidelines, 2006.
[31] C. De Wolf, E. Hoxha, C. Fivet, Comparison of environmental assessment methods when reusing building components: A case study, Sustainable Cities and Society 61 (2020) 102322. https://doi.org/10.1016/j.scs.2020.102322
[32] L.C.M. Eberhardt, A. van Stijn, F.N. Rasmussen, M. Birkved, H. Birgisdottir, Development of a Life Cycle Assessment Allocation Approach for Circular Economy in the Built Environment, Sustainability 12 (2020) 9579. https://doi.org/10.3390/su12229579
[33] M.J. Eckelman, C. Brown, L.N. Troup, L. Wang, M.D. Webster, J.F. Hajjar, Life cycle energy and environmental benefits of novel design-for-deconstruction structural systems in steel buildings, Building and Environment 143 (2018) 421–430. https://doi.org/10.1016/j.buildenv.2018.07.017
[34] G. Brambilla, M. Lavagna, G. Vasdravellis, C.A. Castiglioni, Environmental benefits arising from demountable steel-concrete composite floor systems in buildings, Resources, Conservation and Recycling 141 (2019) 133–142. https://doi.org/10.1016/j.resconrec.2018.10.014
[35] C. Braendstrup, Conceptual design of a demountable, reusable composite flooring system: Structural behaviour and environmental advantages, Master's thesis, Delft University of Technology, 2017. https://api.semanticscholar.org/CorpusID:116715365
[36] EN 15978:2011, Sustainability of Construction Works - Assessment of Environmental Performance of Buildings - Calculation Method, CEN, 2011.
[37] EN 1994-1-1, Eurocode 4: Design of composite steel and concrete structures. Part 1-1: General rules and rules for buildings, CEN, Brussels, 2004.
[38] EN 1993-1-1, Eurocode 3: Design of steel structures. Part 1-1: General rules and rules for buildings, CEN, Brussels, 2005.
[39] EN 1992-1-1, Eurocode 2: Design of Concrete Structures. Part 1-1: General rules and rules for buildings, CEN, Brussels, 2004.
[40] EN 1993-1-8, Eurocode 3: Design of steel structures. Part 1-8: Design of joints, CEN, Brussels, 2005.
[41] EN 1991-1-1, Eurocode 1: Actions on structures - Part 1-1: General actions - Densities, self-weight, imposed loads for buildings, CEN, Brussels, 2002.
[42] ArcelorMittal, Cofraplus® 60, (n.d.). https://construction.arcelormittal.com/fr-en/product/floors/composite-floors/cofraplus-60 (accessed March 1, 2026).
[43] M. Spremic, Z. Markovic, M. Veljkovic, D. Budjevac, Push-out experiments of headed shear studs in group arrangements, Advanced Steel Construction 9 (2013) 139–160.
[44] M. Classen, H.-J. Althaus, S. Blaser, M. Tuchschmid, N. Jungbluth, G. Doka, M. Faist Emmenegger, W. Scharnhorst, Life Cycle Inventories of Metals. Final report ecoinvent data v2.1, No.10, Swiss Centre for Life Cycle Inventories, Dübendorf, 2009.
[45] B. Weidema, R. Hischier, H.-J. Althaus, C. Bauer, G. Doka, R. Dones, R. Frischknecht, N. Jungbluth, T. Nemecek, A. Primas, G. Wernet, ecoinvent report No.2, Data v2.1, 2009.
[46] D. Kellenberger, H.-J. Althaus, T. Künniger, M. Lehmann, N. Jungbluth, P. Thalmann, Life Cycle Inventories of Building Products. Final report ecoinvent data v2.0, No.7, Swiss Centre for Life Cycle Inventories, Dübendorf, 2007.
[47] German Federal Ministry for Housing, Urban Development and Building, Ökobaudat according to EN 15804+A2, 2023. https://oekobaudat.de/OEKOBAU.DAT/datasetdetail/process.xhtml?uuid=f0ae9686-25b1-444c-8474-1f1d078cfed8&version=20.24.070&stock=OBD_2024_I&lang=en
[48] J.B. Guinée, M. Gorrée, R. Heijungs, G. Huppes, R. Kleijn, A. de Koning, L. van Oers, A. Wegener Sleeswijk, S. Suh, H. Udo de Haes, J. de Bruijn, R. van Duin, M. Huijbregts, Handbook on life cycle assessment: operational guide to the ISO standards, Springer Science & Business Media, 2002.
[49] Mission Possible Partnership MPP, Making Net-Zero Steel Possible - An industry-backed, 1.5°C-aligned transition strategy, 2022.
[50] The growing battle for scrap steel in green steel production, Roland Berger (n.d.). https://www.rolandberger.com/en/Insights/Publications/The-growing-battle-for-scrap-steel-in-green-steel-production.html (accessed May 20, 2026).
[51] European steel industry decarbonization from EAF mill perspective: IIO 2025 - EUROMETAL, (2025). https://eurometal.net/european-steel-industry-decarbonization-from-eaf-mill-perspective-iio-2025/ (accessed May 20, 2026).

Građevinski materijali i konstrukcije
Building Materials and Structures
journal homepage: www.buildingmaterialsstructures.com

https://doi.org/10.5937/GRMK2600017C UDK: 624.012.45:69.057.1

Review paper

Demountable connections for structural concrete reusability - State of the art and future directions for reinforced concrete, Part I: slabs

Carević Jelena*[1)], Milićević Ivan[1)], Vidović Milica[1)]

[1)] *University of Belgrade, Faculty of Civil Engineering, Bulevar kralja Aleksandra 73, 11000 Belgrade, Serbia*

Article history
Received: 19 May 2026
Received in revised form: 27 May 2026
Accepted: 29 May 2026
Available online: 12 June 2026

Keywords
precast concrete structures,
dry and semi-dry joints,
demountable connections,
slab-to-slab connections,
slab-to-beam connections,
reusability

ABSTRACT

This paper reviews demountable concrete slab connections as a strategy for reusing precast and existing reinforced concrete elements, with a focus on dry and semi-dry joints that enable assembly and disassembly. It analyses slab-to-slab and slab-to-beam connections, comparing solutions that differ in complexity, level of development and validation, and steel usage. Connections are analysed for two groups: precast slabs and monolithic concrete slabs cut for future reuse. Most proposed solutions are bolted dry connections, typically at a conceptual stage, with limited experimental validation. While some demountable precast joints can achieve performance close to that of monolithic systems, experimental results generally show reduced stiffness and load-bearing capacity. Reuse performance also tends to decline slightly in subsequent life cycles, highlighting the need for validation beyond initial use. Key factors such as slab rigidity significantly influence structural behaviour but remain insufficiently studied. Overall, wider practical application requires more comprehensive experimental and numerical research, especially beyond the first life cycle and system-level performance, along with integration into design standards.

1 Introduction

In contemporary growth-driven, globalised economies, the relentless pursuit of increased production has distanced the construction industry from many sound engineering principles and practices. Traditionally, structures were designed efficiently, using local materials, with proper maintenance, adaptation and reuse of components beyond their initial service life, and with minimised waste generation. However, industrialisation shifted priorities towards cost reduction and maximisation of profit. Consequently, we now face significant environmental challenges, and current scientific and societal efforts seek both to revive neglected principles and to develop new strategies to halt further degradation. Today, the construction industry is rigorously analysing products, processes, and frameworks to reduce environmental impacts. In the post-war era of rapid industrialisation, the concrete industry emerged as a leader, with concrete becoming the second most widely used material in the world after water. This leading position, however, brings a substantial environmental burden. The industry's consumption of natural resources—such as river and crushed stone, cement clinker, and water—the CO_2 emissions produced during cement and concrete manufacture and transport, and the vast amounts of waste generated all place the concrete sector at the forefront of environmental concerns in construction [1].

A wide range of strategies has been proposed to reduce the environmental impact of the concrete industry [2]. In the hierarchy of carbon-reduction strategies, the most effective option is to avoid building new structures by repurposing and refurbishing existing ones and by designing flexible, adaptable buildings. Where this is not possible, new construction should be limited to meeting genuine community needs while maximising the utilisation of buildings and materials [3]. When a building must be dismantled, the preferred approach is careful deconstruction and reuse of its elements, which implies that buildings should be designed for deconstruction and reuse [4]. Finally, waste should be reduced through upcycling, recycling or downcycling of materials. Across all these strategies, reuse is placed at the top of the hierarchy as a key element of the circular economy, which explains the recent surge of interest in the reuse of concrete structural elements. Reuse involves carefully disassembling components from an obsolete "donor" structure and reassembling them in a new "receiving" structure. By prolonging the service life of these components in their original or a comparable function, reuse reduces waste generation, greenhouse gas emissions and the demand for new raw materials [5].

Despite this potential, the implementation of reusable concrete elements in practice remains limited due to market, regulatory and technical barriers. The existing building stock has largely been designed for predominantly monolithic

* Corresponding author:
E-mail address: jelenad@imk.grf.bg.ac.rs

behaviour, with wet, cast-in-place joints, which hinder selective deconstruction and the recovery of undamaged elements at end-of-life. There is no systematic information on the building stock, the types and quantities of possible elements for reuse or the expected dates of availability of those elements [6]. This problem has been recognised by the research community, and several projects are focusing on building such databases [7]. Furthermore, incomplete information on material properties, reinforcement layout, prior loading history and degradation impedes reliable assessment of residual capacity and complicates compliance with current design standards. At the same time, the lack of standardised demountable connection systems and clear business models has constrained the development of a mature market for reclaimed precast components [8].

In response, recent research has focused on demountable and dry connections as key enablers for the reuse of precast concrete elements. Semi-dry systems, such as grouted-dowel or hybrid steel–concrete joints, represent an intermediate step towards circularity; however, the highest level of reusability is achieved with totally dry connections, where precast elements are joined exclusively by mechanical steel devices without any cast-in-place concrete [9]. Dry connections between slabs, beams and columns that allow easy demountability and reusability while providing adequate strength and stiffness are particularly challenging in reinforced concrete structures. The key problems are the greater deformability of dry connections compared to monolithic joints and the behaviour of dry joints in the second life cycle of structures, especially under seismic loading. To remain viable over multiple life cycles, buildings with reusable precast elements must maintain structural safety and serviceability throughout, including adequate durability and fire resistance.

The objective of this study is to provide a critical review of demountable connections—dry, or semi-dry where easily reversible—between concrete elements: (1) slab segments, and slabs and beams, (2) beams and columns and (3) columns and foundations. The connections and joints are analysed from the perspectives of ease of disassembly, reuse potential, behaviour in the first and second life cycles, and strength and deformability. The analysis and results are presented in two companion papers: “Demountable connections for structural concrete reusability – State of the art and future directions for reinforced concrete. Part I: slabs” and “Part II: precast frames”.

This paper is structured as follows. Section 2 discusses the role of reusable slabs as diaphragms. Section 3 reviews demountable slab-to-slab and slab-to-beam connections for new precast slabs and cut monolithic slabs. Section 4 provides a critical discussion and Section 5 summarises the main conclusions and research needs.

2 The role of the concrete slab as a rigid diaphragm

Slabs are primary horizontal load-bearing elements in buildings, transmitting gravity loads to vertical members and acting as diaphragms that tie the structure together and transfer horizontal forces to lateral load-bearing elements (walls and frames) [10]. Reinforced concrete slabs are most commonly cast in-situ as monolithic elements, but when construction speed or industrialisation is a priority, they are often designed as precast units. In precast construction, slabs are typically geometrically optimised to reduce self-weight, with hollow-core slabs (HCS) and double-T slabs being the most widely used solutions. Both slab types are usually designed with cast-in-place toppings to maintain continuity and cannot be easily reused due to the wet connection.

When slabs are designed for reuse, the usual approach is to use simply supported slab segments with dry connections along their longitudinal edges to form a rigid diaphragm. These connections should be designed to resist slip, work together to transmit gravity loads, and provide adequate resistance to vertical shear. The typical approach to concrete slab design assumes a uniform distribution of loads across slab spans for global analysis. This assumption needs to be confirmed for reused precast slabs, or the load analysis should be performed in more detail, with accurate linear or concentrated load distributions in the slabs, accounting for slab widths. However, this would reduce the potential for structural adaptability and limit possible changes in load position on slabs during the second life cycle or after adaptation; for example, the position of partition walls could not be chosen freely. Continuous slabs over beams are not a common choice for reused slabs, as continuity would require strengthening or grouting in the top zone, making disassembly at the end of the life cycle more difficult. The reuse of slabs limits the future structures’ span flexibility, so the idea of connecting slab segments in the longitudinal direction to extend the span is also introduced in some studies. These longitudinal in-span connections should be designed to transfer bending and shear forces, provide a rigid connection, and maintain slab continuity. Another important aspect in the design of reused slabs is the dry slab-to-beam or wall connection. This connection should enable the transfer of horizontal and vertical loads to beams/walls, and, if needed, flexural actions.

Longitudinal edge connections between slab segments should also resist shear forces induced by horizontal loads (wind and seismic action), enabling the uniform distribution of horizontal loads across all main horizontal load-bearing elements. The problem of diaphragm rigidity when designing reusable slabs is similar to the analysis done for untopped precast concrete slabs.

The diaphragm behaviour of reusable precast slabs is closely related to that of conventional untopped precast slabs [11]–[15]. Untopped slabs are typically connected on site by discrete steel connectors placed along the slab joints, without a cast-in-place topping, and their in-plane stiffness is therefore generally lower than that of monolithic floor systems. Studies on untopped precast slabs have shown that it is unsafe to assume rigid diaphragm behaviour a priori without experimental or numerical validation [15], since limited in-plane stiffness may lead to larger diaphragm deformations. Good anchorage of the connectors is essential, and in seismic design the diaphragm should remain elastic; therefore, the strength and stiffness [12] of untopped slab systems without topping need to be verified by testing. These findings are directly relevant to reusable slab systems, as most proposed demountable slab connections also rely on discrete mechanical connectors to transfer in-plane forces and develop diaphragm action. Therefore, reusable slabs should not be assumed to act as rigid diaphragms unless such behaviour is demonstrated through appropriate validation of the connection system.

The rigidity of floor slabs is especially important for the seismic design. Different standards define different limitations and consideration for the use of untopped precast slabs in different seismic zones. In the American standards for seismic design, the untopped precast slabs are not permitted in high seismic zones without appropriate experimental validation and consideration of slab rigidity and

connection ductility [16]–[18]. In the European standards, no specific limitation for untopped precast slabs is stated, but a minimum topping of 70 mm is required for adequate seismic design, limiting the use of these slab solutions in moderate or high seismic zones [19]. It is clear that the rigidity of precast slabs designed for reuse is of the most importance, and that it cannot be assumed as a rigid diaphragm without the adequate analysis of connection testing. The analysis should compare the horizontal movement of slabs or their relative movement to the monolithic slab, or be based on appropriate experimental testing. The EN 1998-1-1 standard [19], for example, declares a slab as a rigid diaphragm if the seismic induced lateral movement is less than 10% higher compared to the case when the slab is assumed as an absolute rigid diaphragm.

These observations underline that the diaphragm behaviour of reusable precast slabs is governed to a large extent by the stiffness and detailing of their connections, and that reliable diaphragm action cannot be ensured without explicit validation of the connection system. In addition to diaphragm action, these requirements emphasise that connection detailing governs vertical and longitudinal force transfer, as well as the practical reusability of slab systems, which motivates the following review of demountable slab connections.

3 Demountable connections that could enable the reuse of slabs

The review above shows that connection behaviour is critical for both the structural performance and the reusability of precast concrete slabs. When designed for reuse, slabs should therefore be conceived as precast segments with in-built connections that allow not only straightforward disassembly, but, more importantly, repeated reassembly in new configurations. Reusability also implies that transport and handling of slab segments should require no fundamental changes to current construction practice. In practical terms, this calls for segmented precast slabs with connections designed to ensure adequate interaction between elements and sufficient stiffness and strength in service. Wherever possible, these connections should be dry, or only partially wet in a way that enables easy demountability without damaging the embedded connection components. While some mechanical parts, such as bolts, washers and nuts, may be replaced in subsequent life cycles, it is crucial that the embedded connection elements retain their integrity during disassembly and reassembly.

Slabs are structural elements with strong potential for reuse, as they account for the vast majority of concrete volume in reinforced concrete buildings. Consequently, current research on slab reuse addresses both the development of precast slabs with reusable connections and the design of connections for cast-in-situ slab segments cut from obsolete structures. Both types of connections should fulfil the same structural functions, although their installation procedures and force-transfer mechanisms differ. Section 3.1 reviews demountable connections for new precast slabs, while Section 3.2 focuses on connections developed for monolithic slabs cut from existing structures.

3.1 Precast concrete slab connections

The idea of designing concrete structures for reusability is not new. One of the earliest demountable structural concepts was introduced in the 1970s and further developed in Europe [5], [20]. Several reusable structural systems were developed in the Netherlands in the 1990s: *Matrixbouw system, CD20 system, SMT system, Bestcon-30 system and Moducon-2000* [21]. These systems are largely closed, meaning that only elements from the same system can be connected to each other. They are similar to conventional concrete flat-slab buildings, typically comprising columns, slabs and walls. The slab segments are directly connected to the column heads and feet via bolts that protrude from the column and pass through pre-drilled holes in the slabs (Figure 1). The slabs used in these systems were ribbed (*Matrixbouw system*), pre-stressed (*CD20 system*) or double T (*SMT system*). No experimental data are available on the behaviour of these systems, and in some cases the connections were grouted (*SMT* and *Bestcon-30 systems*). The main barriers to broader implementation of these systems for reusable concrete structures are: the lack of technical information on behaviour under seismic loading, the lack of design guidelines for these connections and restrictions regarding modularity and custom-made buildings [22][23].

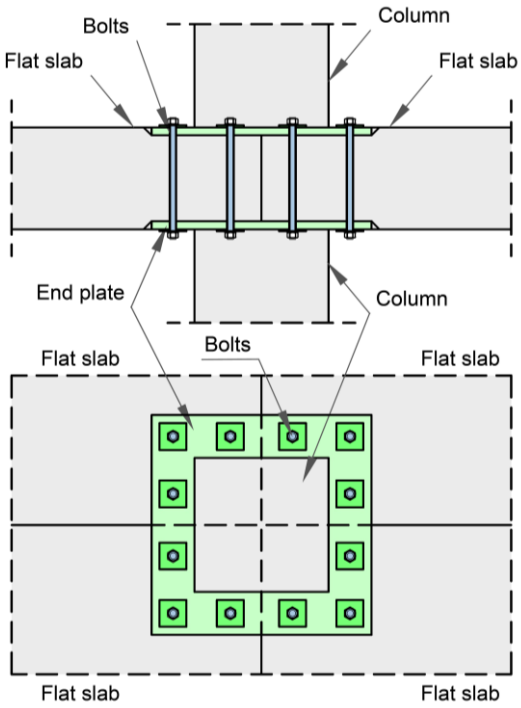

Figure 1. The Matrixbouw system column and flat slab connection - adapted from [21], [22]

Only a handful of new slab-to-slab connections are reported in the literature. They are mostly inspired by composite slab solutions and are designed with mechanical connectors and additional steel elements, such as plates, angles, or shear keys. These connections are either between adjacent slab segments in longitudinal direction, or in the middle of slab spans (mid-section connections).

A conceptual design of slab-to-slab longitudinal connection is presented in [23]–[25], and an adaptation of that connection is shown in Figure 2. Slab segments are longitudinally connected using steel plates and threaded rods. Holes are drilled in precast slabs, and they are connected using steel plates and threaded bars or bolts. Longitudinal shear forces between slabs are transferred through the dowel action of the bolts. Bolts can be pre-tensioned, and in that case, the shear forces are also

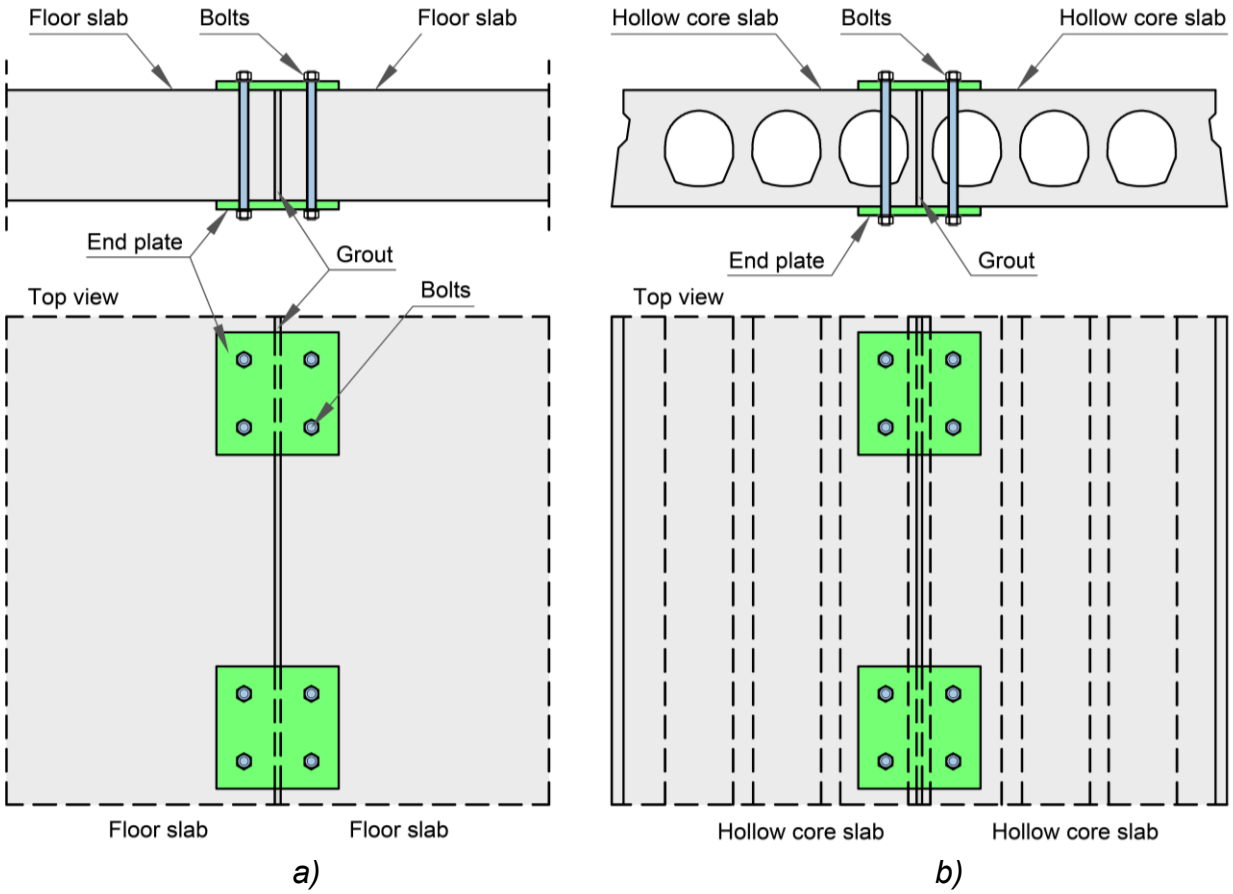

Figure 2. Layout of conceptual design of removable slab-to-slab connections: a) solid reinforced concrete slab segments, b) HCS segments - adapted from [23]–[25]

resisted by the friction between steel plates and slabs [26]. This connection type can generally be applied to flat slabs, double T and hollow-core slabs with minor modifications. However, no details about the geometry of connecting elements are presented, no analysis or experiments regarding the behaviour of the connection were conducted, so this solution is still at the conceptual level.

The same authors suggested one more possible solution for longitudinal connections between slab segments, but it remained on the conceptual level as well (Figure 3) [23], [24]. The slab segments have saw-tooth edges, with adjacent slab units interconnected by embedding the protruding ends of one floor slab unit into the recessed ends of the second slab unit. This connection type, if properly designed, can resist horizontal shear forces, but without any mechanical connectors, it cannot provide adequate resistance for vertical shear forces.

Another slab-to-slab connection was proposed by a different group of authors, but the connection type they proposed and tested was a mid-span connection between slab elements [26]. They proposed four different connection configurations in the slabs mid-span: simple bolted connection (Figure 4 a)), bolted connection with an embedded steel block (Figure 4 b)), bolted connection with a shear key (Figure 4 c)), and bolted connection with a combination of shear key and embedded steel block (Figure 4 d)).

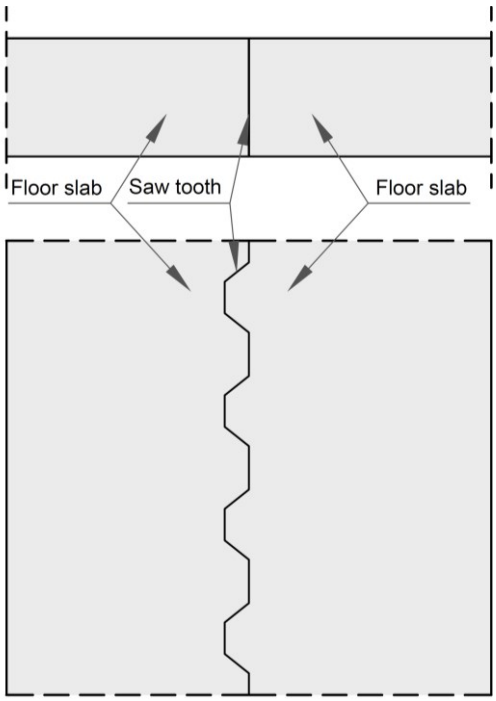

Figure 3. Layout of conceptual design of removable slab-to-slab connections with saw-tooth edges - adapted from [23], [24]

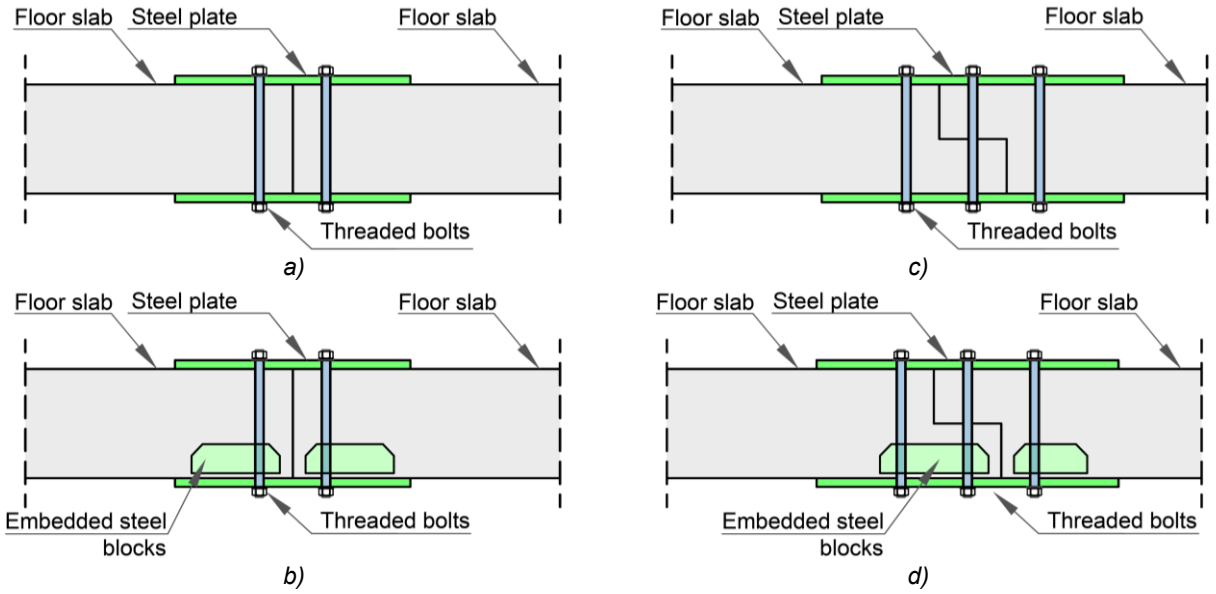

Figure 4. Slab-to-slab mid-span connections: a) simple bolted connection, b) bolted connection with an embedded steel block, c) bolted connection with a shear key, and d) bolted connection with a combination of shear key and embedded steel block - adapted from [26], [27]

The first slab-to-slab connection type they proposed was a mid-span connection with steel plates at the top and bottom of the slab ends, and high-tensile threaded steel bolts. Holes for bolts were protected with steel ducts to prevent the bolts from moving (Figure 4 a)). The second type (Figure 4 b)) was a modification of the previous connection type with an additional steel block with ribs welded to the tensioned slab reinforcement.

The other two connection types were similar to the first two, but with a shear-key. The third connection consisted of shear keys at both ends of slab segments, which were interlocked and connected with high-tensile threaded steel bolts protruding through the full slab depth (Figure 4 c)). And the last connection was a combination of previous types with shear keys strengthened with steel blocks with ribs and threaded bolts (Figure 4 d)).

The authors conducted experimental testing of slabs with these four connection types, and compared them to a reference slab without a mid-span connection. Simple supported 5.2 m one-way slabs (50 cm wide and 16 cm deep) were tested in a four-point bending test. All specimens had 50 cm-wide, 8 mm-thick connecting steel plates. To be efficient, this connection should ensure slab continuity by providing the required bending and shear strengths. Experimental tests showed that all four demountable slab solutions exhibited lower ultimate loads, higher crack widths, and higher deflections than the reference monolithic slab. For slabs with embedded steel blocks, the reduction of strength was highest – around 60%, and for the simple shear key solution, the lowest – around 25% [26]. Embedded steel blocks induced stress concentrations, large crack widths and low bearing capacity. The solution with shear keys and threaded bolts yielded the best results, but more research and modification are needed to validate this type of in-span connection. It is still unclear how to design these connections, how to reinforce the area around the connection, and what is the influence of this connection on global slab behaviour regarding the diaphragm effect and vibrations. Ensuring adequate continuity in slabs (mid-span or other in-span sections) cannot be easily achieved without significant additional steel for connections. In current practice, the design of reused slabs generally does not include in-span connections; instead, simply supported slabs are used, with secondary steel beams if the spans are shorter than desired. This is also a solution with additional steel, but the load transfer is straightforward and uses easy, validated connections.

Connections with interlocking steel elements, mostly plates of different shapes, have been studied as a replacement for traditional welding or bolting. One study focused on the development of demountable interlocking slab-to-slab connections [28]. The connection consisted of two parts: (1) an embedded high-strength steel faceplate with the T-shaped and rectangular-shaped cuts, and (2) H-shaped or rectangular-shaped connectors for in-plane and out-of-plain shear (Figure 5). No detail about the faceplate anchorage was provided in this study. The teeth and connectors interlock, and their shape and number should be defined based on the design shear forces. Steel elements were designed with a 2-mm installation tolerance. A monotonic tension test was conducted to evaluate the in-plane interaction behaviour between shear connectors and embedded steel plates. Steel strength, number of connectors, spacing between cuts, faceplate tooth width and connector shape were varied during the experimental testing. The results showed that this system can provide an in-plane shear transfer. However, these connections were not tested within a concrete slab; anchoring is neither designed nor analysed; the effects of edge distance and reinforcement detail are unknown; and the behaviour of this connection type under seismic loading is not tested.

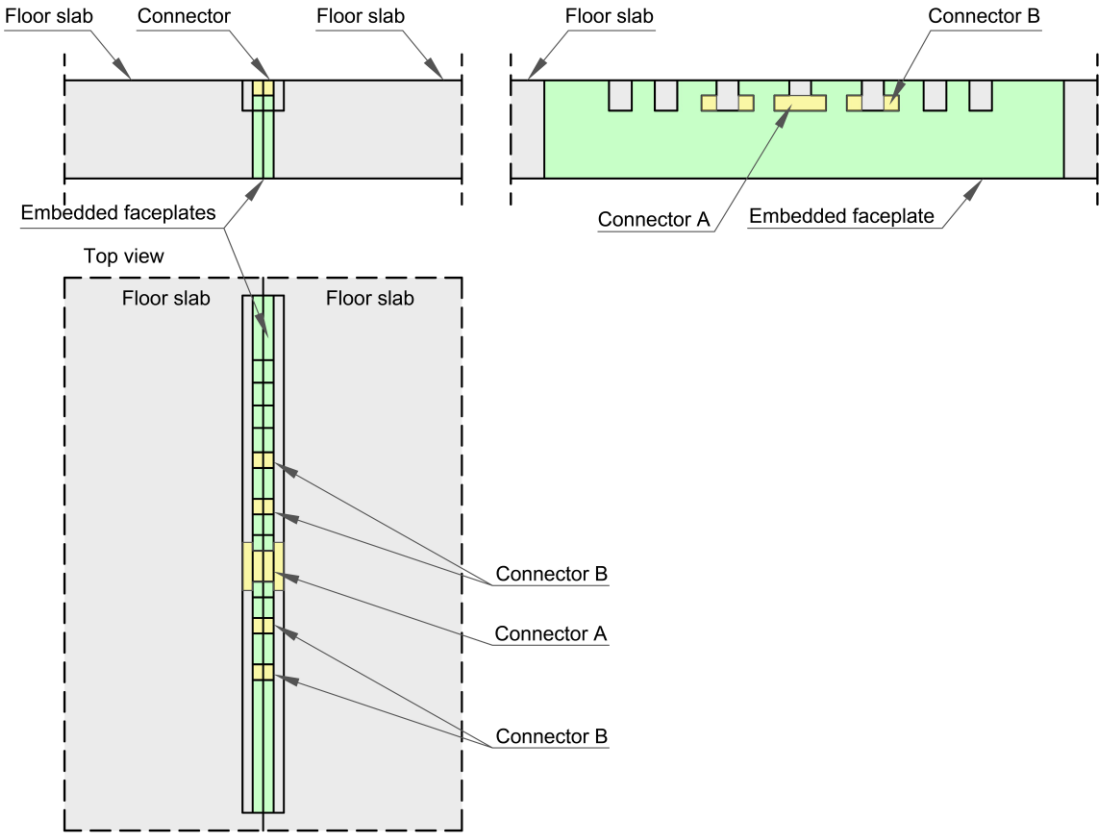

Figure 5. Demountable interlocking connection - adapted from [28]

Another important connection is the slab-to-beam or slab-to-wall connection. These connections should be designed to prevent slip and enable effective flexural and shear transfer. Similar to slab-to-slab connections, connections between slabs and beams are designed using bolts, steel plates, or angles. A few examples found in literature for this type of connection are described below.

One preliminary design idea for demountable slab-to-beam connections is shown in Figure 6. [23]–[25]. Precast concrete slabs are connected with beams using bolts that protrude from the slab through drilled holes, and are embedded for some length in the beam (Figure 6 a)). Two slab segments are also connected with steel plates and bolts on the top side under the beams. The general concept of this connection is that bolts connected to the floor slab are removable, and the bolts connected to the beam are embedded into the concrete (Figure 6 b)). The holes in the steel angles on the beam side are slotted vertically to accommodate relative vertical movement between the beams and slabs under lateral loads. A similar type of floor-to-beam steel connection system is possible for different types of floor slabs (Figure 6 c)). This type of connection can be easily disassembled if the slab is constructed without the topping. If an adequate number of bolts on adequate spacing are selected, this connection can transfer vertical and horizontal shear between the slab and the beam. There are no specific details about this connection in [23]–[25], so it is unclear what the adopted tolerances are,

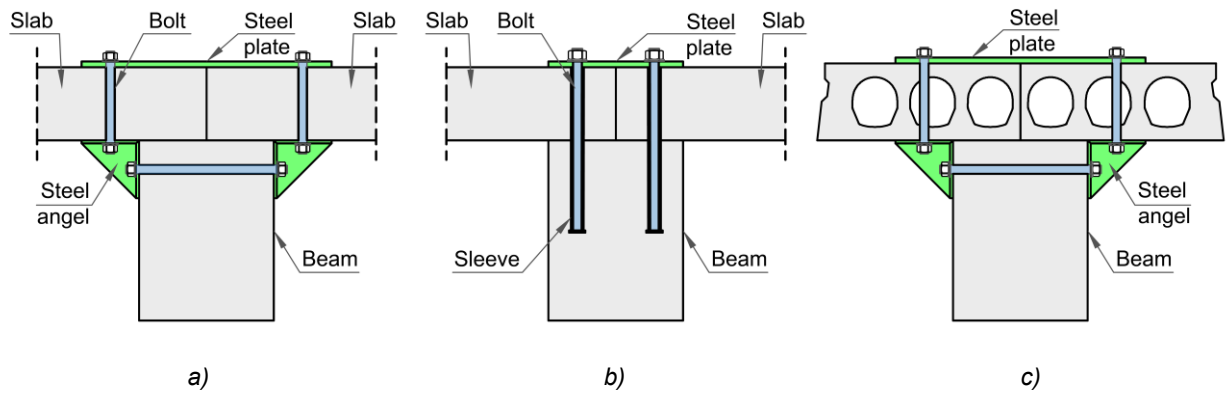

a) *b)* *c)*

Figure 6. a) Solid slab-to-beam connection with bolts and steel plates and angles, b) solid slab-to-beam connection with bolts and steel plates and c) Hollow-core slab-to-beam connection with bolts and steel plates - adapted from [23]–[25]

how they will affect the connection flexibility, or whether this is a longitudinal or transverse connection of slabs to the beam (especially the connection presented in Figure 6 c). Also, there are no experimental or numerical test results for these connections in the present literature, so no clear conclusions about their behaviour and the slab as a whole can be drawn.

In some research studies, an attempt was made to minimise the connections between slab segments in the longitudinal direction by designing larger slab segments that cover the whole grid field [23] [29] [30]. One example of that slab solution is shown in Figure 7 a), together with the concept of bolted connections in the middle (Figure 7 b)) and edge beams (Figure 7 c)). One of those slab-to-beam connection types was demonstrated by Zhang et al. [31] in a ½ scaled three-story demountable precast concrete frame structure, designed for a peak ground acceleration of 0.2g, and tested on a shaking table to evaluate its seismic performance. The structure is made with bolted connections between all concrete elements (foundations, columns, beams and slabs), and the precast reinforced concrete solid slabs were designed to cover one 3.0×4.0 m grid field.

The slabs were designed with a constant height of 60 mm and three connection spots with two bolt holes along each of the four edges, as shown in Figure 7 a). The bolts were embedded in beams, protruding over the beam top in a sufficient length for a precast slab, a washer or a steel plate and a nut (similar to Figure 7 b)). The authors did not provide any additional information about the connection: no bolt type or diameter, nor any mention of bolt anchorage or hole sizes. The study conducted by Zhang et al. [31] demonstrated easy, fast assembly with no need for temporary support for all precast elements, but the demountability or reusability was not evaluated.

The test showed that the precast frame structure was essentially elastic with no cracks in the beams or columns under frequent earthquakes, and that the maximum inter-story drifts were within the limits. No cracks in precast floor slabs were reported, but no specific information about slab behaviour was provided. Based on the global behaviour of the tested structure, the authors of this paper can assume that the slab-to-beam connections provided effective transfer of horizontal forces to the frames. However, the behaviour of slab-to-beam connections is an important factor that needs to be systematically evaluated, considering the behaviour of bolts, the adopted tolerances, the failure mechanism, and the crack development.

Bolted protruded slab-to-beam connections were also proposed by Cai et al. [29] as suitable for reusability and easy demountability. The authors designed a ground-floor house for low- or moderate-seismic zones at the conceptual level, with all connections as demountable steel plates and bolts. Slabs were designed for the entire grid field, so no slab-to-slab connections were introduced, but only bolted slab-to-beam connections. The slab design was not presented in detail, and no slab connection testing was conducted. A push-out test on three concrete blocks connected with these bolted connections was, however, tested within this study (Figure 8). The results showed that after testing, assemblies reached their peak loads, and the specimens quickly lost their bearing capacity. The stiffness of bolted connections was lower than that of welded connections due to slipping, concrete crushing, and bolt deformation [29].

Similar to Cai et al. [29], Akduman et al. [30] proposed bolted slab-to-beam connections for one ground-floor demountable pilot house. The slabs (h=20 cm and L=5.45 or 6.0 m) were designed with different widths (200-235 cm) and without longitudinal connections between slabs (Figure 9). Each slab segment was designed with four corner square profiles (cross-section 50x50 mm and 200 mm in height) embedded to leave space for connectors (8.8-grade threaded bars, 24 mm in diameter). Slabs were connected to the beams with 80x80x10 mm steel square washers and nuts. The connector bars were placed in the corners of slabs with an edge distance of threaded rods 12 cm in the longitudinal direction, and 12 cm in the transverse direction. Rubber sheets were used to improve the transfer of force at the slab-beam connection surface. One slab (20x80x367 cm) was tested in this study in a standard three-point bending test, and only a brief description of the slabs' behaviour during testing was presented.

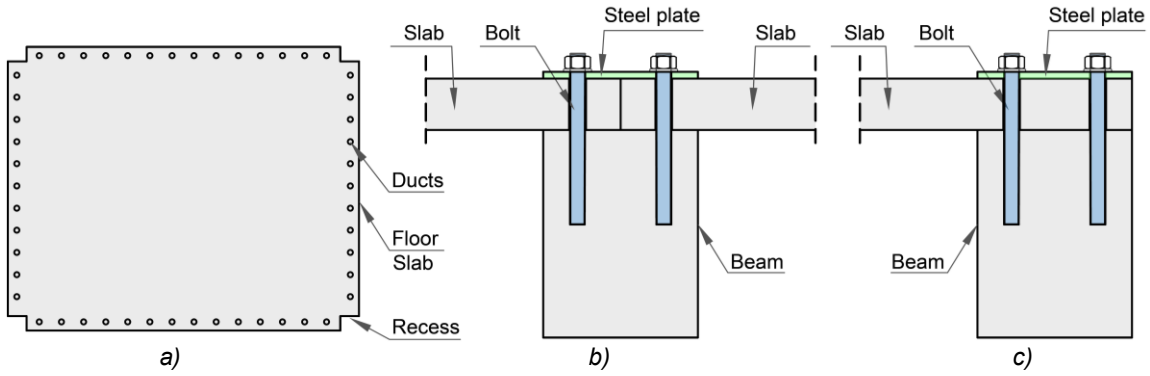

Figure 7. a) Larger slab segments that cover the whole grid field, with b) middle beam and c) edge beam connection - adapted from [23] [29] [30] [31]

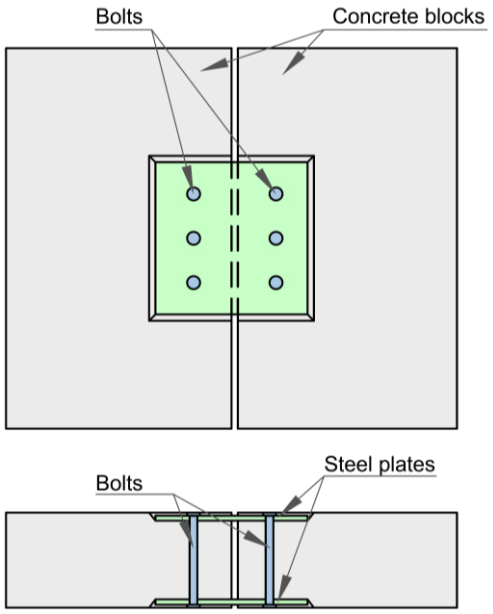

Figure 8. Bolted connection tested by Cai et al. [29]

The authors stated that no reduction in the bearing capacity of the tested slab was observed up to a deflection of 80 mm (the serviceability limit for deflection was 14.3 mm). During this test, the slab was connected to the supporting beams using two corner-threaded bolts, as described above. Rotation of the slab on the supporting lines was reported, but no information about the behaviour of threaded bars or slip in the steel square profiles was provided. No specific test results or validation criteria were presented, so no clear conclusions about the behaviour of this slab and its connections can be drawn. It remains unclear whether a 20-cm slab calibrated to meet deflection criteria at a 3.67 m span can satisfy the same criteria at a 6.0 m span.

Another conceptual idea for a slab-to-beam connection is presented by Almahmood et al. in [26]. The connection consisted of steel plates (or connectors) with ribs embedded in the slab and bolts protruding from the beam (Figure 10). This connection is easily demountable, but it requires more steel elements compared to previous types. The idea is presented as a concept, without any detail on geometry, tolerances, force transfer, reinforcement details, or connection behaviour.

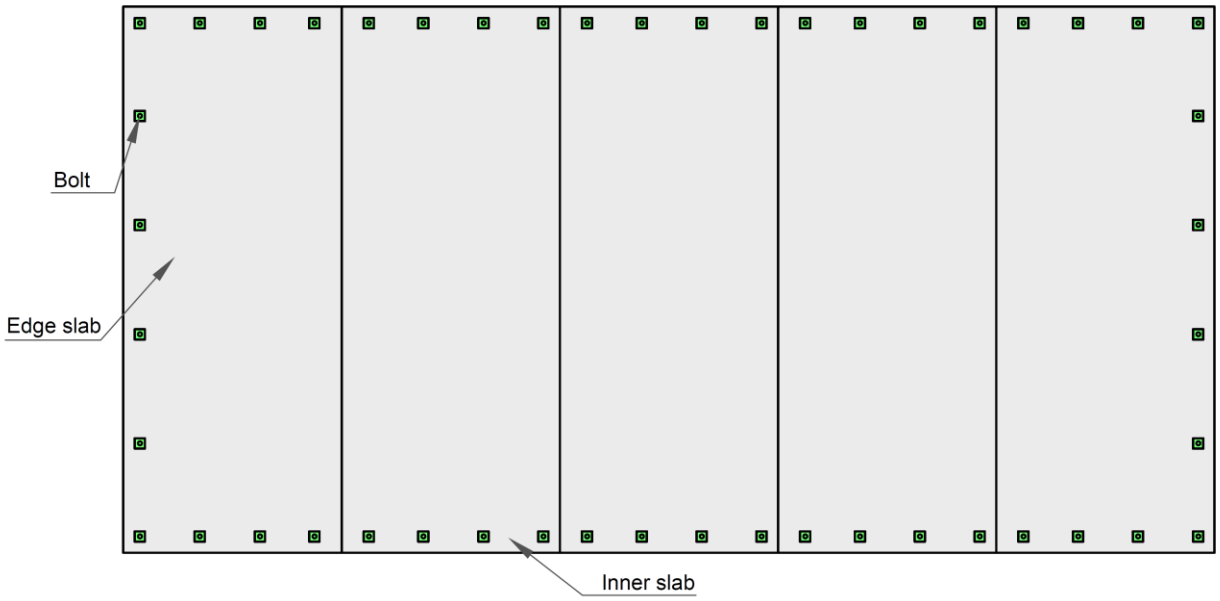

Figure 9. Connection concept for slab segments and beams – adapted from [30]

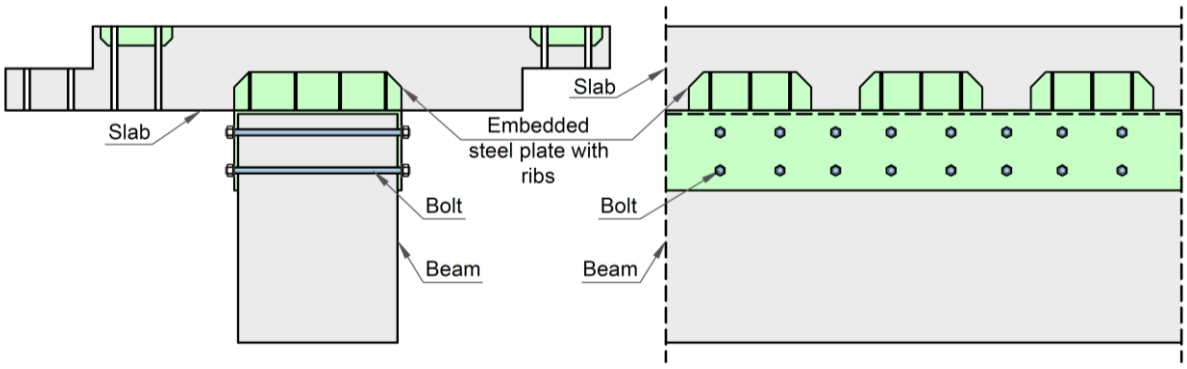

Figure 10. Slab-to-beam connection - adapted from [26]

One research study focused on explaining the behaviour of bolted plate slabs-to-beam connections under vertical loading [32]. Two precast concrete slabs were connected to a supporting beam with steel plates and post-tensioned bolts protruding from both slabs and the beam (Figure 11). Steel plates were positioned on top of the slabs and on the bottom of the beam, and connected with eight post-tensioned bolts. In this study, the assembly shown in Figure 11 was tested in a three-point bending test to induce vertical shear and bending in the connection. Steel plates used in this experiment were 40×20×1.5 cm; concrete slabs were 150×50×(10, 15 and 20) cm; the supporting beam was 50×(25, 35)×15 cm; and the bolts were Ø10, 16 and 20 mm. The holes for the bolts were designed with diameters 2 mm larger than the corresponding bolt sizes, and eight pipes matching the hole sizes were embedded in the slabs.

The influence of four parameters was analysed in this experiment: slab height, beam width, bolt diameter and post-tensioning force in bolts. The results showed that this connection can successfully transfer vertical shear forces and some bending moments. The capacity was lower compared to the monolithic slab, but the authors reported it can be up to 84% of the load-bearing capacity of fully monolithic structure. The capacity for horizontal shear forces was not analysed.

Some slab-to-beam connections, different from these bolt-and-steel-element types, have been analysed or presented conceptually in the available literature. A group of authors, Scalbi et al. [33], is developing a so-called “Cylinders Connection System concept” using cylindrical steel tubes as dowel-type shear connectors to transfer longitudinal shear force between two connected slabs [33]. This design is not presented in detail, and, to the best of the authors' knowledge, it has not yet been validated.

Another demountable solution for the concrete slab-to-beam connection was presented by Li et al. [34]–[36], and the connection concept is shown in Figure 12. This slab-to-beam connection was made with non-embedded high-strength bolted shear connectors to allow easy assembly and disassembly. A steel boxes (Q420 grade) were anchored to the beam, and a steel channel (Q355 grade) to the slab, both fixed with studs. The elements were connected on site using high-strength bolts, without embedding the bolts in concrete [36]. To evaluate the performance of this connection under shear, seven slab-to-beam assemblies were tested in a monotonic push-out test. Each specimen consisted of one beam block and two slab blocks, connected with 2x4 8.8-grade bolts in steel boxes on each side. All samples were designed with the bolt as the weakest link to ensure it fails first under loading, and to maintain the elastic behaviour of steel boxes and channels. The test investigated the influence of bolt diameter (M16, M20, and M24), outer wall thickness of the steel box (8 and 12 mm), channel spacing (150, 200, and 300 mm), and slab concrete strength (C20 and C40) on the behaviour of the connectors. Reusability was analysed by testing all samples across two life cycles. In the first cycle, the load was applied by a hydraulic jack under displacement control in three stages: preloading, service-level loading, and loading to ultimate failure. After failure, samples were reassembled and tested once more using the same loading protocol to simulate the second life cycle.

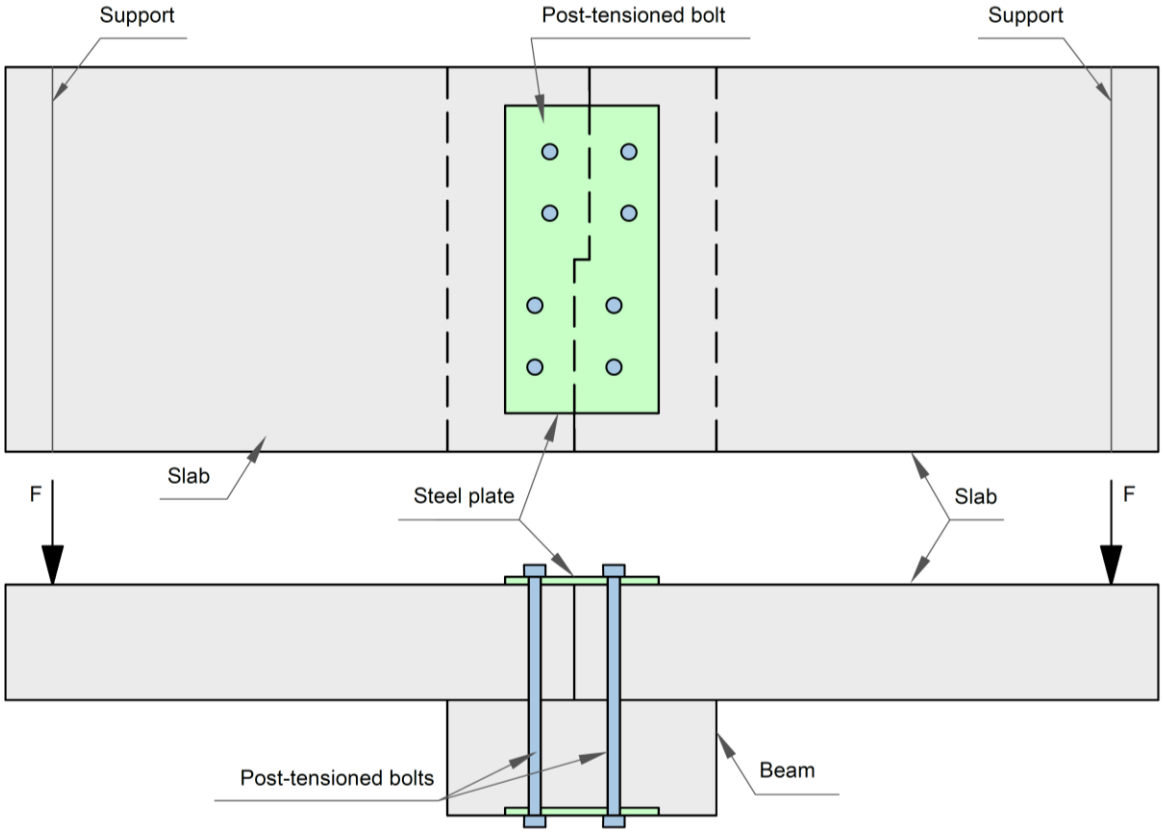

Figure 11. Slab-to-beam connection with post-tensioned bolts – adapted from [32]

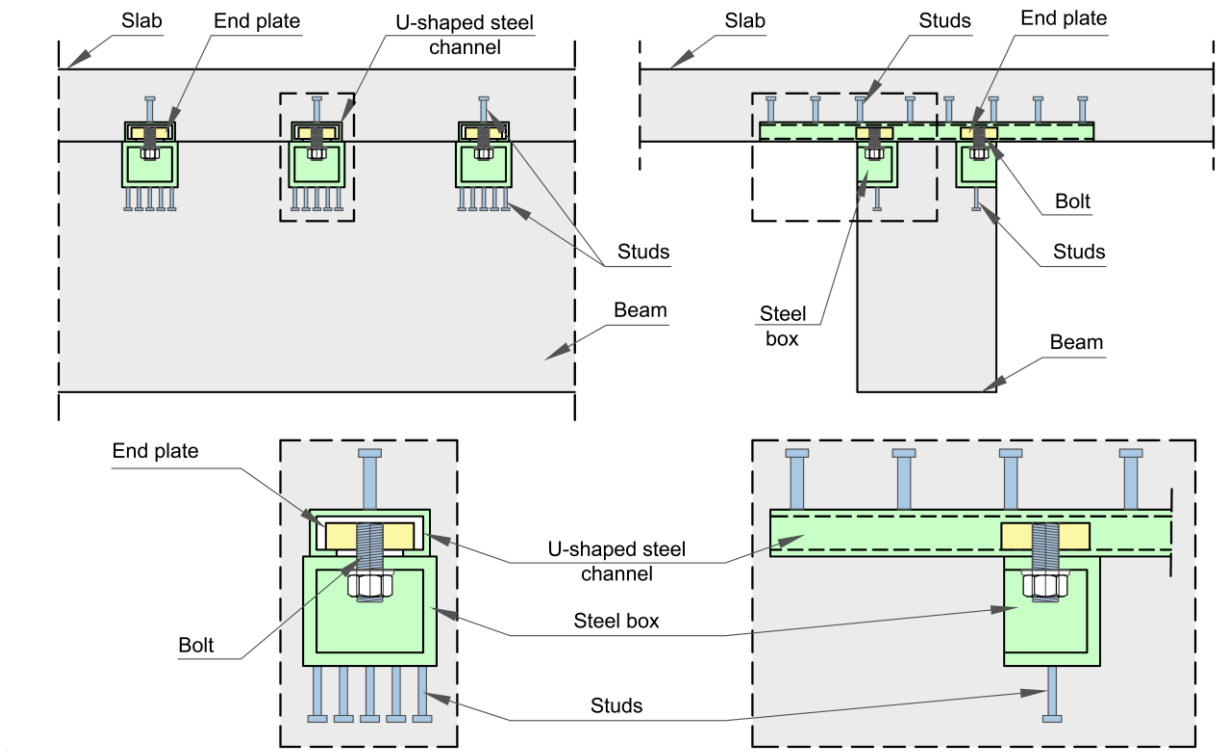

Figure 12. Demountable slab-to-beam connection with steel channels and boxes - adapted from [34]–[36]

Under increasing load, the connection behaved as follows: (1) the connection initially transferred shear by friction due to bolt pretension, (2) followed by a combined friction–bearing mechanism with progressive slip, (3) the bolt shear accompanied with localized concrete cracking, and (4) with all specimens ultimately failing by bolt shear fracture at the beam–slab interface while the concrete members, channel and steel box remained largely undamaged. Variations in bolt diameter, channel spacing, steel box wall thickness and slab concrete strength showed that: (1) larger bolt diameters and reduced channel spacing significantly enhance ultimate shear capacity (with some reduction in ductility for larger bolts), (2) increased box thickness improves capacity but may slightly reduce deformation uniformity, (3) whereas the influence of slab concrete strength on shear resistance is marginal for this setup. During the first loading cycle, the strain of the steel box and the channel remained below the yield strain limit. The disassembly torque measurements demonstrated that bolts can be safely loosened both at service load and after reaching ultimate capacity. The loosening torques were clearly lower than the initial tightening torques, yet still sufficient for adequate tightening under service loading, but low enough to permit practical bolt removal and replacement without damaging the concrete or steel components. In the secondary loading phase, the same specimens were reassembled with new bolts and subjected to the same displacement-controlled loading protocol. Based on the obtained results, Li et al. concluded the following: (1) the failure mode was still governed by bolt shear, (2) the initial slip loads showed minimal variations, (3) the ultimate shear capacity, initial stiffness and peak slip generally decreased by about 5–20% (depending on bolt diameter, channel spacing and box thickness). This study verifies good demountability, reusability and stable mechanical performance of the proposed connection under repeated loading cycles.

In the first loading cycle, all specimens reached ultimate slips larger than 6 mm (typically around 8–13 mm depending on the configuration), fulfilling the EN1994-1-1 [37] ductility criterion, while in the secondary loading, the corresponding ultimate slips remained above 6 mm but were reduced by roughly 5–20%, confirming that the connection still exhibits adequate deformation capacity after reuse. The observed reductions in stiffness and ultimate shear capacity under secondary loading can be attributed to accumulated damage and residual deformations in the steel box–channel region, and to microcracks in the concrete surrounding the connectors, which change the load-transfer mechanism despite the replacement of the bolts.

In addition to purely mechanical dry and semi-dry connections, alternative design-for-disassembly approaches have been proposed that rely on intentionally “weak” mortar joints. Halding [38] investigated lime–cement mortars in joints between HCS and walls, aiming to achieve sufficient in-service shear capacity for horizontal load transfer while facilitating joint removal at end-of-life. Experimental tests on low-strength mortars and a case-study wind analysis showed that selected lime–cement mixes can provide adequate performance during the service life, but their demountability still depends on specialised demolition techniques (such as hydro-demolition or flat jacks), highlighting a different trade-off between structural capacity, connection stiffness and practical disassembly compared to fully mechanical demountable connections.

3.2 Connections of monolithic concrete slabs cut for reuse

The feasibility of reusing existing cast-in-place concrete elements to create a new structure was demonstrated with two pilot projects in Switzerland: a 10-m-spanning post-tensioned segmented "Re:Crete" arch footbridge prototype, and a 233-m^2 parking pavement built with reused concrete walls and slabs [39]–[41].

Reusing cut cast-in-situ slabs for equivalent purposes is in its infancy, but one design-level solution for slab-to-slab and slab-to-beam connections is shown in Figure 13. These connections for the structural reuse of cut cast-in-situ slabs have not been experimentally verified in the existing literature, but the concept is well-known: bolted steel plates and angles. Cut reinforced concrete slabs are supported by 20-cm-wide steel angles installed on the walls with bolts, Figure 13 b). The slabs are placed on the supports previously topped with elastomer and fastened with through-bolts that pass through the full thickness of the slab and the angle leg [39]. Holes for these anchors need to be drilled in slab segments. Joints between two slabs are typically 2-cm wide and filled with mortar.

Two slab segments are also connected with a 25-cm-wide steel plate on the top side and post-installed anchors (Figure 13 a), ensuring transfer of lateral forces. This type of connection can be considered demountable, as steel elements can be unbolted and mortar joints hydro-jetted. This connection system is well-known for its clear force transfer and a straightforward design. There are numerous post-installed anchors available on the market that are demountable, but they will protrude above the slab surface. When considering bolt/anchor connections, important factors include concrete stresses in the vicinity of the mechanical connection. The distance between the anchor and the concrete edge should be analysed, taking existing slab reinforcement into account. Slabs and segments cut from existing structures will usually not have any additional reinforcement at the edges, but only top- and/or bottom-reinforcement mesh. An important aspect of bolted connections is also the tolerance, i.e., the hole diameter relative to the bolt diameter. Tolerances for bolted concrete elements are generally higher than those for steel structures, which can increase the potential for slip under horizontal loads. This should be considered during the design, or the holes should be filled with some epoxy material that allows easy demountability.

These types of slabs are generally intended for unidirectional one/span application in receiving structures, but it is possible to achieve slab continuity to some extent by strengthening the regions subjected to negative bending moments. In the structural model of the target building analysed in [7], reused slabs are assumed to be continuous over the walls. In these regions, a 20–35 mm layer of *Ultra-High-Performance Fibre-Reinforced Cementitious Composite* was applied to the upper surface of the slab to provide structural strengthening where required, ensure continuity at connections, and transfer tensile forces between slab elements. In this way, slabs would not be easily disassembled for further reuse after the second life cycle.

4 Discussion

The reviewed literature indicates that research on reusable concrete slabs and their demountable connections remains in its early stages, both in terms of the number of studies and the maturity of proposed solutions. Most concepts have been introduced at a preliminary or conceptual level, often without full detailing, design procedures, or systematic experimental validation across multiple life cycles. These connections were mostly inspired by precast concrete element connections with bolts or by steel element connections. However, this philosophy cannot be adopted without consideration of specific aspects related to reusability: precast concrete elements' tolerances can be higher compared to steel elements, and the holes shouldn't be grouted to ensure a dry connection; the behaviour of joints will change to some extent after the first life cycle, disassembly, transport and reassembly. The slab connections presented in this paper are divided into two major groups: connections for new precast slabs designed for reuse and connections for previously cut monolithic concrete slabs.

From a structural perspective, a central issue is the diaphragm behaviour of reusable slabs. Similar to untopped precast slabs, dry longitudinal joints and dry slab-to-beam or slab-to-wall connections introduce additional slip and flexibility, so a rigid diaphragm assumption cannot be taken for granted. For reusable systems, further reductions in stiffness arise from design choices made to facilitate demountability, such as segmenting slabs, avoiding cast-in-place toppings, and relying on simply supported spans. This combination directly affects in-plane stiffness, deformation

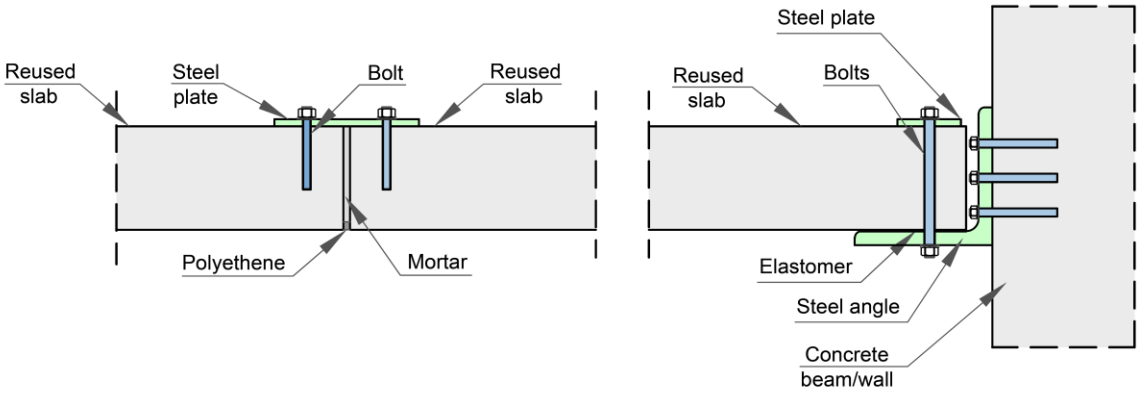

Figure 13. Cut slab segment connections: a) slab-to-slab, b) slab-to-concrete beam/wall [39]

compatibility, vibration characteristics and the distribution of horizontal loads. As a result, the classification of reusable slabs by rigidity becomes an explicit design task that should be based on quantified stiffness from experiments or reliable models, rather than analogy with monolithic floors.

Reusable precast concrete systems introduced in the 1970s demonstrated feasibility but are largely closed and lack accessible test data, restricting their wider, modular, and seismically robust application. More recent concepts for reusability focus on open, modular, and reusable systems with dry connections. Those solutions regarding slab connections are mostly at the conceptual level, or demonstrated in pilot projects without experimental testing, connection classification, or design recommendations. Slab connections for precast reusable slabs are mostly discrete types of connections. The tooth-saw concept is a continuous connection along the longitudinal edges of two slab segments, but it can only transfer horizontal shear forces; to transfer vertical shear forces, additional mechanical fasteners or other connectors are required.

Bolted connections with steel plates and angles are proposed by several authors, but no experimental analysis of those joints was conducted, leaving their bearing capacity, stiffness and influence on global floor behaviour unclear. Available experiments [30] confirm that bolted plate connections can transfer a significant portion of shear and bending loads, but with increased slip, rotations, and reduced stiffness compared to monolithic or welded solutions. Testing of the post-tensioned bolted joint by Baghdadi et al. [32] showed that its capacity can reach up to 84% of the load-bearing capacity of a fully monolithic structure, though the capacity for horizontal shear forces was not analysed. Overall, demountable slab-to-slab and slab-to-beam connections with bolts and steel plates or angles are technically feasible but not yet sufficiently validated and characterised for reliable design, with key aspects such as tolerances, slip, global diaphragm performance, and seismic behaviour remaining open.

Another discrete connection along the slabs' longitudinal edge with interlocking steel plates and elements was proposed by Chen et al. [28]. The absence of anchor plate design, edge distance analysis, and seismic testing means that the structural validity of this connection remains confined to a single in-plane shear mode under monotonic loading — a narrow basis for a system intended for multi-directional force transfer in real floor diaphragms. Until these gaps are addressed, the connection cannot be considered verified for practical use, and adopting it in seismic regions would carry unquantified risk.

The idea of mid-span slab-to-slab connections using bolts, plates, embedded steel blocks and shear keys was introduced by Almahmood et al. [26]. Achieving continuity and diaphragm action through in-span connections demands substantial additional steel and detailing effort, yet design rules, optimal reinforcement arrangements, and their influence on global slab behaviour — particularly diaphragm action and vibrations — remain unclear. As a result, current practical solutions for reusable slabs generally avoid in-span connections and rely on simply supported segments, sometimes combined with secondary steel beams, because these arrangements provide straightforward load paths and well-understood connections.

A unique solution for slab to beam connection was proposed by Li et al. [34]–[36]. To the best of the authors' knowledge, this is the only study to assess a demountable slab-to-beam connection over two distinct life cycles, which renders its findings especially influential despite the much broader scope of research that remains necessary. The observed degradation in shear capacity, stiffness, and slip performance demonstrates that first-cycle behaviour cannot be assumed to persist, and that systematic multi-cycle testing — particularly under seismic loading — must become a standard validation requirement for all dry mechanical connection types.

Reuse of cut monolithic slabs is technically feasible [39]; however, the connection concepts developed so far lack systematic structural validation. Key aspects such as design guidance for edge detailing, slip control, and long-term performance remain undeveloped, leaving the approach largely experimental. Furthermore, measures that ensure adequate continuity and diaphragm action often undermine future reusability. Addressing this issue is essential before cut monolithic slabs can be considered a dependable, demountable system.

A summary of connection and connector types, level of development and testing results in the first and second life cycle for studies presented in this paper is shown in Table 1.

Table 1. Qualitative presentation of connection types, level of development and testing results in the first and second life cycle for studies presented in this paper

Study [ref]	Joint	Connection type	Level of development	Test results – the first life cycle	Reuse validation – the second life cycle
[21], [22]	Flat slab-to-column	Bolted with steel plates	Practical demonstration	Not available	Potential reusability with no validation in the second life cycle
[23]–[25]	Slab-to-slab longitudinal connection	Bolted with steel plates	Conceptual level	No testing	Potential reusability with no validation in the second life cycle
[23]–[25], [29] [30] [31]	Slab-to-beam	Bolted with steel plates	Conceptual level	No testing	Potential reusability with no validation in the second life cycle
[23], [24]	Slab-to-slab longitudinal connection	Saw-tooth	Conceptual level	No testing	Potential reusability with no validation in the second life cycle

[26], [27]	Slab-to-slab mid-span connection	Bolted with steel plates and blocks, shear key	Preliminary testing	Lower ultimate loads, higher crack widths, and higher deflections	Potential reusability with no validation in the second life cycle
[28]	Slab-to-slab longitudinal connection	Interlocking steel plates of different shapes (teeth and connector interlock)	A monotonic steel connector tension test	A steel system can provide an in-plane shear transfer, but no connection testing	Potential reusability with no validation in the second life cycle
[29]	Slab-to-beam	Bolted protruded connections with steel plates	Connection testing on concrete blocks	Lower stiffness	Potential reusability with no validation in the second life cycle
[30]	Slab-to-beam	Bolted protruded connections with steel plates	Practical demonstration	No testing	Potential reusability with no validation in the second life cycle
[32]	Slab-to-beam	Steel plates and post-tensioned protruding bolts	Joint testing	Successful shear transfer and up to 84% of the monolithic structure's load-bearing capacity	Potential reusability with no validation in the second life cycle
[34]–[36]	Slab-to-beam	Non-embedded high-strength bolted shear connectors, steel boxes and channels	Monotonic push-out tests of slab-to-beam assemblies	Failure by bolt shear fracture with the concrete members, channel and steel box undamaged	After second life cycle testing, the ultimate shear capacity, initial stiffness and peak slip decreased by 5–20%
[39]	Slab-to-slab and slab-to-beam for cut monolithic slabs	Bolted with steel plates and angles	Conceptual level	No testing	Potential reusability with hydro-jetting mortar joints, but no validation in the second life cycle

5 Conclusions

The reusability of concrete elements has attracted significant attention in recent years as a possible practice that could shift the concrete construction industry toward sustainability. The idea of reusing concrete elements is currently being studied from market development to demonstration pilot projects. However, a comprehensive experimental analysis of the behaviour of connections between reusable elements was not conducted to an adequate extent for all connection types. This is currently one of the largest obstacles to broader practical implementation of concrete reuse. The authors sought to address this obstacle by analysing the current state of the art in reusable slab connections. Based on the analysis of available literature, the following conclusions regarding slab connections can be made:

– The proposed connection solutions between slab segments and slab-to-beam connections were mostly presented on the conceptual design level, with only a few experimental tests of the connection [28], or joints [26] [27] [32].

– Proposed solutions were mostly bolted connections made with threaded bars or bolts and steel plates or angles.

– All analysed connection solutions were dry connections that can be demounted, but the majority of studies did not validate the easy reusability of connected elements.

– Experimental tests in available literature showed that the bearing capacity and stiffness of dry reusable mid-slab bolted connections and bolted connections between concrete blocks [21], [32] are generally lower compared to the monolithic slab.

– Experimental testing of slab-to-beam connections using steel boxes, channels and bolts [34]–[36] showed that the ultimate shear capacity and initial stiffness decrease by about 5–20% after testing in the second life cycle, confirming that reuse should be validated through testing in both the first and at least the second life cycle.

– Reusable semi-dry connections for monolithic slab segments can be designed with bolts, steel plates, and angles, but no experimental validation is available in current literature.

The review of existing literature on slab-to-slab and slab-to-beam connections designed for reusability indicates a clear lack of systematic research in this area. Future studies should primarily focus on establishing a robust methodology for validating reusability. At present, the conditions under which slab elements can be safely reused remain insufficiently defined, as does their structural performance during a second life cycle, particularly under seismic loading. Furthermore, the stiffness of concrete slabs with reusable connections represents a critical parameter influencing the global structural response and therefore requires comprehensive and systematic investigation.

Acknowledgements

The authors would like to express their gratitude to the CircBoost – Boosting Circular Economy in Construction Industry, funded by the European Union under the Horizon Europe research and innovation programme (Grant Agreement No. 101082068) and Ministry for Education,

Science, and Technology, Republic of Serbia (Grant number 200092).

CRediT authorship contribution statement

Jelena Carević: Conceptualization, Methodology, Data curation, Visualization, Writing - original draft, Writing - review & editing.

Ivan Milićević: Conceptualization, Methodology, Writing - review & editing.

Milica Vidović: Visualization, Writing - review & editing.

Declaration of competing interest

The authors declare that they have no known competing financial interests or personal relationships that could have appeared to influence the work reported in this paper.

References

[1] L. Valentini, "Sustainable sourcing of raw materials for the built environment," *Mater. Today Proc.*, vol. 121, no. May 2023, pp. 427–430, 2023, doi: 10.1016/j.matpr.2023.07.308.

[2] A. Favier, C. De Wolf, K. Scrivener, and G. Habert, "A sustainable future for the European Cement and Concrete Industry Technology assessment for full decarbonisation of the industry by 2050," 2018, doi.org/10.3929/ethz-a-010025751

[3] C. Carroll, Y. A. de Souza, E. Salter, R. Hunziker, L. De Giovanetti, and V. Contucci, "Net-zero buildings: Where do we stand ?," 2021.

[4] C. Montano-Owen and J. Costa, "Creating local economies with complete cycling of concrete," 2025.

[5] J. Devènes, M. Bastien-Masse, and C. Fivet, "Reusability assessment of reinforced concrete components prior to deconstruction from obsolete buildings," *J. Build. Eng.*, vol. 84, no. June 2023, p. 108584, 2024, doi: 10.1016/j.jobe.2024.108584.

[6] I. Bertin, M. Saadé, R. Le Roy, J. M. Jaeger, and A. Feraille, "Environmental impacts of Design for Reuse practices in the building sector," *J. Clean. Prod.*, vol. 349, no. February, 2022, doi: 10.1016/j.jclepro.2022.131228.

[7] A. Parezanović, A. Nadaždi, D. Isailović, N. Višnjevac, and Z. Petojević, "Mapping the urban building stock for a circular economy by integrating GIS and BIM. A case study from Belgrade, Serbia," *Resour. Conserv. Recycl.*, vol. 215, no. November 2024, 2025, doi: 10.1016/j.resconrec.2024.108075.

[8] Z. Al-Faesly, "Feasibility of Reuse in the Concrete Industry," University of Ottawa, 2021.

[9] T. M. Fayyad and A. F. Abdalqader, "Demountable reinforced concrete structures : A review and future directions," *Civ. Eng. Res. Irel. 2020 Demountable*, pp. 218–222, 2020.

[10] *fib bulletin 43, Structural Connection for Precast Concrete Buildings*, International Federation for Structural Concrete, Lausanne, 2008. doi.org/10.35789/fib.BULL.0043.

[11] W. Zhao, S. Liang, R. Pang, X. Zhu, and Z. Zhou, "Experimental and numerical investigation on tension behavior of innovative untopped diaphragm connections," *Structures*, vol. 60, no. January, 2024, doi: 10.1016/j.istruc.2024.105892.

[12] R. Pang, Z. Xu, S. Liang, X. Zhu, and K. Hu, "Experimental and analytical investigation on the in-plane mechanical property of discretely connected precast RC floor diaphragm," *J. Build. Eng.*, vol. 32, no. September 2020, p. 101819, 2020, doi: 10.1016/j.jobe.2020.101819.

[13] R. Pang *et al.*, "Vibration behavior of innovative discretely connected precast concrete sandwich floors," *J. Build. Eng.*, vol. 82, no. March 2023, p. 108313, 2024, doi: 10.1016/j.jobe.2023.108313.

[14] H. Li and W. Zhou, "Behavior of new types of flange connectors of precast double-tees," *Struct. Des. Tall Spec. Build.*, vol. 31, no. 6, pp. 21–24, 2022, doi: 10.1002/tal.1922.

[15] R. Pang, C. Gao, X. Gao, Y. Sun, Z. Xu, and K. Xu, "Shaking table test and numerical analysis of an innovative precast reinforced concrete building structure," *J. Build. Eng.*, vol. 77, no. April, 2023.

[16] R. B. Fleischman, J. Restrepo, S. K. Ghosh, C. J. Naito, and R. Sause, "Seismic design methodology for precast concrete diaphragms part 1: Design framework," *PCI J.*, vol. 50, no. 5, pp. 68–83, 2005.

[17] ACI Committee 318, *Building Code Requirements for Structural Concrete: ACI 318-19*. American Concrete Institute, 2019.

[18] ACI-ASCE Committee 550, *Code Requirements for the Design of Precast Concrete Diaphragms for Earthquake Motions: ACI 550.5M-18*. American Concrete Institute, 2018.

[19] European Committee for Standardization, *Eurocode 8: Design of structures for earthquake resistance — Part 1: General rules, seismic actions and rules for buildings*. 2015.

[20] N. Widmer, M. Bastien-Masse, and C. Fivet, "Building structures made of reused cut reinforced concrete slabs and walls : A case study," in *Proceedings of The Eighth International Symposium on Life-Cycle Civil Engineering (IALCCE 2023), 2-6 July, 2023, Politecnico Di Milano, Milan, Italy*, 2023, pp. 172–179.

[21] H. W. Reinhardt, "Demountable concrete structures - an energy and material saving building concept," *Int. J. Sustain. Mater. Struct. Syst.*, vol. 1, no. 1, p. 18, 2012, doi: 10.1504/ijsmss.2012.050452.

[22] K. van Dijk, P. Boedianto, and A. Kowalczyk, "State of the Art Deconstruction in the Netherlands," *Overv. Deconstruction Sel. Ctries.*, p.95-143, 2000, [Online]. Available: http://www.irbnet.de/daten/iconda/CIB444.pdf.

[23] P. K. Aninthaneni and R. P. Dhakal, "Demountable Precast Concrete Frame–Building System for Seismic Regions: Conceptual Development," *J. Archit. Eng.*, vol. 23, no. 4, pp. 1–10, 2017, doi: 10.1061/(asce)ae.1943-5568.0000275.

[24] P. K. Aninthaneni and R. P. Dhakal, "Environment-friendly Demountable Precast Concrete Frame Building System for Minimization of Seismic Downtime," *16th Symp. Earthq. Eng.*, no. December, pp. 20–22, 2018.

[25] R. P. Aninthaneni, P. K. and Dhakal, "Demountable precast RC frame building system for seismic regions," in *Proceedings of the International Conference on Earthquake Engineering and Seismology (IZIIS-50), New Zealand*, 2016.

[26] H. Almahmood, A. Ashour, D. Figueira, and G. Yıldırım, "Tests of demountable reinforced concrete slabs," *Structures*, vol. 46, no. October, pp. 1084–1104, 2022, doi: 10.1016/j.istruc.2022.10.097.

[27] A. Ashour, D. Figueira, H. Almahmood, G. Yıldırım, A. Aldemir, and M. Şahmaran, "Demountable Reinforced Concrete Structures - A Way Forward to Minimize Energy and Waste in Construction Industry," *Lect. Notes Civ. Eng.*, vol. 349, pp. 72–80, 2023, doi:

10.1007/978-3-031-32519-9_6.

[28] P. Chen, J. Guo, and T. Chan, "Thin-Walled Structures Experimental and analytical investigation on the shear behaviour of a demountable interlocking connection applied in precast floor diaphragms," *Thin-Walled Struct.*, vol. 208, no. October 2024, p. 112696, 2025, doi: 10.1016/j.tws.2024.112696.

[29] G. Cai, F. Xiong, Y. Xu, A. S. Larbi, Y. Lu, and M. Yoshizawa, "A Demountable connection for low-rise precast concrete structures with DfD for construction sustainability-A preliminary test under cyclic loads," *Sustain.*, vol. 11, no. 13, 2019, doi: 10.3390/su11133696.

[30] S. Akduman, R. Aktepe, A. Aldemir, E. Ozcelikci, B. Alam, and M. Sahmaran, "Opportunities and challenges in constructing a demountable precast building using C&D waste-based geopolymer concrete: A case study in Türkiye," *J. Clean. Prod.*, vol. 434, Jan. 2024, doi: 10.1016/j.jclepro.2023.139976.

[31] R. Zhang, T. Guo, and A. Li, "Thin-Walled Structures Experimental investigation into demountable dry connections for fully precast frame structures through shaking table tests," *Thin-Walled Struct.*, vol. 201, p. 112014, 2024, doi: 10.1016/j.tws.2024.112014.

[32] A. Baghdadi, L. Ledderose, and H. Kloft, "Bolted steel plates for rigidly connecting decks to beams in precast concrete flooring systems," *Structures*, vol. 81, no. July, p. 110004, 2025, doi: 10.1016/j.istruc.2025.110004.

[33] A. Scalbi, M. van Mierlo, T. Lambrechts, M. Vullings, and S. Wijete, "Steel cylinder connectors for reversible precast concrete floors: the CCN case study," in *Circularity in the Built Environment: Proceedings of the 2025 conference*, 2025, vol. 6, pp. 167–186.

[34] W. Li, W. Chen, H. Jiang, and H. Su, "Flexural Behavior of Concrete Beam and Slab with Novel Demountable Connectors," *Buildings*, vol. 15, p. 2776, 2025, doi: 10.3390/buildings15152776.

[35] W. Li, W. Chen, X. Lin, L. Chen, H. Lv, and K. Shao, "Cyclic behavior and damage mechanisms of a demountable RC joint : Integrated experimental and analytical study," *Structures*, vol. 79, p. 109609, 2025, doi: 10.1016/j.istruc.2025.109609.

[36] W. Li *et al.*, "Experimental and numerical study on behavior of demountable shear connectors in sustainable reinforced concrete beam-slab," *Constr. Build. Mater.*, vol. 445, no. April, p. 137918, 2024, doi: 10.1016/j.conbuildmat.2024.137918.

[37] CEN/TC 250, *Eurocode 4: Design of composite steel and concrete structures — Part 1-1: General rules and rules for buildings*. European Committee for Standardization, 2004.

[38] P. S. Halding, "Design for Disassembly of Concrete Slabs with Mortar Joints", Buildings, 13(8), 1957, 2023, doi.org/10.3390/buildings13081957.

[39] C. Küpfer, N. Bertola, and C. Fivet, "Reuse of cut concrete slabs in new buildings for circular ultra-low-carbon floor designs," *J. Clean. Prod.*, vol. 448, 141566, 2024, doi: 10.1016/j.jclepro.2024.141566.

[40] J. Devènes, J. Brütting, C. Küpfer, M. Bastien-Masse, and C. Fivet, "Re:Crete – Reuse of concrete blocks from cast-in-place building to arch footbridge," *Structures*, vol. 43, no. February, pp. 1854–1867, 2022, doi: 10.1016/j.istruc.2022.07.012.

[41] C. Küpfer, M. Bastien-Masse, J. Devènes, and C. Fivet, "Environmental and economic analysis of new construction techniques reusing existing concrete elements: two case studies," *IOP Conf. Ser. Earth Environ. Sci.*, vol. 1078, no. 1, 2022, doi: 10.1088/1755-1315/1078/1/012013.

Građevinski materijali i konstrukcije
Building Materials and Structures
journal homepage: www.buildingmaterialsstructures.com

https://doi.org/10.5937/GRMK2600016V UDK: 624.012.45:624.072.2

Review paper

Demountable connections for structural concrete reusability - State of the art and future directions for reinforced concrete, Part II: precast frames

Vidović Milica[*1)], Milićević Ivan[1)], Carević Jelena[1)]

[1)] *University of Belgrade, Faculty of Civil Engineering, Bulevar kralja Aleksandra 73, 11000 Belgrade, Serbia*

Article history
Received: 20 May 2026
Received in revised form: 28 May 2026
Accepted: 29 May 2026
Available online: 12 June 2026

Keywords
precast structures,
dry and semi-dry joints,
demountable connections,
reusability,
frame structures,
sustainable structures

ABSTRACT

This paper presents a comprehensive review of demountable connections in precast concrete frame structures, as a key strategy for the potential reuse of structural elements. The focus is placed on dry and semi-dry joints, which allow relatively simple assembly and disassembly. The paper systematically examines connection solutions for beam-to-column joints, column-to-foundation joints, and column-to-column joints, describing their mechanical devices, force-transfer mechanisms, and typical failure modes. The proposed solutions differ in complexity, construction time, and the amount of steel components used. The review shows that, in certain cases, fully demountable precast joints can achieve adequate resistance and performance comparable to monolithic joints. The most connection solutions demonstrated limited reuse possibilities of precast elements. Only a few studies have experimentally investigated the behaviour of joints in the second life cycle of fully reused precast elements, comparable to that of original joints. Although significant effort was made to identify optimal solutions, their widespread implementation in construction practice will require comprehensive experimental and numerical research focusing on repeated assembly–disassembly cycles and system-level behaviour, as well as their integration into design standards and practical guidelines.

1 Introduction

Reinforced concrete (RC) frames play a major role in RC building structures, forming part of both the gravity-load-resisting and lateral-load-resisting systems. They comprise beams (with or without slabs), columns and beam-to-column joints. The RC frames are most commonly designed and constructed as cast-in-situ (monolithic) moment-resisting frames, capable of resisting the combinations of bending moments, shear forces and axial forces. In this regard, the reliable behaviour of columns and beams at the joint locations, as well as the behaviour of the beam-to-column joints themselves, is of paramount importance for the adequate performance of RC frames under gravity and lateral loads, such as wind and design earthquake loads. For the earthquake events, RC frames acting as a main seismic-load-resisting system are designed as "Strong-Column/Weak-Beam" systems, i.e., with the RC columns that have bending resistance (with axial forces) significantly higher than adjacent RC beams (20-30%, depending on the seismic design code). In this manner, the reliable beam-sway mechanism is provided by forming plastic hinges at the base of the columns and at ends of beams. The beam-to-column joints are often subjected to high stresses under seismic action, and are primarily designed to remain elastic, with sufficient strength and stiffness to ensure the required degree of restraint in the RC frames.

The construction industry is increasingly focused on reducing its environmental impact through circular economy principles – reduce, recycle and reuse, including design for deconstruction of reinforced concrete structures [1-5]. At the end of service life, or when irreparable damage occurs to the monolithic RC frames after the main earthquake event, most columns and beams in RC frame buildings are demolished and the usual sustainable solution is to recycle them. Although reuse of existing monolithic RC elements has the potential to reduce waste generation, greenhouse gas emissions, and consumption of raw materials, its practical implementation remains limited due to technical, regulatory, and market-related barriers [6], [7].

The reinforced concrete frames can also be designed and constructed as precast concrete elements to primarily reduce the construction time. In terms of sustainability, apart from recycling, precast RC frames also have great potential for disassembly, replacement, and even the reuse of columns and beams at the end of their service life.

Based on the broader context of circular construction and reusable precast concrete systems discussed in Part I of this study [8], this paper focuses on demountable connections in precast concrete frame structures. The design of slab-to-slab

[*] Corresponding author:
E-mail address: milica@imk.grf.bg.ac.rs

and slab-to-beam connections is primarily governed by serviceability demands, gravity load transfer and rigid diaphragm requirements [8]. On the other hand, beam-to-column, column-to-column, and column-to-foundation joints represent the critical load-bearing regions of precast frame systems. These connections must ensure reliable transfer of axial forces, bending moments, and shear forces while simultaneously providing adequate stiffness, strength, and ductility. In seismic regions, their role becomes even more significant, as the connection detailing directly influences energy dissipation, plastic hinge formation, residual deformations, and the overall structural response. Therefore, recent research is focused on the development of demountable dry and semi-dry connections that enable easier assembly, disassembly, and reuse of precast elements while maintaining adequate structural performance [9].

The aim of this study is to critically review demountable dry or semi-dry beam-to-column, column-to-foundation, and column-to-column connections from the available literature. The discussion includes not only the load-bearing capacity, stiffness, deformation capacity and energy dissipation of connections and joints but also their assembly and disassembly characteristics, as well as their potential for replacement and reuse beams, columns, foundations and connections.

2 Beam-to-column connections

According to the Fédération Internationale du Béton [10], precast RC frame systems can generally be divided into two major categories, depending on the type and design of the connections between beams and columns: “equivalent monolithic” systems and “jointed” systems. In the former, wet joints are commonly used and are designed and constructed to be equivalent to those in monolithic structures (cast-in-place emulation). Regarding disassembly, replacement and reuse, this type of precast RC frame system has similar drawbacks to actual cast-in-place RC frame structures. In “jointed” systems, dry or semi-dry connections are used. In general, the connections can be formed in two ways: (1) by welding or bolting reinforcing bars, using plates or steel embedments, with dry-packing or local grouting, or (2) utilising unbonded post-tensioned tendons or rods. However, jointed systems are generally considered not to fully emulate the performance of cast-in-place RC frames, although the ductility of the connections can be achieved to some extent.

According to Eurocode 8 [11], the connections in precast concrete structures under earthquake action can be divided into three major categories, regarding their resistance and ductility:

- Connections located well outside critical regions, which do not affect the energy dissipation capacity of the structure;
- Overdesigned connections located within critical regions, but adequately designed for strength based on capacity design rules with respect to the rest of the structure, so that they remain elastic while plastic hinging is shifted outside the connection;
- Connections located within critical regions with substantial ductility.

The choice of the connection category can significantly impact primarily the overall behaviour of the joint under seismic action, and its potential for disassembly, replacement and reuse. In general, the similar categorisation of connections can be applied for gravity loads and wind loads as well, depending on their strength and the location along the beam’s length.

Over the past decades, many different configurations of dry and semi-dry beam-to-column connections with anchor bolts, rods and couplers, were experimentally and numerically studied, either as pinned connections with dowels [12], [13], or as moment resisting (semi-rigid or rigid/fixed) connections [14-16]. The main objective was to gain insight into the cyclic performance of the beam-to-column joints and, in case of moment resisting connections, to achieve the emulation of monolithic beam-to-column joints. However, in general, a little to none consideration on the disassembly of the precast elements was paid.

In the following subsections, the review of the latest research on dry and semi-dry precast beam-to-column joints is presented, which mainly employ mechanical fasteners and connectors, with or without steel plates. However, the joints which include welding of reinforcement with partial grouting, different kinds of dissipative or replaceable devices, as well as innovative post-tensioned connections are also covered. The focus is placed on moment resisting joints.

2.1 Connections with RC corbels

Precast RC columns can be constructed with RC corbels, which are used for supporting precast RC beams (resist shear forces) and to simplify the assembly process during the construction. Traditionally, the beams are simply supported via corbels, i.e., hinged/pinned connections with dowels are usually employed. However, this type of connection can also be designed as moment resistant connection, if appropriate mechanical connectors for continuity of longitudinal reinforcement or anchor bolts are used.

Bournas et al. [17] and Negro et al. [18] have investigated the behaviour of a full-scale three-storey precast RC structure consisting of dapped-end beams and columns with RC corbels, by subjecting the structure to a series of pseudo-dynamic (PsD) experimental tests. As stated by the authors, the dry connections were used because of quick erection, easy maintenance and possible reuse. Two types of dry beam-to-column connections were examined – nominally pinned and moment connections, for two different prototypes of the building. The layout of the connections is presented in Figure 1. The dimensions of wide RC beams were b_b/h_b = 2250/400 mm, while the dimensions of RC columns were b_c/h_c = 500/500 mm, with 2250 mm wide corbels (“capitals”).

For the first prototype of the building, nominally pinned connections were used and, therefore, the columns were expected to work as cantilevers. The connections were realized via two dowels per connection with variable diameter along their length which were protruding from the corbels, as shown in Figure 1 a). The dowels were screwed into anchors at the bottom of steel sleeves in the column corbels. Steel pads were placed between the column corbels and the dapped-end of beams in order to enable relative rotations between the elements. After the seating of the dapped-end beams on the corbels was ensured, the sleeves were filled with a fine non-shrinking grout, while the connection was completed by using top anchoring plates, washers and nuts. The increased diameter of dowels was used to resist high shear demands at the beam-to-column connection (top of the corbel) as a result of their design as “strong” (overdesigned) connections for seismic loads, while the steel anchoring plates were used to resist uplifting forces due to possible overturning. After the testing of the first

prototype, it was concluded that the dowels had sufficient strength to resist high shear forces with small damage, albeit high overall flexibility of structure with cantilever columns and corresponding large displacements. Compared to the reduced shear forces divided by the behaviour factor, the increase of shear forces acting on the dowels can be substantial.

The second prototype of the building was formed from the first prototype, with the activation of the previously embedded, dry mechanical connections, which were supposed to emulate moment (fixed) beam-to-column joints, as shown in Figure 1 b). These connections were provided in order to ensure the continuity of the longitudinal reinforcement crossing the joint, and were considered as ductile connections. Two thick steel plates, used to anchor the two longitudinal rebars with enlarged ends (rivets), were embedded at the top and bottom of ends of the dapped-end beams and corbels. The connection was realized with demountable bolts. In total, four longitudinal rebars at the bottom and four rebars at the top of the connections were continued through the joint. At the joint interfaces between corbel and the beam, the small gaps (approximately 10–15 mm) were filled by a mortar, albeit the control of grouting execution was not possible (grouting was not identical at all joints). It should be emphasized that the holes used for the connecting bolts were not grouted (see Figure 1 b)). During the testing, it was noted by the authors that the emulative joints experienced inelastic behaviour and concrete cracking; however, the strength of the connection was not reached since the plastic hinging was formed at the base of the columns well before the maximum capacity of the connections was reached. Although the beam-to-column joint slip was reduced dramatically in the case of moment resisting joints compared to the pinned joints, the emulative beam-to-column joint response was quite different from a rigid joint and was classified as semi-rigid beam-to-column joint.

After the testing, it seems that the structural elements were disassembled without any major destruction methods, although Bournas et al. [17] have used the term “demolition” in the presented research. The possibility of replacement or reuse was not discussed in the paper. However, since the significant damage of beam-to-column joints was not reached (except for cracking of the beams) even for high peak ground acceleration (0.3g and 0.4g), there was a considerable potential for replacement and possible reuse of beams and columns with this type of connection, especially in low and moderate seismic regions.

Zhong et al. [19] have proposed similar dry bolted connection for moment beam-to-column joints, subjected to cyclic load. The cross-sectional dimensions of the beam were b_b/h_b = 250/400 mm, while the dimensions of the column were b_c/h_c = 450/450 mm. The proposed connection consists of anchoring steel plates with welded longitudinal reinforcement, embedded in dapped-end precast beam and longer corbel (protruding beam) from RC column, with the length smaller than the depth of the beam. Steel plates are connected with demountable bolts. The gaps between steel plates, as well as at beam and column corbel, were filled with rubber layers (cushions). In addition, between the plates and bolts, flexible gaskets (i.e., rubber washers) were provided. The authors have stated that rubber layers were used in order to make a well-distributed contact and prevent any leakage of moisture from the external environment. The rubber washers were used in order to adjust (decrease) the stiffness of RC beams, i.e., to achieve “strong column-weak beam” design concept. Although the authors have indicated that this type of connection can be used for beam-to-column joint with precast slab, only the specimens which simulate the monolithic RC floor slab system with the upper concrete layer cast in-situ were experimentally tested. Therefore, the bolted connectors were only installed at the bottom of the joint, and the vertical dowel protruding from the corbel was not installed.

The cyclic test results have shown that the presented precast solution has similar strength and deformation capacity as monolithic specimen, with lower dissipation energy and approximately 60% lower stiffness. Thus, the joints were classified as semi-rigid. The major damage was concentrated at the connection, while significant cracking of the beam appeared both at sections between the connection and column face and outside the connection (away from the column).

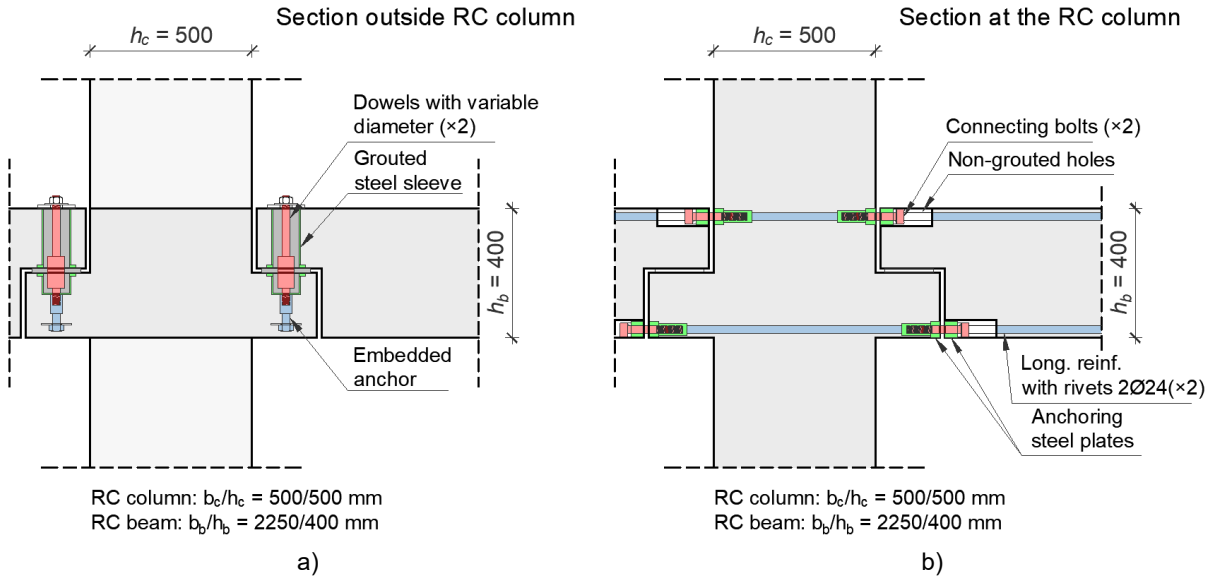

Figure 1. Beam-to-column joints with dapped-end beam: a) pinned connection with dowels, b) moment connection with thick steel plates, longitudinal reinforcement with enlarged ends and demountable bolts (adapted from [17] and [18])

Regarding the disassembly possibilities of the proposed connection, Zhong et al. [19] have concluded that the connectors, such as bolts and flexible layers, were easy to remove after testing. In other words, tested precast specimens showed the advantages of detachable precast specimens after the structure was damaged by an earthquake. However, no discussion of the possibilities of replacement nor reuse was provided in the presented research, and can be considered as low since the major damage occurred in the connection, with significant cracking in beam and protruding corbel.

Ding et al. [20] have conducted experimental cyclic tests on the precast beam-to-column joint with dry connection realized with through anchor bolts presented in Figure 2 a). The joint comprised RC column with dimensions b_c/h_c = 750/750 mm with RC corbel, and T-end RC beam with general dimensions b_b/h_b = 400/750 mm and dimensions $b_{b,T}/h_{b,T}$ = 750/750 mm at the end of the beam. At the back of the T-end beam, the steel pressure plate was provided. Similarly, the pressure plate was embedded in the back of the RC column. After the seating of the beam on the RC corbel was ensured, the connection was realized by eight through bolts M30, inserted in the non-grouted holes, which ensured that anchor bolts were unbonded. However, the 25 mm gap between RC beam and column was grouted. The through anchor bolts were ultimately pretensioned, while the grade of the bolts was varied.

The cyclic test results have shown that failure was attained with severe damage of T-end of the precast beam, with cracks on the steel end plate and the rupture of through anchor bolts at the upper side. The column was not damaged. The joint was classified as semi-rigid, although no comparison with monolithic companion was provided.

Ding et al. [20] have stated that the proposed solution of the dry connection for beam-to-column joint is suitable for post-disaster repair works, by replacing the through anchor bolts as the main load-bearing components (ductile connection), which greatly reduces the repair time and work cost of the joint components. Although it seems from the presented research that the RC column has strong potential for reuse, the repeated testing of the connection with the replaced through bolts should be conducted in order to confirm the adequacy of the RC beam for reuse.

Liu et al. [21] have conducted experimental cyclic tests on the precast beam-to-column joint, which was almost the same as it was analysed by Ding et al. [20], as shown in Figure 2 a). The main difference was that instead of the back plates without stiffeners, the haunched steel end plate (steel angles with stiffeners) was used. In addition, pressure steel plates were placed at the beam's end and RC column, at their interface. Although overall dimensions were the same as tested by Ding et al. [20], different diameter of reinforcement as well as diameters and grade of through bolts were used. Albeit the failure modes were the quite similar, the aforementioned differences led to the increase of the joint strength. The same conclusions regarding the post-earthquake repairment possibilities were drawn as highlighted by Ding et al. [20].

Krishnan and Purushothaman [22] have conducted cyclic test on one-third scaled model of semi-dry connection for beam-to-column joints, as presented in Figure 2 b). The proposed connection consists of precast RC beam (b_b/h_b = 100/120 mm) and column (b_c/h_c = 100/120 mm), steel cleat angle, unbonded vertical and horizontal dissipaters (through anchor rods) and dowel bar protruding from RC corbel. A channel section with steel duct was placed at the beam end. After the seating of the RC beam on the bearing plate at the top of the corbel was ensured, the hole for dowel bar was grouted. Afterwards, the cleat angle was placed, the unbonded anchor rods were inserted and clamped with nuts. The aim of this connection is that the anchor rods are used as dissipaters, i.e., for interaction and dissipation of energy in the connection as a sacrificial fuse (ductile connection). Therefore, their diameter was reduced along the major part of their length. The dowel bar was used for additional anchorage and prevention of the unseating of the beam in case of vertical dissipator failure. A channel section at beam's end was used to prevent concrete damage at the end of the beam. Krishnan and Purushothaman [22] adopted this concept in order to improve previous similar solutions [23], without dowel bar and channel section, which exhibited severe damage of beam's end and corbel. Furthermore, geopolymer concrete with recycled concrete aggregate (GCRCA) was used for RC elements, in order to supplement sustainable precast construction.

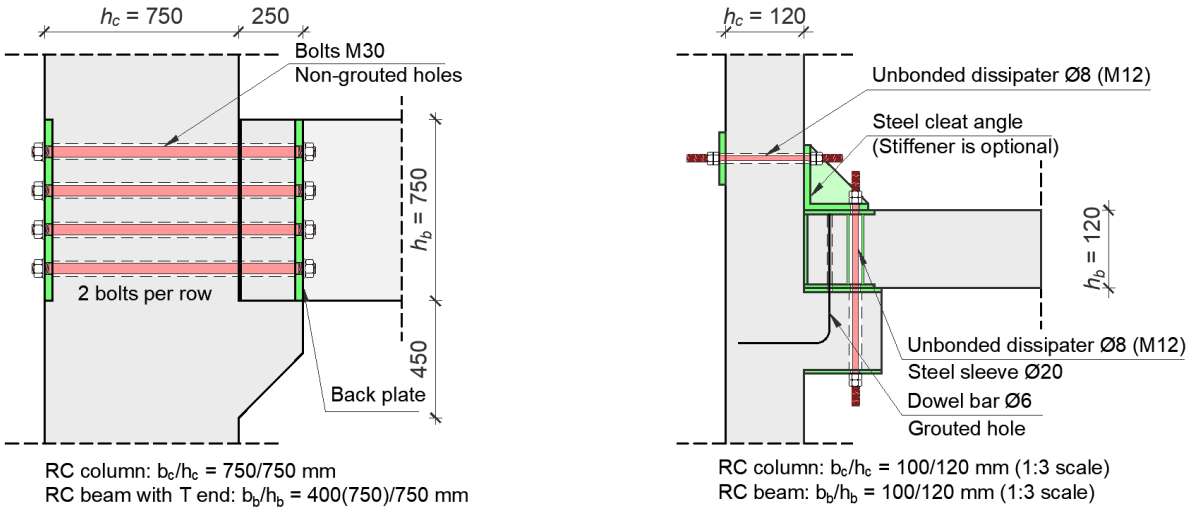

Figure 2. Beam-to-column joints with RC corbels and through bolts: a) adapted from Ding et al. [20], b) adapted from Krishnan and Purushothaman [22]

The specimens with and without stiffeners on the cleat angles were tested under cyclic loads and compared to the equivalent, fully cast-in-situ (monolithic) specimen. Only the connections with stiffeners exhibited dissipater failure (shear/tension) with mainly flexural cracks at the beam end. The RC columns remained undamaged. In all cases, precast specimens had almost the same or higher strength than the monolithic specimen. However, other seismic performance indicators were lower than for the monolithic specimen (e.g., ductility, secant stiffness, energy dissipation, etc.). Therefore, the proposed connection could be classified as semi-rigid and was recommended mainly for low seismicity regions and, in some cases, for moderate seismicity regions.

Krishnan and Purushothaman [22] have stated that both the concept of minimal structural damage and easily demountable precast systems can be achieved in proposed precast beam-to-column connection with single stiffener and unbonded dissipators. The demountability alone seems possible for all tested configurations of the connection, albeit dowel bar was in fact grouted. However, the replacement and reuse possibilities were not discussed in the paper. The RC column did not experience cracking nor damage and, therefore, there is a potential for its reuse. The possibility for reuse of RC beam should be examined in further research.

2.2 Connections with steel boxes or shoes embedded in beam

In order to simplify the construction of precast beam-to-column joints with dry connections, by excluding the necessity of temporary supports and complicated formwork, as well as to enable easier disassembly of the joint and replacement of the damaged parts of the connection, a few solutions with steel boxes and shoes embedded in beam were proposed.

Zhang et al. [24] have conducted experimental research on the dry connections realised with steel top connector and steel concealed corbel, as shown in Figure 3 a). Both of them are designed as steel boxes opened on the one side, top and bottom, respectively. A rectangular shear groove is left at the column interior face, corresponding to the concealed corbel, with bottom threaded anchor rods embedded in the column which extend out of the shear groove. After the concealed corbel is attached to the column by means of washers and nuts, the beam with the notch corresponding to the rest of the concealed corbel can be placed. At the bottom of the beam, threaded couplers (“screwed sleeves”) with the threaded anchor rods are previously embedded. The bottom connection is realised by inserting and tightening the connecting bolts. At the top of the beam, the steel box connector is embedded, with long threaded anchor rods plug welded to it. In RC column, threaded couplers and anchor rods are previously embedded. The top connection is realised by inserting and tightening the connecting bolts. Boxes were not grouted.

The specimen was tested under cyclic load and compared to the equivalent, fully monolithic specimen. The results have shown that the precast joint had 40% lower initial stiffness than cast-in-situ joint and, therefore, the connection can be classified as semi-rigid. The strength of the precast joint had the same or higher resistance than cast-in-situ joint, depending on the load direction (higher resistance is achieved when bottom side is compressed, due to concealed corbel). However, the energy dissipation and displacement ductility were smaller, since the majority of the inelastic deformations were concentrated in the connectors (top box and concealed corbel, as well as connecting bolts), while the beam outside the connection experienced cracking. Failure of precast joint occurred due to concrete damage at the bottom of the beam, at the location of concealed corbel. The column experienced some cracking, but remained without significant damage.

Zhang et al. [24] have stated that the proposed dry connection can concentrate the plastic damage on the steel connectors that are easy to replace, which could improve the recoverability of structural performance and building functions. However, due to high yielding strength, steel boxes cannot be used as damping devices and, therefore, the authors have recommended that the material of the boxes can be replaced with mild steel or the reduction of cross-sectional area can be implemented, in order to improve energy dissipation capacity of the joint. In the author’s opinion, further research is needed in order to establish the possibility for replacement and reuse of RC columns and beams. Since the columns remained elastic with slight cracking, the possibility for reuse is considerable.

Zhang et al. [25] have conducted experimental shaking table tests on 1/2-scale specimen of the precast concrete three-storey frame structure with fully demountable dry connections between all structural elements – slabs, beams, columns and foundations. The layout of the connection in beam-to-column joints was similar to the presented in Figure 3 a). The main difference was that all threaded anchor rods in RC beams were connected to steel box connector and concealed corbel by means of threaded couplers (or extended nuts). The same applies for the top connectors in RC column, while the bottom threaded rods were the same as shown in Figure 3 a). Furthermore, the longitudinal ribs in steel boxes were designed as energy-dissipation plates, made out of soft steel (ductile connection). The structure was designed with aim that the initial stiffnesses of steel box connectors in precast beam-to-column joints are equal to the elastic bending stiffnesses of cast-in-situ beam-column joints with the same cross-sections. The structure was designed to sustain peak ground acceleration (PGA) of 0.2g. The test results have shown that for PGA of 0.2g, cracks in the beams as well as relative sliding between steel box connectors and the beams occurred. For PGA of 0.4g, damage was mainly concentrated on the box connectors and the concrete of some beams (yielding of the beam reinforcement occurred), while the columns remained undamaged. The maximum storey drift was 0.166% for PGA of 0.07g (frequent earthquakes) and 0.935% for PGA of 0.4g (rare earthquakes). Apart from quick and relatively easy assembly of the structure with the proposed connections, Zhang et al. [25] have highlighted that damaged beams were easily removable and thus replaceable, which contributes to the structural sustainability in terms of seismic resistance. Since the columns remained elastic, the possibility for reuse is considerable.

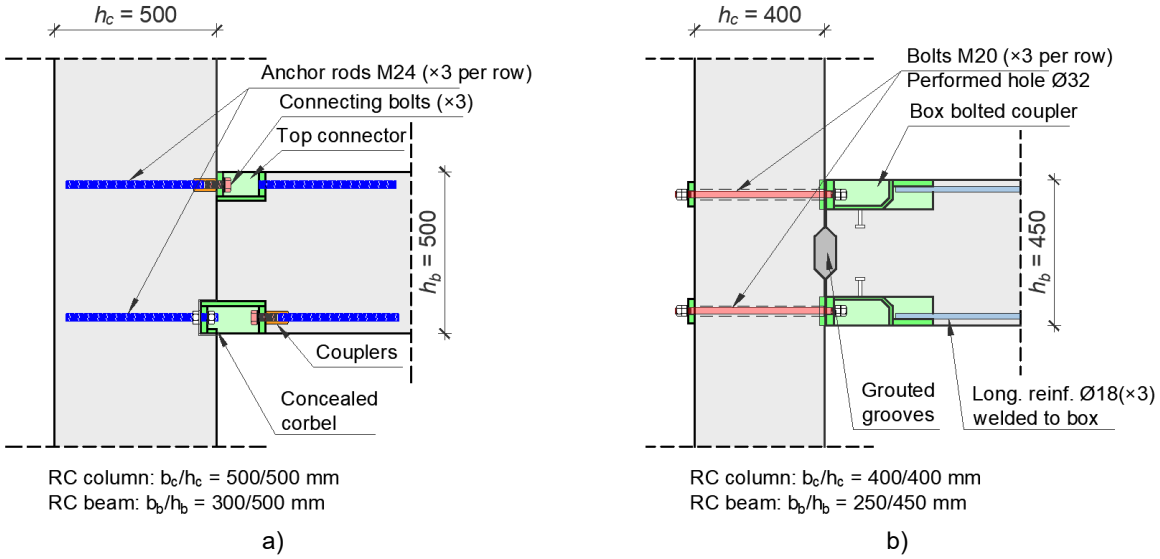

Figure 3. Beam-to-column joints with steel boxes: (a) connection with concealed corbel end threaded rods (adapted from Zhang et al. [24]), (b) connection with grouted grooves and through anchor bolts (adapted from Zhang et al. [26])

Zhang et al. [26] have proposed the alternative layout of beam-to-column connection with steel boxes, as presented in Figure 3 b). The top and bottom boxes are embedded in beam, with welded longitudinal reinforcement. The connection is realised by clamping and preloading horizontal through anchor bolts embedded in RC column. The shear key at beam-column interface was also provided, which was ultimately grouted. The basic concept was to use high strength bolts and boxes, in order to ensure that plastic hinges in the beams are formed away from the column face. Compared to the monolithic companion, the cyclic test results indicated that the proposed precast beam-to-column joint can achieve higher strength and similar secant stiffness, displacement ductility and cumulative energy dissipation. The possibilities for the disassembly, replacement and reuse were not discussed in the paper. However, due to nature of the connection that comprises embedded steel box with welded reinforcement and embedded anchors, it can be considered that the disassembly of the joint is possible while only the replacement of the beam and reuse of column after earthquakes can be considered reliable.

Liu et al. [27] have suggested that the demountable beam-to-column connection can be achieved by connecting steel shoes embedded in RC beam and mechanical couplers with rebar anchor embedded in RC column by demountable threaded bars, in a similar manner as it is usually done in column-to-foundation connections (see Section 3.2). It was argued that the connection can be achieved without using RC corbel; however, considering the effect of errors in elements' dimensions and installation on the construction, there is a certain gap between the contact plane of beam and column which can affect the shear resistance of the connectors. Therefore, the single shear tests on the single connectors were performed in direct shear and flexural shear conditions. It was demonstrated that in case of larger gaps between beam and column, the failure of couplers can occur. The simple method for prediction of shear resistance of the single connector with mechanical coupler in relation to the gap width was proposed.

2.3 Connections with steel end plates or steel angles

Although the solutions for demountable beam-to-column joints presented in previous subsections showed generally good performance in terms of strength and displacement capacity, with assured "strong column-weak beam" concept, most of them had lower stiffness and dissipation energy capacity than corresponding monolithic joints, which classifies them as semi-rigid with limited energy dissipation capacity. In order to improve these characteristics and the simplicity of demountable precast beam-to-column joints, a few research groups have conducted tests on the connections which employ steel end plates or steel angles, with demountable connecting bolts or through anchor bolts located outside beam cross-sectional dimensions.

Senturk et al. [28] have conducted experimental tests on precast beam-to-column joints realised by steel end plate with stiffeners embedded in beam and demountable bolts, as presented in Figure 4 a). Longitudinal reinforcement with rivet head (enlargement) at the end was inserted in the end plate. The extended nuts (couplers) were welded to the positioning steel plate and embedded in the precast column. In addition, the anchoring reinforcement was welded to embedded extended nuts. Different layouts of anchoring reinforcement in RC columns were examined. The connection is realised by connecting beam end plate to the column by inserting demountable bolts, which were pretensioned. The bolts and extended nuts were designed to remain in the elastic range (overdesigned connection).

The specimens were tested under cyclic load and compared to the equivalent, fully cast-in-situ (monolithic) specimen. The failure modes of precast joints were very similar to the failure modes of monolithic specimens, with considerably higher ductility, dissipation energy and ultimate deformation capacity while providing the same level of resistance and initial stiffness. Localized damage of the connection was also prevented by distributing the plastic deformations throughout the beam element. The columns remained undamaged. Therefore, it was stated that the design of the connection can be based on the traditional approaches.

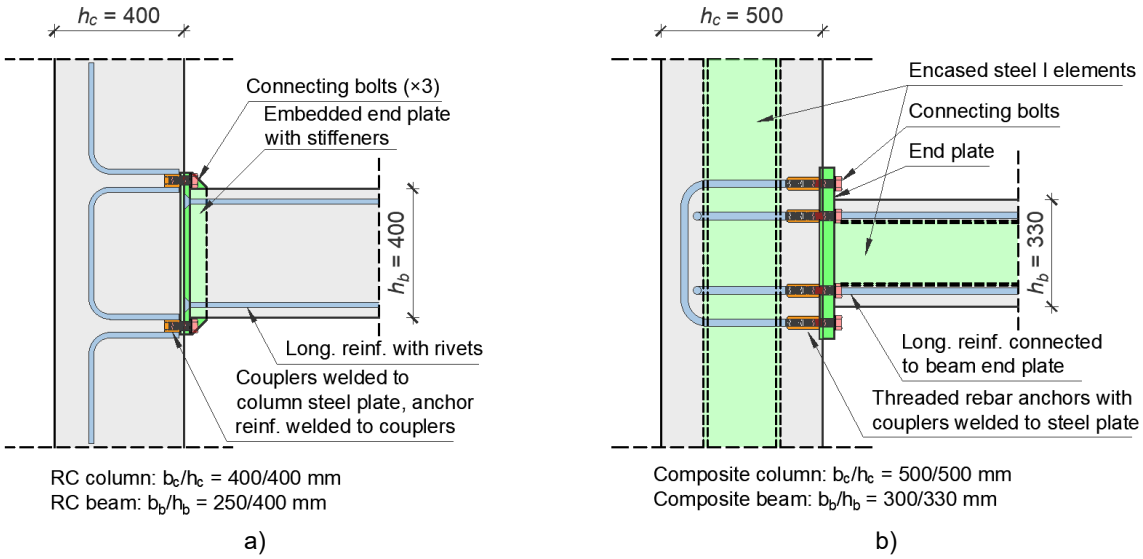

Figure 4. End plate connections in beam-to-column joints: (a) RC joint end plate and stiffeners (adapted from Senturk et al. [28]), (b) composite joint with extended end plate without stiffeners (adapted from Nzabonimpa et al. [29])

Senturk et al. [28] have stated that the developed bolted moment connection system for precast beam-column joints of RC frame structures in seismic regions, offers several advantages such as rapid assembly and disassembly, reusability, and replaceability if damaged during an earthquake event. It should be noted that the reuse possibilities relate solely to the RC column, while the reuse of the beams should be further tested.

Nzabonimpa et al. [29] have experimentally tested similar dry connection, with the use of extended end plate without stiffeners, in the composite precast beam-to-column joints, as shown in Figure 4 b). In precast beams and columns, steel elements with I-section were embedded. In the column, the threaded couplers were welded to the positioning steel plate, while anchoring was achieved with U-shaped reinforcement with threaded ends inserted in couplers. In composite beam, the steel element was welded to the end plate, while the type of connection between longitudinal reinforcement and end plate was varied (threaded ends with nuts, welded to plate). The connection is realised by inserting the demountable bolts in couplers. The same layout of the connection was proposed for the purely precast reinforced concrete joints, albeit this connection was not experimentally tested.

The specimens were tested under cyclic load and compared to the equivalent, fully cast-in-situ (monolithic) specimen of composite beam-to-column joint. The testing results showed that the best performance of the precast joint was exhibited when thick end plate is used (45 mm), with the similar overall behaviour as the monolithic joint, i.e., necking and fracture of the longitudinal reinforcement in the beam and without damage in column (overdesigned connection). The disassembly, replacement and reuse possibilities were not discussed in the paper. However, in the authors' opinion, the similar conclusions can be drawn as it was done by Senturk et al. [28].

It should be noted that the anchoring system in columns in the presented research, i.e., extended nuts and couplers with anchor reinforcement, provide relatively simple disassembly process and reuse of the column and embedded connectors. In order to optimise these types of connections, a group of researchers from University of Belgrade have conducted studies on single connector embedded in precast concrete elements, subjected to pure tension and pure shear loads [30]- [33]. The guidelines for load-displacement behaviour of single anchor were provided, which can be used for estimation of the load-displacement behaviour and optimisation of precast beam-to-column joints.

Aninthaneni et al. [34] have conducted experimental tests on the emulative dry connections in beam-to-column joints, with steel end plate embedded in the beam and through anchor bolts (rods), as shown in Figure 5 a). The cross-sectional dimensions of the beam were b_b/h_b = 350/400 mm, while the dimensions of the column were b_c/h_c = 700/600 mm. The end plate with vertical and horizontal stiffeners is embedded in the beam, with longitudinal reinforcement (25 mm in diameter) with bends welded to the end plate and anchored by passing through the slotted holes in horizontal stiffeners. In addition, two 25 mm diameter bent-up bars were also welded to the embedded plates to effectively transfer the shear force and relocate the plastic hinge to in front of the connection. The connection is realised by inserting through anchor bolts and clamping them with nuts to the steel plate at the back of the column. The anchor bolts were pretensioned. The larger lever arm of the through bolts and the use of the stiffeners was adopted in order to increase bending resistance and stiffness of the connection, which ensures that the connection remains rigid and elastic while the beam reaches its bending moment capacity (overdesigned connection).

Experimental cyclic tests were conducted on two specimens with the identical layout. In the first test, the joint was tested until the failure which occurred in the precast beam outside of the connection. Afterwards, the connection was disassembled and the beam was demounted. In the second test, the new beam was connected to the column which was used in the first test. The testing results of these two specimens showed that there was no significant difference between their behaviour, with the plastic hinging occurring in the beam outside the connection. It was demonstrated that the behaviour of the tested joint was the very much similar to the wet jointed/monolithic concrete beam-to-column joints. It was also demonstrated that the

tested end plate connection has better energy dissipation than the connection with some ductile connectors.

Aninthaneni et al. [34] have stated that the proposed dry beam-to-column connection is demountable, and that in the laboratory the damaged beam could be replaced with a new beam without much difficulty. More detailed discussion regarding the feasibility and replacement of the beams of building structures in real-life conditions is discussed by Aninthaneni and Dhakal [35]. If the damage in a demountable precast RC frame structure is restricted solely to the beams, the replacement of the damaged beams after earthquake with the identical new ones would result in a frame structure as it was before the damage. In other words, the reusability of the RC column was confirmed by test results in the presented research.

Li et al. [37] have conducted the cyclic tests on the embedded end plate connection similar to the one presented in Figure 5 a), with the aim to optimize the components of the connection. The cross-sectional dimensions of the beam were b_b/h_b = 200/500 mm, while the dimensions of the column were b_c/h_c = 400/400 mm, with the 620 mm distance between M24 through bolts. The main tested parameters were: thickness of end plate (16 mm and 20 mm), use of vertical stiffeners (with and without) and welding of longitudinal reinforcement to horizontal stiffeners (with and without). The bent-up bar with 12 mm in diameter were not welded to the horizontal stiffeners.

The specimens were tested under cyclic load and compared to the equivalent, fully cast-in-situ (monolithic) specimen. The results have shown that the final failure mode of precast concrete connections depended highly on the rotational stiffness of the connection. In case of thinner end plate without vertical stiffeners, the failure occurred in the end plate, with significantly lower resistance than obtained for monolithic specimen, but with better ductility. For thicker end plate with stiffeners, the crushing of concrete occurred in the beam, at the location of the connection, with increased moment capacity, but with decreased ductility. Li et al. [37] have highlighted the importance of the adequate detailing of beam reinforcement as well as the connection itself, in order to obtain adequate performance of the joint. Since the column and joint core remained intact, it was stated that it is possible to rapidly replace the damaged components after earthquake.

Aninthaneni et al. [36] have conducted cyclic experimental tests on the dry connection realised with steel angles with stiffeners, and horizontal and vertical through anchor bolts, as shown in Figure 5 b). Steel ducts were embedded in the beam and column, with corresponding reinforcement detailing, in order to enable the insertion of through anchor bolts and the connection with the steel angles. Bolts were pretensioned after the assembly of the joint. In addition to the presented layout (type 1 connection), the second layout (type 2 connection) with the embedded steel web plates in both beam and column, which are connected with the four bolts at the beam-to-column interface, was tested. It should be noted that the beam edge distance from the vertical anchor bolts was smaller than in case of type 1 connection. In both cases, natural rubber sheet or dental plaster were used to achieve good surface contact between the steel connection and the precast elements, since the precast elements' surfaces were not perfectly levelled and legs of steel angle were not exactly perpendicular.

The cyclic test results showed the type 1 connection has the similar resistance as predicted for cast-in-situ joint, with considerable displacement ductility. At the final stages of testing, the slip between the connection and the beam exceeded the clearance between the bolts and the ducts, and the bolts started to bear against the steel duct which induced bearing stress (i.e., bursting stress) into the concrete resulting bearing and direct tensile split vertical cracks, which ultimately passed through beam cross-section. In case of type 2 connection, similar behaviour was noticed, with significantly higher degree of concrete damage and spalling due to smaller edge distance of the vertical bolts, with minor cracking outside of the connection. However, the damaged beam was removed, repaired with high-early-strength grout, and reused in the subsequent test. Ultimately, the repaired specimen was able to reach the nominal strength of the cast-in-situ joint; however, significant strength degradation after 2.5% lateral drift was detected.

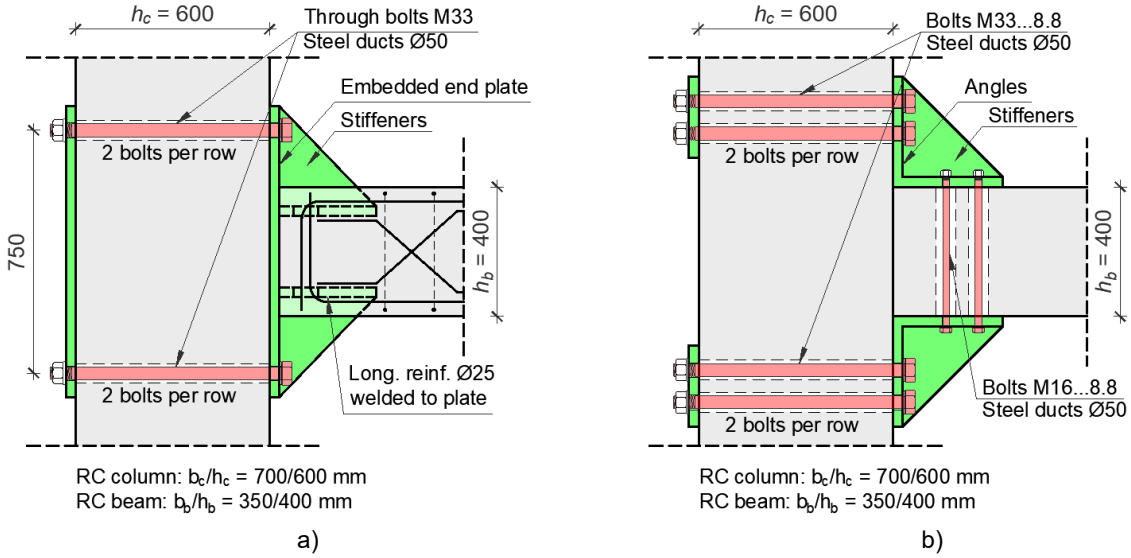

Figure 5. Moment beam-to-column connections with through bolts: a) connection with embedded steel end plate and stiffeners (adapted from Aninthaneni et al. [34]); b) connection with steel angles and stiffeners (adapted from Aninthaneni et al. [36])

Aninthaneni et al. [36] have stated that the precast elements can be demounted and that the undamaged components can be reused, while the damaged beams can be replaced with the new ones in a relatively short time.

2.4 Connections with steel dampers and fuses

In order to improve the shortcomings of previously presented connection solutions, in terms of reusability of all precast concrete elements, an effort was made by several research groups to investigate the possibility of using different steel (metallic) elements as damping devices and fuses – sacrificial elements to dissipate seismic energy. These steel elements would provide sufficient stiffness and damping simultaneously, while reducing the damage in the precast beams and columns (ductile connections). In addition, some of the proposed connections were oriented towards establishing detachable configurations, with aim not only to simplify the assembly and reduce construction time and costs, but also to provide the possibility of disassembly as well as replacement (repair) after earthquake events. It should be noted that the simplicity of the connection and manufacturing process, as well as the total amount of steel used in the connection vary between the proposed solutions.

Wu et al. [38] have experimentally tested the beam-to-column joint with demountable connection realised by steel damper, as shown in Figure 6 a). The metallic damper was composed from short "dog-bone" element (i.e., weakened I-section element, with gradually reduced flange width in the middle section by 50% compared to the full flange width), and thick end plates welded to the "dog bone" element. In precast beam, longitudinal reinforcement with threaded ends was placed in the positioning steel plate at the beam end, with threaded ends protruding from the beam. In the column, threaded couplers (sleeves) were welded to the positioning steel plate while U-shaped anchoring reinforcement with threaded ends was inserted into couplers. The connection is realised by firstly connecting the damper to the beam's end by nuts, then lifting the beam and damper to the expected location and finally connecting the damper to the column by inserting the demountable bolts into couplers.

The specimen was tested under cyclic load and compared to the equivalent, wet jointed precast specimen. Test results showed that the significant plastic damage was concentrated on the damper while column and beam remained elastic (tiny cracks appeared on the beam with no damage on the nuts and threads on the end of longitudinal reinforcement). The specimen with damper showed somewhat lower flexural strength and stiffness compared to specimen with wet joint, although the dog-bone damper was weakened to act as a sacrifice element (in order to protect the concrete components). In addition, the displacement capacity, energy dissipation, as well as strength and stiffness degradation were better than in case of wet jointed specimen.

Since the nuts and threaded ends of longitudinal reinforcement were not damaged, Wu et al. [38] have stated that the connection was easily fully disassembled. Although the possibility of reuse of precast elements was not explicitly analysed in the paper, in the authors' opinion, there is a high potential for reuse of beams and columns, with replaced "dog bone" dumper.

Bai et al. [39] have conducted experimental tests on connection with reduced beam steel section ("dog-bone" element), similar to the one presented in Figure 6 a). The main difference was that the anchoring reinforcement in column and beam were welded to embedded steel elements with end plates, which protruded from the column and beam. The connection was realised by connecting embedded steel elements to the "dog-bone" element by means of high strength bolts. Different configurations of the connections were tested. The test results showed that the strength of non-replaceable parts should be at least 50% higher than replaceable parts of the connection in order to obtain desirable behaviour of the joint – the plastic deformation in the "dog-bone" element and negligible damage of precast elements (ductile connection). In this regard, the authors have performed tests on the three "post-repaired" specimens with reused precast elements and replaced "dog-bone" element. These specimens exhibited stable seismic behaviour, thus proving the possibility of reuse for precast beams and columns.

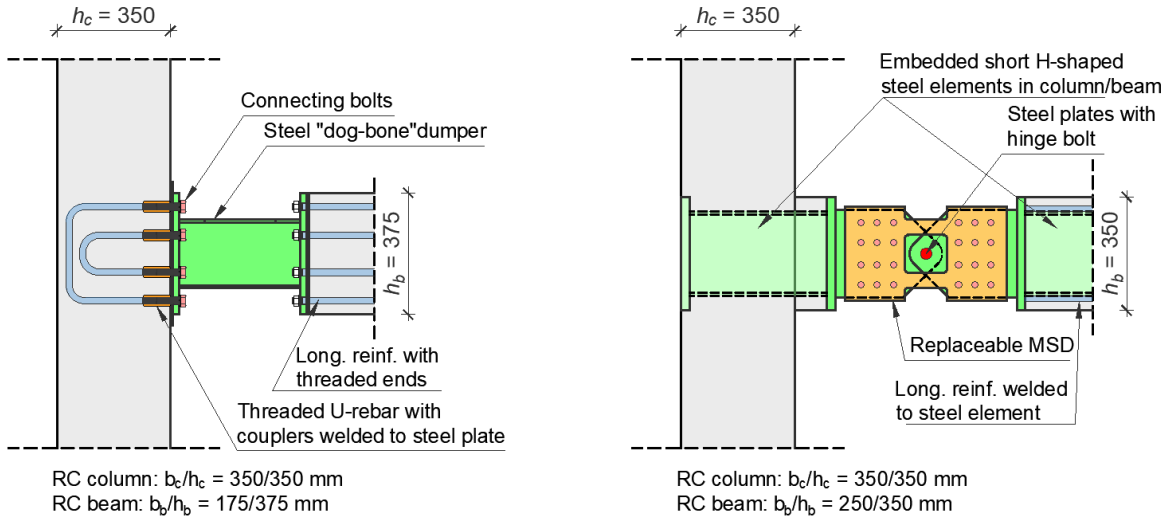

Figure 6. Beam-to-column joints with steel dampers: a) connection with steel "dog-bone" element (adapted from Wu et al. [38]), b) connection with steel "multi-slit devices – MSD" (adapted from Huang et al. [40])

Huang et al. [40] have experimentally investigated another type of energy dissipation connection system in precast beam-to-column joints, as shown in Figure 6 b). The connection consists of H-shaped steel elements embedded in column and beam, with beam longitudinal reinforcement welded to the element. The embedded H-shaped elements of beam and column have extension plates which protrude from their ends. These extension plates are connected with pinned joint at the centre of the connection, via hinge bolt, in order to resist shear loads. Afterwards, the "multi-slit devices – MSD" (steel plates with slits/holes) are connected to the protruding extension plates via bolts. These MSDs are used as one of the main structural elements, with aim to provide flexural capacity for the joint, and additional energy dissipation capacity through the plastic flexural deformation of steel. Different layouts of slits in MSD were analysed in the presented study.

The specimens were tested under cyclic load and compared to the equivalent, monolithic specimen. In case of the proposed connection, the plastic deformation and damage were mainly concentrated on the steel strips of MSD, while the precast beam and column remained within the elastic stage during the entire loading process. The overall seismic performance of the precast joints was better than that of the monolithic joint, in terms of the resistance, deformation capacity, energy dissipation capacity and ductility. In addition, the initial stiffness of the precast joints was also greater than or similar to that of the monolithic joint.

Huang et al. [40] have stated that MSD plates can be replaced directly during post-earthquake recovery in order to conduct the rapid repair of the structures. They discussed the feasibility and effectiveness of the proposed precast joint from the perspective of seismic safety performance.

The same concept of connection with hinge bolt and dissipating steel plates with slits, but with different layouts of the connection (steel elements, anchoring systems, level of complexity, etc.) were investigated by different authors [41], [42], [43]. The conclusions regarding the overall behaviour, damage distribution and the replacement possibilities of precast joints were similar.

2.5 Connections with partial in-situ concreting

Over the past years, a significant effort was made towards reducing the in-situ concreting and grouting in precast beam-to-column joints with nominally wet connections, in order to achieve emulation of monolithic joints and provide the possibility of deconstruction and reuse at the same time.

Ong et al. [44] have suggested that the demountable beam-to-column joints can be achieved with steel elements (I-section element with end plate) embedded in precast beam and protruding beam from the column, with minimal in-situ concreting, as shown in Figure 7 a). The longitudinal reinforcement is welded to the embedded I-section element. After the alignment of beam and column was achieved, the connection is realised with connecting bolts, tightened with the design torque. Finally, the joint is encased with a suitable cast-in-situ material. This type of connection can be used for the precast slab without topping (i.e., without continuity of longitudinal reinforcement, as shown in Figure 7 a or with cast-in-situ connection with the slab. In addition, for reused precast beam in the structure with different spans than the spans in the original building, the solutions with the span extension units (steel elements), connected by bolts and oversized holes or by welding, were proposed.

Instead of beam-to-column joints, four-point bending experimental tests under monotonic load were conducted on the precast beams with different configurations (without topping and continuity of longitudinal reinforcement, with topping and continuity of longitudinal reinforcement, and with bolted extension unit). These tests were conducted in order to simulate the behaviour of beam-to-column joints with hogging moments. After the initial tests under serviceability loads, further examination of reused beams was conducted. Tested reused specimens showed satisfactory behaviour.

Ong et al. [44] have provided detailed description of the deconstruction process of the initially tested beams under serviceability loads, as well as repair and reconstruction process for the reused beams, which were tested until

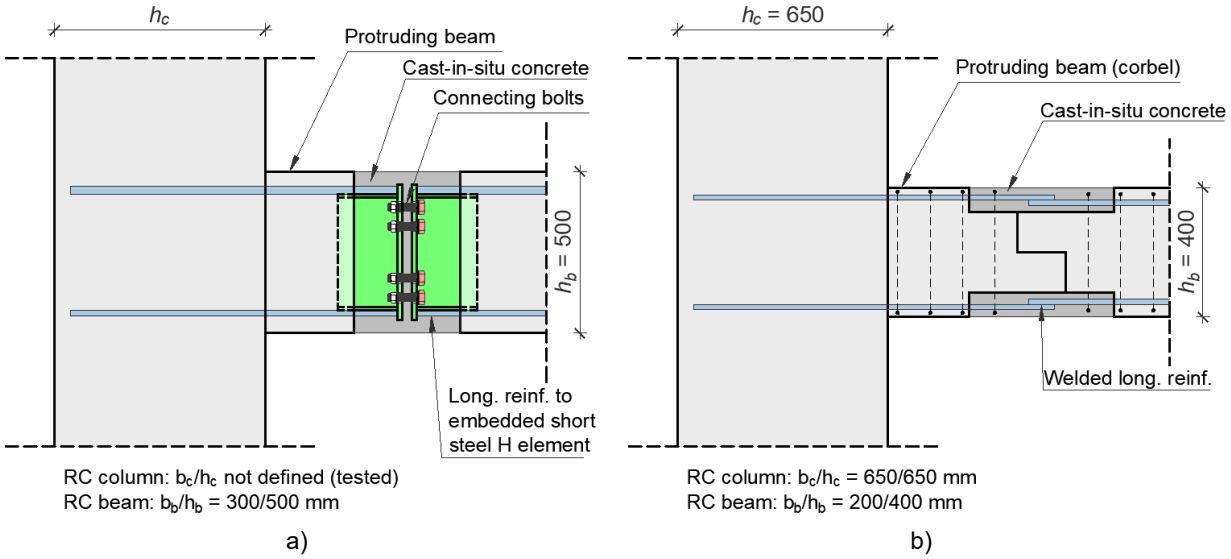

Figure 7. Beam-to-column joints with partial cast-in-situ concreting: (a) bolted connections with embedded steel plates (adapted from Ong et al. [44]), (b) connections with dapped-end beam and welded longitudinal reinforcement (adapted from Xiao et al. [45])

failure. During deconstruction, demolition work was noisy and time consuming, albeit small concrete volume which was removed. Furthermore, there was a necessity for cutting some bolts, due to damage of the threaded part of the bolts, while some damage to the nearby stirrups and embedded steel elements was also noticed. Several recommendations were given for mitigating the observed difficulties in deconstruction.

Xiao et al. [45] have conducted cyclic experimental tests on the demountable precast beam-to-column joints, with dapped-end beam and welded longitudinal reinforcement, as shown in Figure 7 b). The connection included protruding beam extending from the column, with small corbel for supporting precast beam. After the seating of the beam was ensured, the longitudinal reinforcement was overlapped and welded in-situ. Finally, the small amount of in-situ concreting was provided. The connection was moved away from the column face, in order to ensure plastic hinging at the beam near the column, and avoid major damage in the connection. In order to improve sustainability of the proposed solution, specimens with natural aggregate concrete (NAC) and recycled aggregate concrete (RAC) were tested.

The specimens were tested under monotonic and cyclic loads, and were compared to the equivalent, monolithic (cast-in-situ) specimen, both with NAC and RAC. The testing results have shown that the proposed precast beam-to-column joint has similar strength, initial stiffness, stiffness deterioration, energy dissipation and ductility as monolithic joints, while the majority of the damage occurred in the protruding beam. In general, RAC specimens showed relatively lower ultimate strength compared to the NAC specimens, both for monolithic and precast joints, but within a reasonable limit.

Xiao et al. [45] have conducted deconstruction of precast specimens after testing. The small portion of cast-in-place concrete was carefully removed with mechanical jack-hammer, in order to ensure minimal damage as possible. Afterwards, the welded longitudinal reinforcement was cut off, and the specimens were separated in two parts. It was stated that during the execution of deconstruction process, mechanical removal process was not so difficult and very little debris was generated. The suggestions for improving the connection were highlighted, primarily the increase of length of the welded longitudinal reinforcement in order to achieve full continuity of reused beam. However, the behaviour of the reused precast joint was not examined. Since the connection is placed outside the critical region, with major damage occurring in the protruding beam of RC column, the proposed connection can provide potential reuse only of precast beam.

In the subsequent research, Xiao et al. [46] and Ding et al. [47] have performed cyclic experimental tests on the similar precast beam-to-column joint as shown in Figure 7 b), with aim to experimentally investigate the reuse possibility of precast beams. The main difference in the connection layout was the addition of embedded steel elements, both in precast beam and protruding beam from precast column, in order to provide shear transfer between beam and column. Specimens of interior beam-to-column joints, with natural aggregate concrete (NAC) and recycled aggregate concrete (RAC), were tested. The specimens with reused beams and new columns were constructed from the original specimens which were previously tested under cyclic displacements corresponding to 2% interstorey drift ratios. It was demonstrated that both original and reused precast joints have adequate seismic performance, similar to the monolithic joints. Xiao et al. [46] have conducted Life cycle assessment (LCA) and showed that the proposed precast beam-to-column joint would increase the carbon emission at the first construction process, but would reduce total carbon emission. In addition, the use of RAC in the proposed precast joint had the lowest carbon emission, reduced by approximately 13% compared with monolithic NAC joint.

2.6 Post-tensioned connections with dissipating elements

Although generally classified as non-emulative joints, precast beam-to-column joints connected with unbonded post-tensioned strands were proven to be an adequate solution for multi-storey precast moment frame building structures, with quicker construction speed, large self-centring capabilities (small residual deformations) and an ability to undergo large nonlinear lateral displacements without significant damage of structural elements (columns, beams and unbonded strands remain in the elastic range). However, their greatest setback is that the lateral displacement demands under seismic action may be higher than acceptable, due to insufficient energy dissipation capacity [48]. In order to address this issue, several solutions which could enhance energy dissipation of the joints were proposed in the past decades, although generally increase the cost and difficulty in construction. In recent years, apart from the enhancement of energy dissipation, the focus of the research was on the disassembly and replacement of the specific connection components which are expected to dissipate energy during earthquakes, i.e., steel components such as unbonded mild steel bars, steel angles, steel braces, etc.

Wang et al. [49] have conducted cyclic experimental tests on the interior post-tensioned precast beam-to-column joints with steel jackets and mild steel bars, as shown in Figure 8 a). Steel tubes were horizontally embedded into the column and adjacent beams at the centreline of the beams, in order to accommodate the unbonded post-tensioned strand used to pre-stress the beams against the column. The steel jackets with welded studs were anchored to the end of precast beams, which were used to prevent concrete spalling and crushing at the interface with the column during loading. For the same reason, the steel jacket was used for the column. Supporting angles were connected to the column, which were used to provide seating of the beam and transmission of shear forces. Replaceable steel angles were connected to the beam jacket via bolts (four angles per beam). Replaceable mild steel bars with reduced cross-sectional area along the length were inserted into previously embedded tubes into column, and were subsequently welded to the replaceable angles. The mild steel bars were used as dissipaters. Similar layout of the connection was also examined, with mild steel bars bolted to the steel jacket at the beam's end, without replaceable angles, albeit partially encased beam jackets (with only vertical plates and end plate) and column without steel jacket were used.

The specimens were tested under cyclic loads, and were compared to the equivalent, monolithic (cast-in-situ) specimen. For precast specimens, yielding mainly occurred in the mild steel bars, while the post-tensioned strand and longitudinal reinforcement in the beams remained in the elastic region. The width of concrete cracks outside the connection remained below the value of 0.4 mm at 2% drift ratio. Residual deformations were negligible, even after drift ratios of approximately 5.5%. The strength of precast joint was similar to the monolithic joint. It was demonstrated that the precast joint has somewhat higher cumulative energy dissipation capacity up to 2%, while for higher drifts

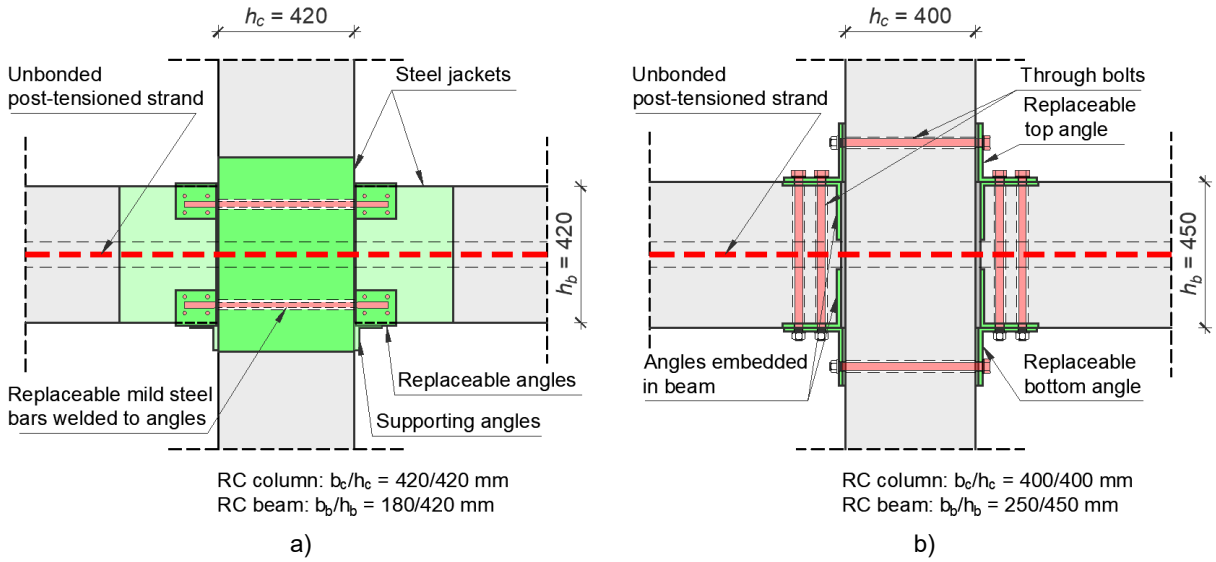

Figure 8. Beam-to-column joints with post-tensioned connections: (a) connections steel jackets and replaceable bar and angles (adapted from Wang et al. [49]), (b) connections with replaceable steel angles and through bolts (adapted from Cai et al. [50])

monolithic joint has considerably higher energy dissipation capacity. The initial stiffness of precast joint was the same as that of monolithic joint until the opening of the gap between beam and column; afterwards, however, the stiffness of precast joint declines.

After first testing, the precast specimen was retrofitted by replacing mild steel bars and post-tensioned strands, and reused for additional testing. The mild steel bars and the replaceable angles were removed by cutting off mild steel bars (welded to the replaceable angles). It was stated that the replacement of mild steel bars after loading of the original specimen took only 2 hours, with 2 workers. The seismic performance of the reused precast joint was very similar (and even better for some parameters) to the performance of original precast joint. Thus, the possibilities of disassembly, replacement and reuse of both precast column and beam were confirmed.

Cai et al. [50] have conducted cyclic experimental tests of the exterior post-tensioned precast beam-to-column joints with replaceable steel angles and through bolts. The layout of the joint is presented in Figure 8 b) for interior joint, for simplicity reasons. The replaceable angles were used as dissipaters (dissipating fuses). The bottom replaceable angles were also used for seating of the beam. The connection is realised by connecting replaceable top and bottom angles to precast beam and column, with vertical and horizontal through bolts. The bolts were pretensioned after the assembly process was completed, and designed for strength. In addition, at the end of the beams, the embedded steel angles were provided in order to prevent local damage and crushing of the concrete at the beam-column interface. The effect of different parameters was investigated, such as initial post-tensioning force, thickness of steel angles, angle dimensions, beam depth, etc.

Test results have shown that cracking only occurred at the beam end, and near the steel angles in all specimens. It was demonstrated that an increase in the initial post-tension force, beam depth, or leg thickness of the steel angles could lead to an improvement in load-carrying capacity and increase in the initial stiffness of tested specimens. The increase of thickness of the steel angles also could lead to a significant increase in the dissipated energy.

After initial testing, specimen with the best performance was retrofitted by replacing demountable steel angles and was reused for additional test. This reused specimen exhibited almost identical hysteretic behaviour as the original specimen, with slight reduction im strength as well as the reduction of initial stiffness to some extent, due to cracking of beam after the initial testing of the original specimen. However, in the late loading stages, the stiffness, energy dissipation and maximal displacement of both specimens were very similar. Somewhat larger residual drifts of reused specimen were detected. Since the overall behaviour of the reused specimen was similar to the original specimen, the possibilities of disassembly, replacement and reuse were confirmed.

3 Column-to-column and column-to-foundation connections

Connections between precast columns and foundations, as well as between adjacent column parts, play a critical role in ensuring reliable force transfer and overall structural integrity. These joints must provide adequate strength, stiffness, and ductility while maintaining stable behaviour under service and seismic loads. In seismic regions, particular attention is given to the ability of connections to dissipate earthquake-induced energy. This can be achieved either by allowing the formation of plastic hinges, similar to conventional monolithic RC systems, or by enabling controlled rocking mechanisms at the column base, which reduce residual deformations and limit structural damage [51].

To satisfy these performance requirements, connection systems must be carefully designed in accordance with capacity design principles, ensuring that inelastic deformations occur in predetermined and ductile regions while protecting critical connection components [52]. In recent years, increasing emphasis has been placed on the development of innovative demountable connections, which facilitate not only structural performance but also disassembly, repair, and potential reuse of structural elements. Such systems are typically based on mechanical joining techniques and are classified as dry or semi-dry

connections, distinguishing them from traditional cast-in-place solutions [52]–[54].

A review of the available literature indicates that demountable column-to-foundation (CF) and column-to-column (CC) connections can be broadly categorized according to the type of mechanical device used for force transfer. The most commonly investigated and applied systems include: steel flange plate connections, column shoe (steel shoe) connections, and steel jacket connections. Each of these systems exhibits distinct load transfer mechanisms, seismic performance characteristics, and levels of demountability and reusability, which are discussed in detail in the following sections.

3.1 Connections with steel flange plate

This type of connection is used for column-to-foundation (CF) and column-to-column (CC) connections. The connection consists of column longitudinal reinforcement (CLR), a steel flange plate, and external bolts or anchor bars. The CLR is first connected to the steel flange plate, after which the steel plate is fixed to the foundation or lower column using anchor bars or bolts. Figure 9 illustrates the typical configuration of CF and CC connections incorporating a steel flange plate. In practice, the flange plate is often strengthened by welded steel jacketing plates and stiffeners, as also shown in Figure 9. The dimensions of the steel flange plate generally exceed those of the column cross-section, allowing the anchor bars or bolts to be positioned outside the column perimeter. Various types of anchor bars are used in such connections, including threaded bars, reinforcing bars, and hybrid systems combining reinforcement, couplers, and bolts, as shown in Figure 9. Anchor bars may be either straight or bent, and may be threaded along their entire length or only over the portion extending from the foundation.

To ensure effective force transmission between the CLR and steel plate, several solutions have been proposed: welding, CLR with rivet head, and threading the CLR bar end followed by fastening with a nut or a coupler-bolt assembly [56]. These solutions are illustrated in Figure 10. In welded configurations, the CLR may be connected to a steel jacketing plate (Type A), a steel flange plate (Type B), or to weldable steel sleeves (Type C), as shown in Figure 10. Type D in Figure 10 represents solution where CLR had rivet

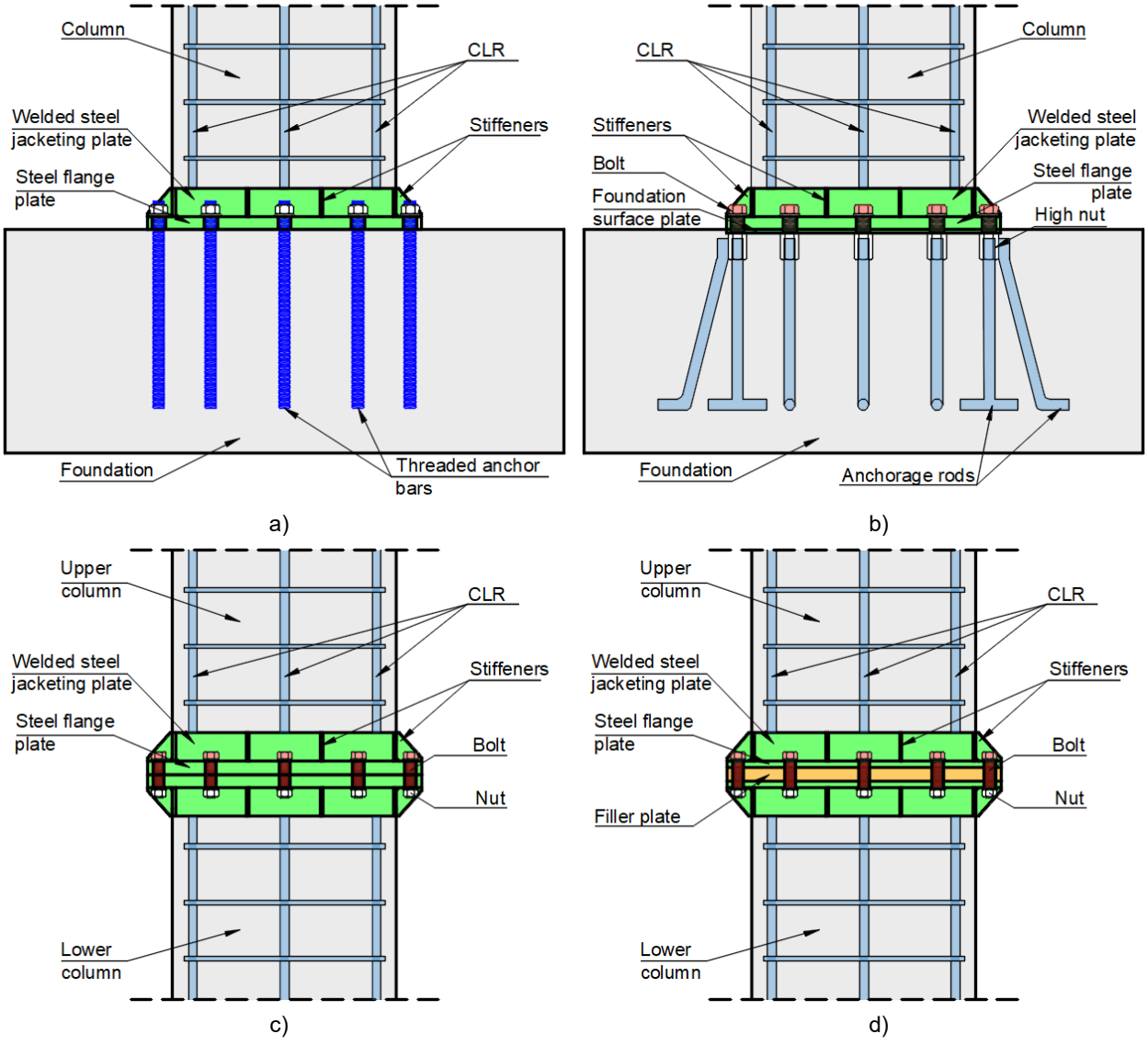

Figure 9. Typical configuration of steel flange plate connections: a) CF connection, b) CF connection adapted from Pul et al. [55], c) CC connection, d) CC connection with filler plate

head. Three types of connection with threading CLR end are also shown in Figure 10: threaded CLR with exposed nut (Type E), threaded CLR with nut installed in the pit (Type F) and threaded CLR secured with coupler and bolt (Type G).

In this section, different solutions for CF and CC connections presented in Figure 9 were discussed. The proposed solutions differ in the type of CLR and steel flange plate connection, as presented in Figure 10.

The welding procedure was commonly used in previous research [57]–[61]. Orlando and Piscitelli [58] had tested CF connection on cantilever columns subjected to monotonic and cyclic loads. In their study, the connection between the column longitudinal reinforcement (CLR) and the steel flange plate corresponded to Type A. The column cross-sectional dimensions were b_c/h_c = 400/400 mm, while the CLR was adopted as 8 Ø16. For the experimental setup, a steel beam (HE400B) was used instead of a reinforced concrete (RC) foundation. The steel flange plate was connected to the beam using eight M24 grade 10.9 bolts. The proposed connection corresponds to what is shown in the Figure 9 a).

The monotonic test results indicated ductile behaviour, characterized by significant plastic deformation beyond the elastic limit, with an ultimate drift ratio of approximately 5%. In cyclic tests, failure of the CLR was not observed, as the tests were terminated upon reaching the capacity of the loading equipment. The yielding force and maximum load of the CF connections under monotonic and cyclic loading occurred at similar drift ratios, with slightly higher drift capacity observed in the monotonic tests. The CF connection was intentionally overdesigned, resulting in cracking localized in the RC column.

Based on the experimental results, the authors concluded that the proposed CF connection satisfied capacity design requirements. Furthermore, they suggested that this type of connection could also be applied in column-to-column (CC) joints, where it is expected to behave as a full-strength connection. Although the possibility of demountability was not addressed in the study, the overdesigned configuration implies that failure would likely occur in the CLR after reaching the ultimate limit state, meaning that only the foundation could potentially be reused.

A direct welding solution was also proposed by Aktepe et al. [59] and Akduman et al. [60], in which a Type B connection between the column longitudinal reinforcement (CLR) and the steel flange plate was adopted. To enhance the force transfer mechanism between the reinforced concrete (RC) column and the steel components of the connection, anchorage rods (steel bars) were welded to the steel jacketing plate. The column dimensions were b_c/h_c = 250/150 mm with 6 Ø10 used as CLR. The connection between the steel end plate and the RC foundation was achieved using embedded threaded bars. After positioning the column on the foundation, high-strength nuts were tightened onto eight threaded rods with a diameter of 14 mm. This configuration corresponds to the connection detail shown in Figure 9 a).

Akduman et al. [60] compared behaviour of cantilever columns with monolithic CF connection and proposed demountable CF connection under cyclic load. The CF connection zone showed no damage during the testing. All deformation appeared in the end of the RC column with more concrete spalling and crushing compared to the monolithic specimen. The failure of demountable specimen was due to crushing confinement concrete zone and CLR buckling, while the failure of monolithic specimen was only due to the crushing of confinement concrete zone. Authors [60] demonstrated that demountable specimens had better performance than monolithic specimens, with higher drift capacity, greater energy dissipation and higher initial stiffness as well as maximum lateral load capacity.

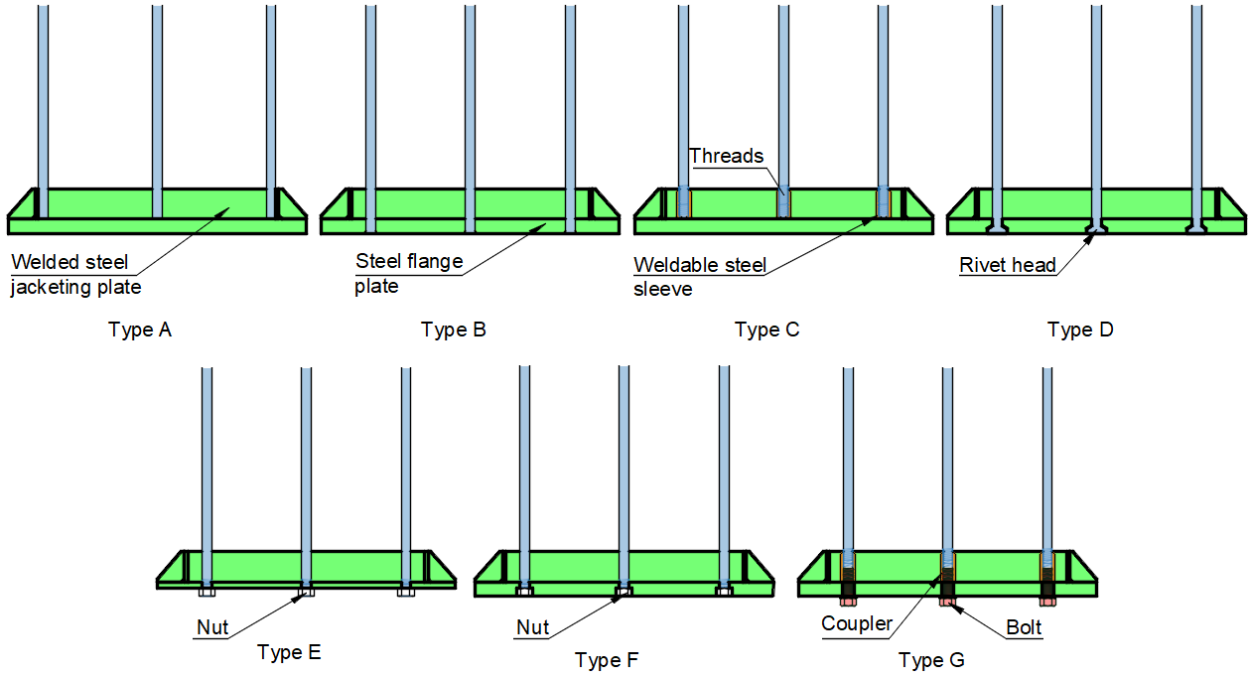

Figure 10. CLR-steel flange plate connections

In addition, the same authors proposed an alternative connection type [8]. They used RC flange instead of steel end plate. The RC flange was reinforced with bars, steel plates or combination of these two and castes together with the column. The column longitudinal reinforcement was bent 90 degrees and welded to the RC flange reinforcement or steel plates. During the RC flange casting holes for threaded rods were made. They observed that under cyclic load, CF connections with RC flange failed to achieve proper capacity design behaviour due to the damage that appeared in the RC flange.

Although the authors stated that the proposed connection is fully demountable, the disassembly procedure was not explicitly demonstrated. It can be concluded that for lower drift ratios the RC column and foundation could potentially be reused. However, at higher drift demands, significant damage of RC column would occur, leaving only RC foundation with anchor rod reusable. Usage of connection with steel plate was highly recommended for both beam and column applications in seismic active zones [59], [60].

Indirect welding of longitudinal reinforcement bar to the steel plate was proposed by Zhang et al. [57] and Liu et al. [61]. Both studies adopted type C concept presented in Figure 10, in which weldable steel sleeves were screwed to the column threaded rebar and then welded to steel plate. Zhang et al. [57] tested CC connection under eccentric compression, the layout of connection is schematically shown in Figure 9 c). The study considered variations with or without steel jacketing plate and stiffeners. In addition, different types of shear keys were used: shear connectors (steel beam) and shear studs, all welded to the steel flange plate. The column had square cross section with dimensions b_c/h_c = 250/250 mm, and CLR was four 16-mm-diameter bars. The connection detail at the end of upper and lower column were identical, and the CC connection was achieved using preloaded M20 high-strength bolts, with grade 10.9. For cast-in-place and demountable connected CC connections the failure occurred due to yielding of CLR on the tension side and concrete crushing on compression side. Under eccentric compression load demountable CC connections outperformed cast-in-place columns in terms of deformability, but cast-in-place columns performed better in terms of load bearing capability.

Liu et al. [61] tested both CC and CF connection in cantilever columns under cyclic load. The section size of all specimens was b_c/h_c = 400/400 mm, with different CLR. The cast-in-place column was reinforced with 12 Ø18, whereas the columns with CC connection had 12 bars with diameters of 18, 22, 28 mm. The column with CF connection had 12 Ø22 for CLR. The CC connection was completed with the utilization of high-strength bolts for connection between two steel end plates. Specifically, 16 M24 bolts were used for the demountable CC connections, while the CF connection used 20 M32 anchor bars embedded in the RC foundation. The threaded anchor bars were welded to the anchor plate embedded inside the foundation.

All specimens were tested under cyclic loading, and the performance of CC and CF connections was compared with that of monolithic columns and columns incorporating grouted sleeve CC connections. Failure of all specimens occurred due to flexural mechanisms. The crack propagation patterns were similar for monolithic columns and those with CC and CF connections. An increase in CLR ratio resulted in reduced crack spacing. The authors concluded that the location of the connection had a negligible influence on the development of flexural cracks.

Demountable specimens exhibited higher cumulative energy dissipation and greater resistance compared to the monolithic specimen. The highest ultimate drift ratio was observed in the proposed CC connection, while both the grouted sleeve and CF connections also achieved higher drift capacities than the cast-in-place column. The CC and CF connections demonstrated comparable performance in terms of strength, ductility, and energy dissipation. Following the tests, the demountability of the connections was verified. The column was successfully detached from the foundation, and subsequent removal of concrete revealed that the steel flange plate, welds, and connections between the CLR and steel sleeves remained intact. Based on these observations, the authors [61] concluded that the proposed connection system is reliable.

The innovative demountable CF connection was proposed by Pul et al. [55]. Instead of welding rebar to the steel plate CLR with rivet head was used (Type D in Figure 10). The steel end plate was manufactured with rivet head rod holes. Again, the steel jacketing plate and stiffeners were also used in proposed solution. At the upper surface of RC foundation, the foundation surface plate was installed, as presented in Figure 9 b). The high nuts were welded to the surface steel plate and rebar anchors were screwed into them. High nuts and anchor rods remain embedded into the RC foundation. The steel flange plate was fixed to the surface foundation plate with the M20 10.9 grade high-strength bolts. The CLR was ten 16-mm diameter bars, whereas the cross-section of columns was b_c/h_c = 400/250 mm. The monolithic and demountable cantilever columns were tested under cyclic load.

Cracking in the demountable specimens initiated at lower drift ratios compared to the monolithic specimen; however, yielding occurred earlier in the monolithic column. Both systems exhibited a flexural failure mode, characterized by concrete cover spalling and buckling of the CLR. Notably, the onset of concrete cover spalling was delayed in the demountable specimens. Pul et al. [55] concluded that the proposed CF connection exhibits behaviour comparable to monolithic systems in terms of energy dissipation, initial stiffness, ultimate drift ratio, and ductility. The design philosophy aims to maintain the steel plates and bolts within the elastic range, thereby concentrating damage within the RC column. Consequently, only the foundation remains suitable for reuse.

Nzabonimpa et al. [62], [63] and Hong et al. [64] developed new way of connecting longitudinal rebar to the steel plate. Their approach was to use steel end plate with holes for rebar. The CLR that was threaded at the end and it was fixed to the steel plate with nuts. Two different solutions were proposed the one with thin plate and the other with thick plate (Type E and F in Figure 10). The thick plate enables making the pits for the nuts and threaded rebar to fit into. The surface of the end steel plate remains flat, and position of rebar in upper and bottom column remains same. In contrast, the use of a thin plate requires the addition of a filler plate (steel or concrete) to accommodate the protruding nuts and to fill the gap between opposing steel plates. In this case, the nuts remain exposed on the plate surface. The connection between the two steel end plates is achieved using 18 M20 bolts. The configuration without a filler plate is illustrated in Figure 9 c), while the configuration with a filler plate is shown in Figure 9 d). Unlike other solutions, these studies [62]–[64] did not incorporate steel jacketing plates or stiffeners. The column dimensions were b_c/h_c = 500/500 mm and CLR 4 Ø25.

The cyclic behaviour of cantilever columns with CC connections using thin and thick plates was evaluated and compared with that of cast-in-place columns. For specimens with thick plates, failure occurred due to concrete cover spalling and buckling of the CLR, while the steel flange plate remained intact. In contrast, specimens with thin plates exhibited noticeable deformation of the steel plate. The results indicated that connections with sufficiently stiff and strong (i.e., thick) steel plates could achieve structural behaviour comparable to monolithic joints and effectively act as rigid connections with similar stiffness and deformability. However, specimens with thin plates demonstrated inadequate performance, including a significant reduction in strength and an inability to form rigid joints. Disassembly of the connections was successfully performed, confirming the feasibility of reusing both the upper and lower column segments.

The type G connection, presented in Figure 10, was adopted and experimentally tested by Zhou et al. [56]. Instead of welding, the CLR with threaded end was connected to the steel flange plate using a coupler-bolt assembly. The welding procedure was performed on steel jacketing plate and steel stiffeners. The overall configuration of the tested connection is similar to that shown in Figure 9 a). A total of 24 pre-stressed M24 grade 12.9 high-strength anchor bolts, together with an anchor plate, were embedded in the RC foundation. The square column section with dimensions b_c/h_c = 800/800 mm was reinforced with 32 bars of 20 mm diameter. The cantilever columns were tested under cyclic load. At the end of testing, longitudinal rebars buckling was observed with significant concrete crushing. Authors [56] concluded that CF connection had favourable flexural mode characterized by concrete cracking, yielding of the CLR, concrete cover spalling and crushing, and eventual fracture of the reinforcement. Although only a limited analysis of the results was presented, the authors concluded that the connection showed adequate flexural performance.

Following the tests, the steel flange plates were successfully demounted from the column. The steel components and bolted connections remained intact, demonstrating the feasibility of demountability for this connection type. Both the foundation and the steel elements of the connection were deemed reusable.

3.2 Connections with steel shoe embedded in column

In the literature, several solutions for column-to-foundation (CF) and column-to-column (CC) connections using column shoes have been presented [51], [52], [54], [65]. Column shoes are currently manufactured by various companies as prefabricated elements or manufactured by welding steel plates. The connection mechanism is based on load transfer from the CLR to the column shoe through lap splicing. Reinforcing or steel bars are pre-welded to the column shoe, and the CLR is lapped with these welded bars. A single column shoe may be designed to accommodate one or multiple CLR bars. All proposed solutions had two types of welded rebars: (1) Type 1 rebar used for overlapping with column longitudinal rebar, and (2) Type 2 rebar used for improving the column shoe-concrete connection and stress transfer [51], [52], [54], [65]. The CC and CF connections are completed after fixing column shoes for foundations or lower column. The embedded anchor bars or coupler-bolt assembly are used for connecting column shoe and foundation/lower column. The upper and lower nuts were used, lower one for adequate positioning of column and upper one for fixing the column shoe. Commonly the column shoes are either welded to the integral plate or used as standalone elements. The difference from steel flange plate connection solution is in use of grout. After erecting column on foundation or lower column, the gap between column shoe and concrete surface is poured with non-shrink grout. Contrary to the steel flange connections, the column cross-sectional dimensions remain unchanged at the connection zone. The characteristic example of column shoe connections is presented in Figure 11.

The cyclic response of the CF connections in cantilever columns was investigated by Nascimbene and Bianco [52]. In their study, four column shoes welded to an integral steel plate were used, as shown in Figure 11. The protruding anchoring bolts anchored into the foundation were used for connecting the column shoes to foundation. Three diameters of anchor bolts and corresponding column shoe were used M24, M30 and M39. The CLR was 12 Ø 16 and 4 Ø 20, and column cross-section b_c/h_c = 400/400 mm. For shear resistance, they added steel pins, which were embedded half in foundation half in grout.

Based on the experimental results, the authors concluded that the behaviour of the anchor bolts governs the overall response of the CF connection. The anchor bolts were the only components that exhibited nonlinear behaviour, while no significant damage was observed in other parts of the specimens. The connections demonstrated sufficient strength and ductility to resist seismic actions. Although reusability was not explicitly addressed, the minimal damage to the column suggests that reuse may be feasible. The authors also recommended a more rational design of the column, because the CLR did not reach the yielding point during testing.

Similar connection set-up, without an integral plate was tested by Wang et al. [65]. Researchers tested seismic performance of both CF and CC connections and compared results to the cast in situ column. All columns had CLR as four 18 mm- diameter bars, and b_c/h_c = 300/300 mm cross-section dimension. The column shoes were produced by welding steel plates. The M22 grade 10.9 studs threaded at both ends were used for anchoring. For the CC connections the studs were anchored in the lower column, with the lower threaded end of the stud connected to the CLR using rigid coupling sleeves. When it is about the CF connections the same principle is applied, instead of the column longitudinal rebar bent bar were used. To increase shear capacity of connection shear keys were added and one stirrup between two precast elements. Only one sample without shear keys and additional stirrup was tested.

The failure point was defined as detaching the column shoe from the concrete. The CF connection specimens exhibited the lowest lateral load at first cracking, while the CC connections showed minor damage. After testing cantilever columns under cyclic load, author suggested usage of these connection only in the region of minimal bending moment. They reported poor seismic performances of the CF connections compared to the cast in situ columns. The weak bond between the grout and the column shoe was identified as the critical issue, leading to early cracking, pinched hysteretic response, and reduced energy dissipation capacity. The authors [65] also concluded that shear keys are not necessary when the connection is located in the central region of the column.

Dal Lago et al. [54] tested different connection types under cyclic load among them the connection with column shoes, similar to the one shown in Figure 11. All columns had a square cross section of 400 mm sides, and CLR as 8 Ø16.

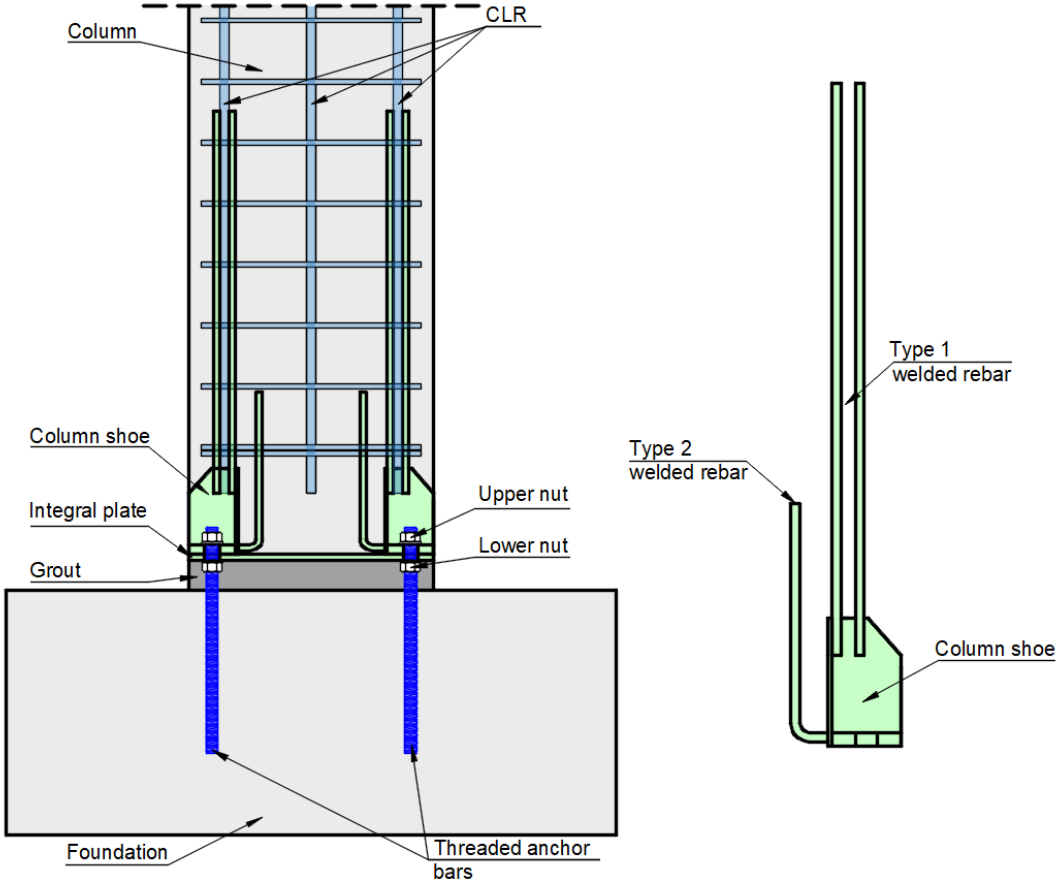

Figure 11. The CF connection with the column shoe

Threaded anchors were used for fixing column to the foundation. The bar anchor was threaded only on the part that is protruding from the foundation. After testing column cantilever samples under cyclic load, a good overall ductility of the specimen is shown by the envelope curve that should correspond to the monotonic behaviour. The connection presents the combination of rocking model and forming of plastic hinges. The failure occured due to the exceeding the capacity of anchors. The pinching effect that occurred significantly reduced seismic response characteristics of connections. However, the authors suggested that over dimensioning of anchors and overlapping of column longitudinal rebar should be more carefully taken into account in the capacity design.

The CF connection with column shoes and unbonded prestressing tendons was tested by Sripongngam et al. [51]. The column shoes were used for transferring forces from column to foundation, corresponding to the solution showed in Figure 11. Unbonded prestressed tendons are installed along the column and extended into the foundation to provide rocking behaviour. The dimensions of cross-section of column were b_c/h_c = 320/320 mm, and the adopted CLR was 8 bars with diameter of 16 mm. Authors [51] used energy-dissipating (ED) bolts (DB16, DB20, and DB25) to connect the column shoes to the foundation. These bolts are designed to enhance seismic performance by dissipating energy under cyclic loading. Columns with column shoes and cast-in-place column were tested and their responses were compared.

For the specimens with the demountable connection, the cracks were localized around the joint region, while the cast-in-place column displayed cracks throughout the upper and lower column region. The significant concrete spalling was considered as failure point during the testing. Overall, the demountable system exhibited reduced flexural damage compared to the cast-in-place column. However, the cast-in-place specimen showed higher ductility and greater overall energy dissipation capacity. The use of ED bolts led to concentration of inelastic deformations within the bolts, allowing the RC column to remain largely elastic. The authors classified this system as a low-damage solution, demonstrating stable cyclic behaviour with only minor reductions in strength and stiffness compared to the monolithic specimen. It was also observed that the performance of the system was sensitive to the level of overdesign of the connection. An appropriate overdesign ratio is necessary to achieve the desired low-damage behaviour. Higher overdesign ratios result in behaviour similar to cast-in-place systems with greater damage of columns, while lower ratios lead to reduced energy dissipation capacity with lower damage of columns.

Orlando and Piscitelli [58] tested a connection system conceptually similar to column shoe connections based on lap splicing. The column dimensions and connection to the steel foundation beam were the same as in case of steel flange plate connection. Instead of separated column shoes, they used single flanged unions, where the bars welded to steel flange were overlapping with column longitudinal rebar.

They concluded that overlapping gives higher moment resistance of column cross section compared to the continuous bars. Therefore, the plastic hinge can be formed in the section that is outside the connection, which should be taken into account. Compared to the connection type with directly welded column longitudinal bars to the steel end plate, this connection type showed lower dissipation capacity, but higher strength.

Another connection type that can be classified within this group was proposed by Quing et al. [66], [67]. The authors used a system similar to column shoes, using a steel box; however, instead of a lap-splice mechanism, force transfer from the CLR was achieved by threading the bar ends and screwing them into the steel box. The steel box was anchored with bent high-strength rebar embedded into the foundation. The upper and lower reinforcing bars had the same diameter, but the lower bars were of higher strength and were designed to remain elastic during testing, in order to prevent local plastic deformations and potential loosening of the threaded connection. The shear keys were also adopted, as presented in Figure 12. In the first study, the authors [66] compared behaviour of the cantilever precast specimens with monolithic specimens under cyclic loads. The tested columns had a square cross-section of 400 mm, with CLR consisting of eight bars of 25 mm diameter.

The monolithic specimens exhibited concrete cracking and spalling over a relatively shorter region compared to the columns with the proposed CF connection. In contrast, columns with steel boxes showed a greater number of cracks and a more extensive damage zone. Inelastic deformations in these specimens were concentrated above the top of the steel box, resulting in a longer plastic hinge region compared to the monolithic columns. Failure occurred in flexure, accompanied by rupture of the CLR. The demountable specimens exhibited higher lateral load capacity but relatively lower deformation capacity compared to the monolithic specimens. Additionally, their energy dissipation capacity was lower.

In a subsequent study, the authors [67] investigated cantilever columns with different mechanical connection devices, including grouted steel sleeve systems, steel box connections, and hybrid configurations comprised of these two solutions. Among these, only the steel box connections demonstrated potential for reuse. The steel box specimens exhibited strength and stiffness degradation comparable to those with grouted sleeve connections, while the hybrid systems showed improved overall performance but lacked reusability. The author [66], [67] did not discuss demountability process or reuse of elements. Although the demountability process and reuse were not explicitly examined, it can be inferred that, after reaching the ultimate limit state, only the foundation and the lower reinforcement—remaining in the elastic range—would be suitable for reuse.

3.3 Connections with column steel jacket

The steel jacket connections represent a hybrid solution that combines characteristics of RC columns and concrete-filled tube (CFT) columns [68], [69]. The lower portion of the column is manufactured as a CFT element, while the remaining height consists of a conventional precast RC column. The CF and CC connections are placed at the CFT end of the column, where the steel tube provides a robust interface for load transfer. Additional external steel plates are connected either to the CFT ends of adjacent columns or between the CFT end and the foundation. The CLR is bent and welded to the steel part of CFT end of the column, ensuring continuity of force transfer between the concrete and steel elements.

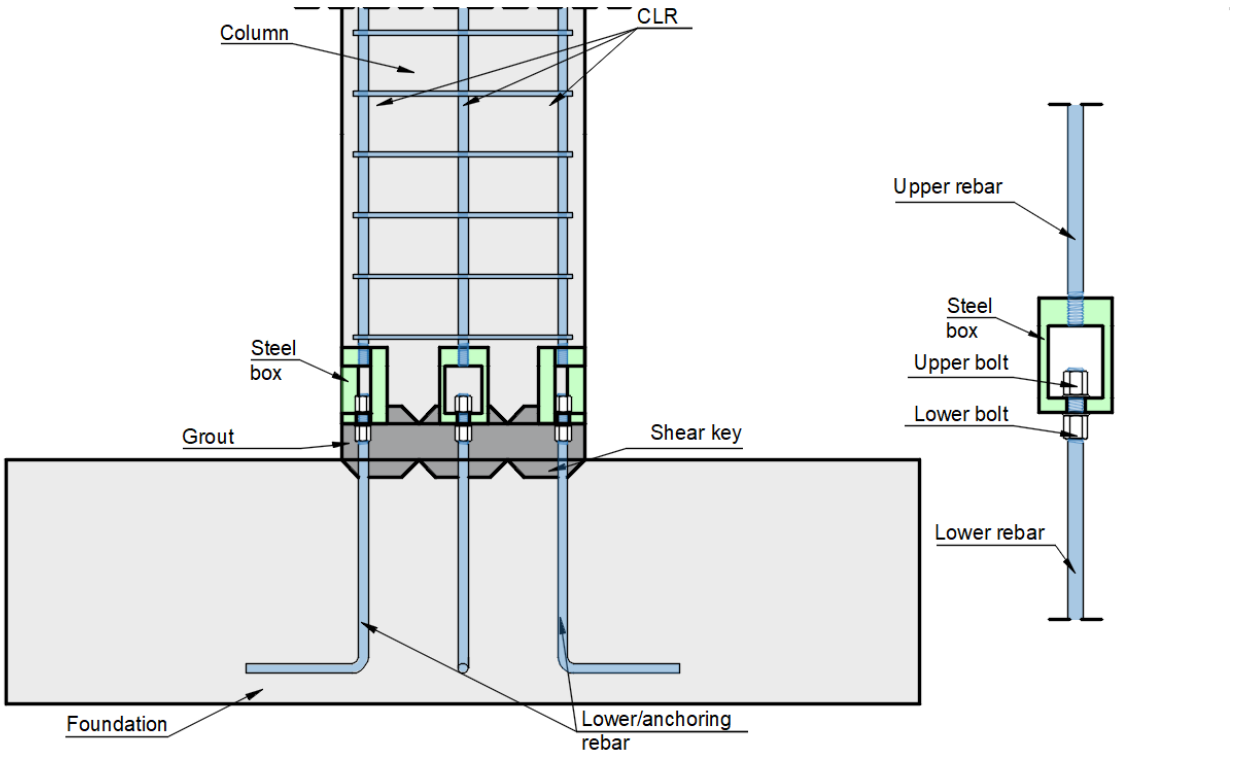

Figure 12. The CF connection with the steel box adapted from Quing et al. [67]

Guo et al. [68] proposed the replaceable solution of CF connection, which is illustrated in Figure 13. The column consisted of upper RC part and lower CFT part. The connection assembly included the CFT column part, embedded anchor bolts, the steel fuses (plates with slits), the buckling restraints and the padding blocks. The CFT part of column had two cross sections, with the narrower end. The gap between the steel fuse and narrow CFT cross section was filled with padding blocks. The steel fuse was connected to the embedded anchor bolts in CFT part of column. The two preinstalled bolts in the padding block were used to fix the buckling restraints against the steel fuses. Connection between the foundation and column was provided by connecting the steel fuses to the embedded anchor bolts in foundation.

The experimental investigation of cantilever column behaviour under cyclic load was performed. The cross-section of RC column part was b_c/h_c = 400/400 mm, while the narrow CFT column part had dimensions b_c/h_c = 240/240 mm. Twenty-four high strength anchor bolts with 24 mm in diameter were used to connect the steel fuses and CFT column and twenty embedded anchor bolts with 30 mm in diameter were used to connect the steel fuses and the foundation. Authors [68] varied padding block material and tested reparability of connection. Each specimen was tested twice: first to a drift ratio of 2%, and then, after disassembly and replacement of the steel fuses and padding blocks, to a drift ratio of 4%. From the experimental results, it was concluded that the seismic response of the specimen was mainly characterized by slipping and plastic deformations of steel fuses, followed by buckling at larger drift ratios. The rest of the connection elements remained unaffected. Up to the 2% drift ratio, the steel fuses deformed, but the disassembly procedure was performed without obstacles. The main conclusion of experimental testing was that the request of reparability was satisfied, and that the behaviour of the samples in the first and second testing was the same. Generally, in terms of seismic performance, all specimens showed adequate behaviour.

The comparable connection with steel jacket was developed by Yuan et al. [70]. They proposed the CC connection that is formed of two RC columns placed together into so-called the steel plate hoop. In this system, the CLR from the two columns is not directly connected; instead, the bars are bent at the column ends. During fabrication, holes are formed at the column ends, allowing bolts to pass through both the concrete sections and the surrounding steel hoop. The bolts are then secured with nuts, as illustrated in Figure 14 a). In this way two columns are connected without welding the CLR to the steel elements of connection or embedding steel elements into the concrete elements.

The seismic performance of the proposed system was evaluated through cyclic testing of cantilever columns and compared with cast-in-situ specimens. In addition, the length and the thickness of steel plate hoop were varied. The column cross-sectional dimensions were b_c/h_c = 400/400 mm, while the CLR were adopted as 8 Ø22. The embedded bolts were M22 with the steel category HRB400. The results showed that specimens with thicker and longer steel plate hoops did not exhibit tearing or buckling of the steel jacket during testing. Only minor concrete cover spalling was observed at the column base, and upon removal of the steel hoop, the internal concrete remained in good condition. In contrast, specimens with thinner steel hoops developed dense cracking at the column ends, accompanied by localized crushing of the cover concrete in the compression zone. Overall, the prefabricated columns demonstrated slightly higher strength and comparable stiffness relative to cast-in-situ columns. The proposed CC connection exhibited behaviour similar to monolithic construction, indicating its potential applicability in precast concrete frame systems in seismic regions.

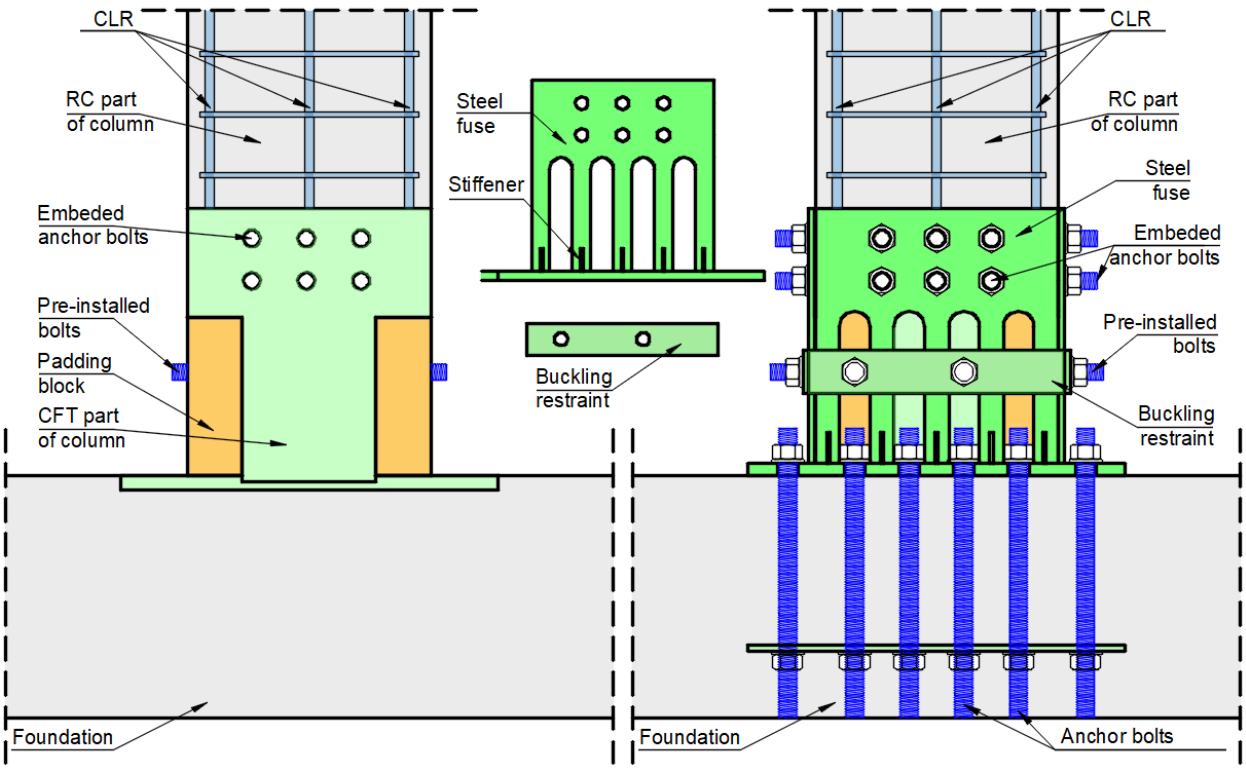

Figure 13. The configuration of the CF connection adapted from Guo et al. [68]

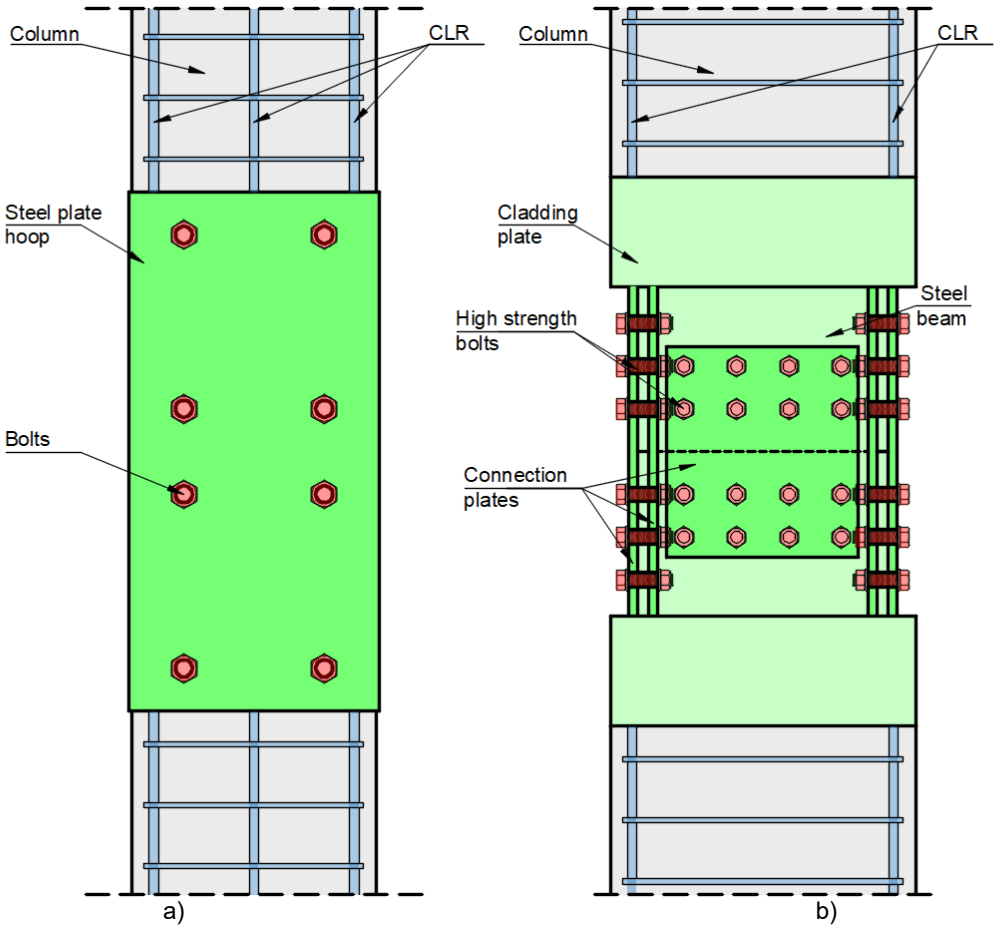

Figure 14. The configuration of the CC connection: a) adapted from Yuan et al. [70] and b) adapted from Zhan et al. [69]

The disassembly process was performed for the columns with thicker steel hoop plate, but the possibility of reuse was not discussed. It can be concluded that with the proper design of the steel hoop plate all connection elements could possibly be reused.

Zhan et al. [69] proposed similar solution for the CC connections, which is presented in Figure 14 b). The CFT part was connected to the RC part of the column with the studs, welded to the inner side of the cladding plate. In addition, CLR is welded to the interior of cladding plate. An I-shaped steel beam is also welded to the cladding plate, and the connection between two columns is achieved by joining the steel beams at the ends of the CFT segments using external steel plates, bolts, and nuts. The dimensions of column cross section were b_c/h_c = 500/500 mm, while the CLR were adopted as 4 Ø25.

The authors conducted only a finite element (FE) analysis to evaluate the behaviour of the proposed connection in comparison with a monolithic column under both monotonic and cyclic loading. The results indicated that the overall behaviour of the demountable connection is comparable to that of the monolithic system. At lower drift ratios, both systems exhibited similar responses, while at higher drift levels, the columns with CC connections showed slightly reduced strength. However, the ductility coefficient was higher for the columns with CC connections, and the yielding point remained similar for both samples. The demountability of the proposed connection was not addressed in the study. Furthermore, in the absence of experimental validation, it is difficult to discuss the level of damage of individual components, and the potential for reuse of the connection elements.

4 Discussion

4.1 Beam-to-column connections

In this section, different solutions for demountable precast beam-to-column joints were presented and discussed in terms of their strength, stiffness and ductility under lateral loads as well as their potential for disassembly, replacement and reuse after being subjected to the serviceability or ultimate load conditions. In general, the connections can be formed in two ways: (1) by welding or bolting reinforced bars, plates or steel embedments, with dry-packing or local grouting, or (2) by utilizing the unbonded post-tensioned tendons or rods.

It was demonstrated that the assumptions regarding the location of the connection (placed within or outside the critical region of the beam) and design of the connection (overdesigned or designed for ductility) can have major impact not only on the overall mechanical performance of the beam-to-column joints, but also on the extent of replacement or reuse possibilities.

A general, qualitative comparison of performance indicators of precast beam-to-column joints in respect to the monolithic joints or wet precast joints, is presented in Table 1. It can be seen that the precast joints with RC corbels and connections with steel boxes, with the connectors located within beam depth, have similar or higher bending resistance

compared to the monolithic joints. However, the initial stiffness, displacement ductility and energy dissipation are either similar or lower, which may require additional elements for ensuring lateral stiffness of the building structure, such as steel braces or RC walls. The performance indicators of connections with steel end plates or angles are generally better, since the through anchor bolts were placed outside beam's depth. Connections with dampers and fuses have good performance, particularly in terms of displacement ductility and energy dissipation capacity. Precast joints with semi-dry connections have similar performance as monolithic joints. Finally, joints with post-tensioned connections and dissipaters also have similar performance as monolithic joints, except the energy dissipation capacity. However, these joints have large self-centering capabilities with small residual deformations.

Table 1. Qualitative comparison of performance indicators of precast beam-to-column joints in respect to monolithic or wet precast beam-to-column joints

Precast connection type / Study	Connection category	Bending resistance	Initial stiffness (Type of joint rigidity)	Displacement ductility	Energy dissipation
Connections with RC corbels [17], [19], [20], [21], [22]	Ductile	Similar or higher	Lower (semi-rigid)	Similar or lower	Similar or lower
Connections with steel boxes [24], [25], [26]	Ductile or overdesigned	Similar or higher	Similar or lower (semi-rigid)	Similar or lower	Similar or lower
Connections with end plates or steel angles [28], [29], [34], [36], [37]	Overdesigned	Similar	Similar (rigid)	Similar or higher	Similar or higher
Connections with dampers and fuses [38], [39], [41], [40], [42], [43]	Ductile	Similar or higher	Similar or higher (rigid)	Higher	Higher
Connections with partial in-situ concreting [45], [46], [47]	Placed outside critical region of beam	Similar	Similar or higher (rigid)	Similar	Similar
Post-tensioned connections with dissipating elements [49], [50]	Ductile	Similar	Similar (rigid)	Similar	Similar or lower

Possibilities of disassembly, replacement and reuse for each connection type are presented in Table 2. In all cases, the disassembly of the connections was considered possible or explicitly demonstrated by authors, albeit the difficulty and extent of the necessary works varied between the solutions. As stated earlier, the replacement and reuse possibilities strongly depend on the design assumptions and the location on the connection, i.e., the location where the major damage occurs. Since the "strong column-weak beam" concept was employed in almost all cases, with small to none damage occurring in columns, the majority of the proposed solutions could potentially provide at least the reuse of precast columns. The exceptions are joints with corbels or protruding beams which experienced high extent of the damage during testing. In case of connections with dampers and fuses, as well as the post-tensioned connections, which are designed to ensure practically elastic behaviour of precast beams and columns, it seems that both beams and columns have great potential for reuse.

It should be noted, however, that in the research presented in this section, the possibilities for reuse of precast beam-to-column joints are mainly commented and examined after the failure of the tested specimens was reached. In other words, these situations mainly correspond to the repairment of structure after strong earthquakes. It is a completely different question if the structural elements can be disassembled, relocated and reused after frequent earthquakes or at the end-of-life scenario, with the similar behaviour as the original structure. In those circumstances, the level of damage to the structural elements is expected to be much lower, and possibility of reuse of both beams and columns is expected to be higher. Further research is needed to address these aspects of the replacement and reuse.

Finally, the presented solutions for demountable precast beam-to-column joints vary in their complexity, the construction time, difficulty of disassembly and the amount of steel components, which ultimately prevails in the decision-making process regarding the use of specific connection type.

Table 2. Qualitative presentation of disassembly, replacement and reuse potential possibilities for precast beam-to-column joints

Precast connection type (Study)	Major damage	Disassembly	Replacement	Reuse
Connections with RC corbels [17], [20], [21], [22]	Connection and/or beam	Yes, relatively easy	Connection and/or beam	Column or none
Connections with steel boxes [24], [25], [26]	Boxes, bolts and/or beam	Yes, relatively easy	Connection and/or beam	Column
Connections with end plates or steel angles [28], [29], [34], [35], [36], [37]	Beam	Yes, relatively easy	Beam and connection	Column
Connections with dampers and fuses [38], [39], [40], [41], [42], [43]	Connection	Yes, relatively easy	Connection	Column and beam
Connections with partial in-situ concreting [44], [45], [46], [47]	Protruding beam from the column	Yes, requires hammering and cutting	Connection	Beam
Post-tensioned connections with dissipating elements [49], [50]	Dissipating elements	Yes, can require cutting	Dissipating elements	Column and beam

4.2 Column-to-foundation and column-to-column connections

The reviewed studies demonstrate significant progress in the development of demountable CF and CC connections for precast reinforced concrete structures. A wide range of solutions has been investigated, primarily distinguished by the type of mechanical device used to transfer forces, including steel flange plates, column shoes, and steel jacket systems.

Table 3 summarizes the performance indicators of the previously reviewed connection types. The analysis includes only studies in which the behaviour of precast demountable connections was compared with that of equivalent monolithic specimens. Despite differences in detailing, most proposed connections aim to achieve structural performance comparable to monolithic systems while enabling partial or full demountability.

Across all connection types, experimental and numerical investigations consistently indicate that properly designed demountable connections can satisfy strength, stiffness, and ductility requirements. Flexural failure mechanisms dominated, characterized by concrete cracking, reinforcement yielding, spalling, and, in some cases, bar buckling or fracture. This confirms that capacity design principles can be achieved, with inelastic deformations concentrated in ductile regions.

However, the location and distribution of damage vary depending on the connection concept. Steel flange plate systems often rely on overdesign to ensure that damage occurs in the column rather than in the connection, resulting in stable and predictable behaviour but limited reusability of the column. The column shoe connections seismic performance strongly depends on the behaviour of anchor elements and the bond between grout and steel components. Capacity design requirements are generally satisfied, with damage concentrated either in the column or in designated ductile components such as anchor bolts or energy-dissipating devices. Steel jacket systems, particularly those incorporating replaceable components such as steel fuses or energy-dissipating bolts, allow better control over the location of inelastic deformations.

The qualitative presentation of demountable CC and CF connection in terms of reusability is also shown in table 3. Among the investigated systems, only a limited number of studies explicitly validated demountability through experimental disassembly and reassembly procedures [29], [56], [61]–[63]. The systems presented in these studies allowed damaged components to be removed and replaced after seismic loading, while the primary structural elements (e.g., foundation, steel plates, or even column segments) remained mostly intact. In contrast, many solutions rely on overdesign principles, which ensure that the connection remains elastic while damage is concentrated in the RC column. In such cases, reuse is typically limited to the foundation and embedded steel components, as the column itself experiences irreversible damage.

In terms of demountability and reuse, solutions proposed by Guo et al. [68] incorporating replaceable components show clear advantages. The steel fuses solution enables repair and reuse of key structural parts, while other systems indicate potential but lack experimental verification; consequently, reuse is typically limited to steel components and foundations.

Table 3. Qualitative comparison of performance indicators of precast CC and CF joints in respect to monolithic joints and qualitative presentation of disassembly and reuse potential possibilities for CF and CC joints

Study	Connection type	Mechanical device	Bending resistance	Initial stiffness	Displacement ductility	Energy dissipation	Major damage	Disassembly	Reuse
[59], [60]	CF	Steel flange plate/welding	Higher or similar	Higher or similar	Similar	Higher or similar	Column/buckling of CLR	Not performed/ potentionaly relatively easy	Foundation
[61]	CF	Steel flange plate/welding	Similar	Similar	Higher	Higher	Column	Performed without obstacles	Foundation
[61]	CC	Steel flange plate/welding	Higher or similar	Similar	Higher	Higher	Column	Performed without obstacles	Lower column
[55]	CF	Steel flange plate/rivet head CLR	Similar	Similar	Similar	Similar	Column/buckling of CLR	Not performed/ potentionaly relatively easy	Foundation
[62], [63], [64]	CC	Steel flange plate/threaded CLR	Similar	Similar	Similar	Similar	Column/buckling of CLR/steel plate deformation	Performed without obstacles	Upper and lower column
[65]	CF	Column shoe	Similar	Similar	Similar	Similar	Column/bond between grout and column shoe	Not performed/ potentionaly relatively easy	Foundation
[65]	CC	Column shoe	Similar or higher	Similar or higher	Similar or higher	Similar or higher	Column/bond between grout and column shoe	Not performed/ potentionaly relatively easy	Upper column
[54]	CF	Column shoe	Similar	Similar	Similar	Similar	Failure of anchor bolt	Not performed/ potentionaly relatively easy	Foundation
[51]	CF	Column shoe	Similar or lower	Similar or lower	Similar or lower	Similar or lower	Column	Not performed/ potentionaly relatively easy	Foundation
[66], [67]	CF	Column shoe/steel box	Similar	Similar	Similar	Similar	Column	Not performed/ potentionaly relatively easy	Foundation
[70]	CC	Steel jacket	Similar	Similar	Similar	Similar	Column	Performed without obstacles	Upper and lower column

5 Conclusions

The reuse of concrete elements has gained considerable attention in recent years as a promising approach for improving the sustainability of the concrete construction industry. Although comprehensive experimental and numerical investigations of the behaviour of demountable connections between precast frame elements has been conducted, the reusability of elements and their connections remains limited for many connection types. This lack of detailed knowledge represents one of the major barriers to the wider practical application of structural concrete reuse. Therefore, the authors aimed to address this challenge by reviewing and analysing the current state of the art for demountable connections in precast frame systems.

Based on the analysis of available experimental and numerical research of precast beam-to-column joints and frames, which is mainly focused on the performance under cyclic (seismic) loads, the following conclusions regarding precast beam-to-column connections can be drawn:

– Most of the presented connections were realised with bolts or threaded rods, couplers (threaded sleeves), and

steel elements such as plates, boxes, angles, I-sections, etc. Other connections include welding of some components (mainly longitudinal reinforcement or threaded rods), partial in-situ concreting or prestressing via post-tensioned strands.

– The behaviour of precast beam-to-column joints depends strongly on the adopted design approach and on the location of the connection relative to the beam-to-column interface. Although adequate strength can be achieved in all the moment-resisting connections presented, other seismic performance indicators, such as stiffness, ductility and energy dissipation, vary across the solutions. In this regard, at present, the most promising solutions seem to be connections with steel end plates or angles (with connectors placed outside the beam's depth), partial in-situ concreting, and connections with steel dampers and fuses.

– All analysed connection solutions can be demounted. Apart from bolted connections, this also applies to connections that involve welding of some components and partial in-situ concreting. In the latter cases, although hammering and cutting were employed, some authors have stated that the mechanical removal process was not too difficult and time-consuming.

– It was demonstrated that the replacement and reuse possibilities also depend on the adopted design approach and the location of the connection, i.e., the location of the major damage under imposed load (monotonic or cyclic). The majority of the analysed connection solution could provide the reusability of precast columns. The exceptions are precast joints with protruding beams (long corbels) extending from precast column, which experienced damage during testing. However, in those cases, it was demonstrated by some authors that the reuse of precast beams is possible with new columns. The reuse of both beams and columns seems to be possible for the connection solutions that employ dissipating connections, which mitigate damage from beams and columns, such as connections steel dampers, fuses and dissipaters.

– For practical implementation, the reuse possibilities of precast beams and columns, as well as their connections, should be carefully examined and verified. The scenarios at the end-of-life of the building or after frequent (low intensity) earthquakes might contribute to these possibilities. Finally, the complexity, the construction time, difficulty of disassembly and the amount of steel components used for the connection, can ultimately prevail in the decision-making process regarding the use of specific connection type for precast frames.

From the literature review of demountable column-to-foundation (CF) and column-to-column (CC) connections, the following conclusions can be drawn:

– Demountable connections are primarily realised with steel-based mechanical devices, such as steel plates, bolts, threaded bars, and couplers, which enable force transfer and potential disassembly.

– The CF and CC connections are predominantly investigated under cyclic loading conditions, with focus on capacity design behaviour and comparison to monolithic reinforced concrete specimens

– Overall, demountable CF and CC connections represent a viable alternative to traditional monolithic construction, offering comparable structural performance with added benefits in terms of adaptability and potential reuse.

– Achieving a fully reusable system requires careful balance between capacity design, damage control, and connection detailing. While significant progress has been made, further experimental validation and design optimisation are needed to fully realise the potential of demountable precast concrete systems

– Experimental validation of demountability is still scarce, particularly regarding repeated assembly–disassembly cycles and long-term performance.

– The majority of studies focus on individual components or simplified configurations, with limited investigation of system-level behaviour in realistic structural frameworks.

Acknowledgements

The authors would like to express their gratitude to the CircBoost – Boosting Circular Economy in Construction Industry, funded by the European Union under the Horizon Europe research and innovation programme (Grant Agreement No. 101082068) and Ministry for Education, Science, and Technology, Republic of Serbia (Grant number 200092).

CRediT authorship contribution statement

Milica Vidović: Conceptualization, Methodology, Data curation, Visualization, Writing - original draft, Writing - review & editing.

Ivan Milićević: Conceptualization, Methodology, Data curation, Visualization, Writing - original draft, Writing - review & editing.

Jelena Carević: Visualization, Writing - review & editing.

Declaration of competing interest

The authors declare that they have no known competing financial interests or personal relationships that could have appeared to influence the work reported in this paper.

References

[1] M. Stamenić, "Mix design of concrete incorporating fine recycled concrete aggregates – a review," Build. Mater. Struct., vol. 68, no. 3, p. 2500008S, 2025.

[2] A. Radović, V. Carević, and S. Marinković, "Impact of the water-curing time on the carbonation initiation period of high-volume limestone powder concrete," Build. Mater. Struct., vol. 68, no. 2, p. 2500004R, 2025, doi: 10.5937/grmk2500004r.

[3] J. Dragaš, S. Marinković, V. Radonjanin "Prediction models for high-volume fly ash concrete practical application: mechanical properties and experimental database," Build. Mater. Struct., vol. 64, no. 1, pp. 19–43, 2021.

[4] A. Favier, C. De Wolf, K. Scrivener, and G. Habert, "A sustainable future for the European Cement and Concrete Industry Technology assessment for full decarbonisation of the industry by 2050," 2018, doi.org/10.3929/ethz-a-010025751

[5] J. Devènes, M. Bastien-Masse, and C. Fivet, "Reusability assessment of reinforced concrete components prior to deconstruction from obsolete buildings," *J. Build. Eng.*, vol. 84, no. June 2023, p. 108584, 2024, doi: 10.1016/j.jobe.2024.108584.

[6] I. Bertin, M. Saadé, R. Le Roy, J. M. Jaeger, and A. Feraille, "Environmental impacts of Design for Reuse practices in the building sector," *J. Clean. Prod.*, vol. 349, no. February, 2022, doi: 10.1016/j.jclepro.2022.131228.

[7] Z. Al-Faesly, "Feasibility of Reuse in the Concrete Industry," University of Ottawa, 2021.

[8] J. Carević, I. Milićević, M. Vidović, "Demountable connections for structural concrete reusability - State of the art and future directions for reinforced concrete, Part I: slabs" Build. Mater. Struct., (under review).
[9] T. M. Fayyad and A. F. Abdalqader, "Demountable reinforced concrete structures : A review and future directions," *Civ. Eng. Res. Irel. 2020 Demountable*, pp. 218–222, 2020.
[10] fib, *fib bulletin 27 - Seismic design of precast concrete building structures*, vol. 1994. 2003.
[11] European Committee for Standardization, *Eurocode 8: Design of structures for earthquake resistance — Part 1: General rules, seismic actions and rules for buildings*. 2015.
[12] B. Zoubek, T. Isakovic, Y. Fahjan, and M. Fischinger, "Corrigendum to 'Cyclic failure analysis of the beam-to-column dowel connections in precast industrial buildings' [Eng. Struct. 52 (2013) 179-191]," *Eng. Struct.*, vol. 57, p. 276, 2013, doi: 10.1016/j.engstruct.2013.09.036.
[13] N. Batalha, H. Rodrigues, A. Arêde, A. Furtado, R. Sousa, and H. Varum, "Cyclic behaviour of precast beam-to-column connections with low seismic detailing," no. June 2021, pp. 1–19, 2022, doi: 10.1002/eqe.3606.
[14] C. W. French, M. Hafner, and V. Jayashankar, "Connections between precast elements - failure within connection region," vol. 115, no. 12, pp. 3171–3192, 1990.
[15] R. E. Englekirk, "Development and Testing of a Ductile Connector for Assembling Precast Concrete Beams and Columns," *PCI J.*, vol. 40, no. 2, pp. 36–51, 1995.
[16] K. S. Elliott, G. Davies, M. Ferreira, H. Gorgun, and A. A. Mahdi, "Can precast concrete structures be designed as semi-rigid frames? Part 1 – The experimental evidence," *Struct. Eng.*, vol. 81, no. 16, pp. 14–19, 2003.
[17] D. A. Bournas, P. Negro, and F. J. Molina, "Pseudodynamic tests on a full-scale 3-storey precast concrete building : Behavior of the mechanical connections and floor diaphragms," *Eng. Struct.*, vol. 57, pp. 609–627, 2013, doi: 10.1016/j.engstruct.2013.05.046.
[18] P. Negro, D. A. Bournas, and F. J. Molina, "Pseudodynamic tests on a full-scale 3-storey precast concrete building : Global response," *Eng. Struct.*, vol. 57, pp. 594–608, 2013, doi: 10.1016/j.engstruct.2013.05.047.
[19] Y. Zhong, F. Xiong, J. Chen, A. Deng, W. Chen, and X. Zhu, "Experimental Study on a Novel Dry Connection for a Precast Concrete Beam-To-Column Joint," *Sustainability*, vol. 11, no. 17, p. 4543, 2019, doi: doi:10.3390/su11174543.
[20] K. Ding, Y. Ye, and W. Ma, "Seismic performance of precast concrete beam-column joint based on the bolt connection," vol. 232, p. 111884, 2021, doi: 10.1016/j.engstruct.2021.111884.
[21] J. Liu, Y. Liu, and D. Yu, "Experimental and Numerical Studies on the Seismic Performance of New Assembled Concrete Frame," *Buildings*, vol. 13, p. 329, 2023, doi: https://doi.org/10.3390/ buildings13020329.
[22] T. Krishnan and R. Purushothaman, "Effect of stiffeners in cleat angle based precast beam-column connections under reverse cyclic loading," *Structures*, vol. 25, pp. 161–172, 2020, doi: 10.1016/j.istruc.2020.03.012.
[23] R. Vidjeapriya and K. P. Jaya, "Experimental Study on Two Simple Mechanical Precast Beam-Column Connections under Reverse Cyclic Loading," *J. Perform. Constr. Facil.*, vol. 27, no. July/August, pp. 402–414, 2013, doi: 10.1061/(ASCE)CF.1943-5509.0000324.
[24] R. Zhang, Y. Zhang, A. Li, and T. Y. Yang, "Experimental study on a new type of precast beam-column joint," *J. Build. Eng.*, vol. 51, p. 104252, 2022, doi: 10.1016/j.jobe.2022.104252.
[25] R. Zhang, T. Guo, and A. Li, "Thin-Walled Structures Experimental investigation into demountable dry connections for fully precast frame structures through shaking table tests," *Thin-Walled Struct.*, vol. 201, p. 112014, 2024, doi: 10.1016/j.tws.2024.112014.
[26] H. Zhang, W. Huang, J. Li, and W. Quan, "Seismic behavior of precast concrete beam-to-column connection with double box bolted couplers," *Eng. Struct.*, vol. 326, p. 119499, 2025, doi: 10.1016/j.engstruct.2024.119499.
[27] C. Liu, X. Chen, X. Mao, B. Zhu, and B. Liu, "Shear resistance of an anchoring coupler applied in demountable concrete connection at varying shear positions," *Structures*, vol. 55, pp. 866–875, 2023, doi: 10.1016/j.istruc.2023.06.088.
[28] M. Senturk, S. Pul, A. Ilki, and I. Hajirasouliha, "Development of a monolithic-like precast beam-column moment connection : Experimental and analytical investigation," *Eng. Struct.*, vol. 205, p. 110057, 2020, doi: 10.1016/j.engstruct.2019.110057.
[29] J. D. Nzabonimpa, W. K. Hong, and S. C. Park, "Experimental investigation of dry mechanical beam–column joints for precast concrete based frames," *Struct. Des. Tall Spec. Build.*, vol. 26, no. 1, Jan. 2016, doi: 10.1002/tal.1302.
[30] B. Milosavljević, I. Milićević, M. Pavlović, and M. Spremić, "Static behaviour of bolted shear connectors with mechanical coupler embedded in concrete," *Steel Compos. Struct.*, vol. 29, no. 2, pp. 257–272, 2018, doi: 10.12989/scs.2018.29.2.257.
[31] I. Milićević, B. Milosavljević, M. Pavlović, and M. Spremić, "Bolted connectors with mechanical coupler embedded in concrete: Shear resistance under static load," *Steel Compos. Struct.*, vol. 36, no. 3, pp. 321–337, 2020, doi: 10.12989/scs.2020.36.3.321.
[32] I. Milićević, B. Milosavljević, M. Spremić, R. Mandić, and M. Popović, "Local behaviour of the connector with mechanical coupler and rebar anchor under tension load," *Build. Mater. Struct.*, vol. 66, no. 2, p. 2300002M, 2023, doi: 10.5937/grmk2300002m.
[33] I. Milićević, B. Milosavljević, and M. Spremić, "Behavior of Demountable Connections with Taper Threaded Mechanical Coupler (TTC) and Rebar Anchor Under Tension Load," *Buildings*, vol. 15, no. 6, pp. 1–30, 2025, doi: 10.3390/buildings15060928.
[34] P. K. Aninthaneni, R. P. Dhakal, J. Marshall, and J. Bothara, "Nonlinear Cyclic Behaviour of Precast Concrete Frame Sub-Assemblies With 'Dry' End Plate Connection," *Structures*, vol. 14, pp. 124–136, 2018, doi: 10.1016/j.istruc.2018.03.003.
[35] P. K. Aninthaneni and R. P. Dhakal, "Demountable Precast Concrete Frame–Building System for Seismic Regions: Conceptual Development," *J. Archit. Eng.*, vol. 23, no. 4, pp. 1–10, 2017, doi: 10.1061/(asce)ae.1943-5568.0000275.

[36] P. K. Aninthaneni, R. P. Dhakal, J. Marshall, and J. Bothara, “Seismic performance of sub-assembly of a demountable precast concrete frame building,” in *Proceedings of the Tenth Pacific Conference on Earthquake Engineering, Building an Earthquake-Resilient Pacific*, 2015, no. 6-8 November 2015, pp. 189–198.

[37] Z. Y. Li, S. B. Kang, H. He, W. Q. Lu, H. J. Liu, and C. J. Lu, “Seismic behaviour of precast concrete beam-column connections with bolted end plates,” *Structures*, vol. 58, no. October, p. 105343, 2023, doi: 10.1016/j.istruc.2023.105343.

[38] C. Wu *et al.*, “A detachable configuration for the precast beam-column connection using metallic damper as connector : Experimental investigation,” *J. Build. Eng.*, vol. 65, p. 105597, 2023, doi: 10.1016/j.jobe.2022.105597.

[39] J. Bai, J. He, C. Li, S. Jin, and H. Yang, “Experimental investigation on the seismic performance of a novel damage-control replaceable RC beam-to-column joint,” *Eng. Struct.*, vol. 267, p. 114692, 2022, doi: 10.1016/j.engstruct.2022.114692.

[40] W. Huang, G. Hu, and J. Zhang, “Experimental study on the seismic performance of new precast concrete beam-column joints with replaceable connection,” *Structures*, vol. 35, pp. 856–872, 2022, doi: 10.1016/j.istruc.2021.11.050.

[41] W. Li, W. Chen, X. Lin, L. Chen, H. Lv, and K. Shao, “Cyclic behavior and damage mechanisms of a demountable RC joint : Integrated experimental and analytical study,” *Structures*, vol. 79, p. 109609, 2025, doi: 10.1016/j.istruc.2025.109609.

[42] L. Xie, J. Wu, J. Zhang, and C. Liu, “Experimental study of mechanical properties of beam-column joint of a replaceable energy-dissipation connector-precast concrete frame,” *J. Build. Eng.*, vol. 43, p. 102588, 2021, doi: 10.1016/j.jobe.2021.102588.

[43] Z. Wang, D.-C. Feng, and G. Wu, “Experimental Study on Seismic Behavior of Precast Bolt-Connected Steel-Members End-Embedded Concrete (PBSEC) Beam-Column Connections,” *Buildings*, 2022.

[44] K. C. G. Ong, Z. S. Li, L. R. Chandra, C. T. Tam, and S. D. Pang, “Experimental investigation of a DfD moment-resisting beam – column connection,” *Eng. Struct.*, vol. 56, pp. 1676–1683, 2013, doi: 10.1016/j.engstruct.2013.08.006.

[45] J. Xiao, T. Ding, and Q. Zhang, “Structural behavior of a new moment-resisting DfD concrete connection,” *Eng. Struct.*, vol. 132, pp. 1–13, 2017, doi: 10.1016/j.engstruct.2016.11.019.

[46] J. Xiao, Z. Chen, T. Ding, and B. Xia, “Effect of recycled aggregate concrete on the seismic behavior of DfD beam- column joints under cyclic loading,” *Adv. Struct. Eng.*, vol. 24, no. 8, pp. 1–15, 2020, doi: 10.1177/1369433220982729.

[47] T. Ding, J. Xiao, E. Chen, and A.-R. Khan, “Experimental Study of the Seismic Performance of Concrete Beam-Column Frame Joints with DfD Connections,” vol. 146, no. 4, p. 04020036, 2020, doi: 10.1061/(ASCE)ST.1943-541X.0002576.

[48] M. J. N. Priestley and J. R. Tao, “Seismic Response of Precast Prestressed Concrete Frames With Partially Debonded Tendons,” *PCI J.*, vol. 38, no. 1, pp. 58–67, 1993.

[49] H. Wang, E. M. Marino, P. Pan, H. Liu, and X. Nie, “Experimental study of a novel precast prestressed reinforced concrete beam-to-column joint,” *Eng. Struct.*, vol. 156, pp. 68–81, 2018, doi: 10.1016/j.engstruct.2017.11.011.

[50] X. Cai, Z. Pan, Y. Zhu, N. Gong, and Y. Wang, “Experimental and numerical investigations of self-centering post-tensioned precast beam-to-column connections with steel top and seat angles,” *Eng. Struct.*, vol. 226, p. 111397, 2021, doi: 10.1016/j.engstruct.2020.111397.

[51] N. Sripongngam, N. Wonghiran, P. Thongou, S. Thianthong, E. Yooprasertchai, and C. Jaturapitakkul, “Development and experimental study of innovative precast column – footing connections with self-centering and energy-dissipating bolts,” *Structures*, vol. 86, no. December 2025, p. 111305, 2026, doi: 10.1016/j.istruc.2026.111305.

[52] R. Nascimbene and L. Bianco, “Cyclic response of column to foundation connections of reinforced concrete precast structures: Numerical and experimental comparisons,” *Eng. Struct.*, vol. 247, no. August, 2021, doi: 10.1016/j.engstruct.2021.113214.

[53] D. Figueira, A. Ashour, G. Yıldırım, A. Aldemir, and M. Şahmaran, “Demountable connections of reinforced concrete structures: Review and future developments,” *Structures*, vol. 34, no. September, pp. 3028–3039, 2021, doi: 10.1016/j.istruc.2021.09.053.

[54] B. Dal Lago, G. Toniolo, and M. Lamperti Tornaghi, “Influence of different mechanical column-foundation connection devices on the seismic behaviour of precast structures,” *Bull. Earthq. Eng.*, vol. 14, no. 12, pp. 3485–3508, 2016, doi: 10.1007/s10518-016-0010-9.

[55] S. Pul, M. Senturk, A. Ilki, and I. Hajirasouliha, “Experimental and numerical investigation of a proposed monolithic-like precast concrete column-foundation connection,” *Eng. Struct.*, vol. 246, no. September, p. 113090, 2021, doi: 10.1016/j.engstruct.2021.113090.

[56] Q. Zhou, Y. Liu, and Y. Li, “Load transfer mechanism of precast concrete piers with demountable connections,” *Eng. Struct.*, vol. 261, Jun. 2022, doi: 10.1016/j.engstruct.2022.114287.

[57] Q. Zhang *et al.*, “Behavior and design of demountable and replaceable RC columns with bolted flange connections under eccentric compression,” *Eng. Struct.*, vol. 310, no. March, 2024, doi: 10.1016/j.engstruct.2024.118138.

[58] M. Orlando and L. R. Piscitelli, “Experimental investigation on static and cyclic behaviour of flanged unions for precast reinforced concrete columns,” *Eur. J. Environ. Civ. Eng.*, vol. 22, no. 8, pp. 927–945, 2018, doi: 10.1080/19648189.2016.1229226.

[59] R. Aktepe *et al.*, “Fully demountable column base connections for reinforced CDW-based geopolymer concrete members,” *Eng. Struct.*, vol. 290, no. May, p. 116366, 2023, doi: 10.1016/j.engstruct.2023.116366.

[60] S. Akduman *et al.*, “Structural performance of construction and demolition waste-based geopolymer concrete columns under combined axial and lateral cyclic loading,” *Eng. Struct.*, vol. 297, no. May, p. 116973, 2023, doi: 10.1016/j.engstruct.2023.116973.

[61] J. Liu, Y. Xue, C. Wang, J. Nie, and Z. Wu, “Experimental investigation on seismic performance of mechanical joints with bolted flange plate for precast concrete column,” *Eng. Struct.*, vol. 216, no. September 2019, p. 110729, 2020, doi: 10.1016/j.engstruct.2020.110729.

[62] J. D. Nzabonimpa, W. K. Hong, and J. Kim, "Mechanical connections of the precast concrete columns with detachable metal plates," *Struct. Des. Tall Spec. Build.*, vol. 26, no. 17, pp. 1–14, 2017, doi: 10.1002/tal.1391.

[63] J. D. Nzabonimpa and W. K. Hong, "Structural performance of detachable precast composite column joints with mechanical metal plates," *Eng. Struct.*, vol. 160, no. June 2017, pp. 366–382, 2018, doi: 10.1016/j.engstruct.2018.01.038.

[64] J. Y. Hu, W. K. Hong, and S. C. Park, "Experimental investigation of precast concrete based dry mechanical column–column joints for precast concrete frames," *Struct. Des. Tall Spec. Build.*, vol. 26, no. 5, pp. 1–15, 2017, doi: 10.1002/tal.1337.

[65] G. Wang, Y. Li, Z. Li, and J. M. Ingham, "Experimental and numerical study of precast concrete columns with hybrid bolted splice connections," *Structures*, vol. 28, no. August, pp. 17–36, 2020, doi: 10.1016/j.istruc.2020.08.042.

[66] Y. Qing, C. Wang, S. Meng, and B. Zeng, "Experimental study on the seismic performance of precast concrete columns with thread-bolt combination couplers," *Eng. Struct.*, vol. 251, no. PA, p. 113461, 2022, doi: 10.1016/j.engstruct.2021.113461.

[67] Y. Qing, Y. Yuan, C. L. Wang, S. Meng, and B. Zeng, "Experimental study of precast columns with a hybrid joint incorporating bolted couplers and grouted sleeves," *J. Build. Eng.*, vol. 74, no. February, pp. 1–17, 2023, doi: 10.1016/j.jobe.2023.106878.

[68] Y. T. Lu, Z. X. Guo, Y. Liu, and S. H. Basha, "Performance of prefabricated RC column with replaceable Column-Base connection under cyclic lateral loads," *Eng. Struct.*, vol. 240, no. April, p. 112343, 2021, doi: 10.1016/j.engstruct.2021.112343.

[69] H. Zhan, M. Ye, J. Jiang, Y. Gao, C. W. Zheng, and S. C. Duan, "Structural performance of detachable precast concrete column-column joint," *Heliyon*, vol. 10, no. 5, pp. 1–17, 2024, doi: 10.1016/j.heliyon.2024.e27308.

[70] D. Yuan, Q. Shang, C. Han, J. Sun, and Q. Li, "Seismic Performance of Precast Concrete Column-to-Column Joint Using the Steel Plate Hoop and Bolts Connection," *Adv. Civ. Eng.*, vol. 2023, 2023, doi: 10.1155/2023/6636781.

Building Materials and Structures

GUIDE FOR AUTHORS

In the journal *Building Materials and Structures*, the submission and review processes take place electronically. Manuscripts are submitted electronically (online) on the website http://www.buildingmaterialsstructures.com**.** The author should register first, then log in and finally submit the manuscript in English language, which should be in the form of editable files (e.g. Word) to enable the typesetting process in journal format. All correspondence, including Editor´s decision regarding required reviews and acceptance of manuscripts, take place via e-mail. Contributions to the journal shall be submitted in English language.

TYPES OF ARTICLES

The following types of articles are published in *Building Materials and Structures:*

Original scientific article. It is the primary source of scientific information, new ideas and insights as a result of original research using appropriate scientific methods. The results are presented briefly, but in a way to enable readers to assess the results of experimental or theoretical/numerical analyses, so that the research can be repeated and yield with the same or results within the limits of tolerable deviations.

Review article. It presents the state of science in particular area as a result of methodically systematized, analyzed and discussed reference data. Only critical review manuscripts will be considered as providing novel perspective and critical evaluation of the topics of interest to broader BMS readership.

Preliminary report. Contains the first short notifications of research results without detailed analysis, i.e. it is shorter than original research paper.

Technical article. Reports on the application of recognized scientific achievements of relevance to the field of building materials and structures. Contain critical analysis and recommendations for adaption of the research results to practical needs.

Projects Notes. Project Notes provide a presentation of a relevant project that has been built or is in the process of construction. The original or novel aspects in design or construction should be clearly indicated.

Discussions. Comment on or discussion of a manuscript previously published in *Building Materials and Structures*. It should be received by the Editor-in-Chief within six months of the online publication of the manuscript under discussion. Discussion Papers will be subject to peer review and should also be submitted online. If Discussion Paper is selected for publication the author of the original paper will be invited to respond, and Discussion Paper will be published alongside any response that the author.

Other contributions

Conference Reports. Reports on major international and national conferences of particular interest to *Building Materials and Structures*. Selected and/or awarded papers from the ASES Conferences are published in Special issues.

Book Reviews. Reviews on new books relevant to the scope of *Building Materials and Structures*.

PREPRINTS

These are the author's own write-up of research results and analysis that has not been peer reviewed, nor had any other value added to it by a publisher (such as formatting, copy-editing, technical enhancements and the like). Authors can share their preprint anywhere at any time. If accepted for publication, we encourage authors to link from the preprint to their formal publication via its Digital Object Identifier (DOI). Preprints should not be added to or enhanced in any way in order to appear more like, or to substitute for, the final versions of articles.

MANUSCRIPT STRUCTURE

The manuscript should be typed one-sided on A4 sheets. Page numbers should be included in the manuscript and the text should be single spaced with **consecutive line numbering** - these are essential peer review requirements. The figures and tables included in the single file should be placed next to the relevant text in the manuscript. The corresponding captions should be placed directly below the figure or table. If the manuscript contains Supplementary material, it should also be submitted at the first submission of the manuscript for review purposes.

There are no strict rules regarding the structure of the manuscript, but the basic elements that it should contain are: Title page with the title of the manuscript, information about the authors, abstract and keywords, Introduction, Materials / Methods, Results/Discussion, and Conclusions.

The front page

The front page contains the title of the manuscript which should be informative and concise; abbreviations and formulas should be avoided.

Information about the authors are below the title; after the author's name, ORCID, a superscript number is placed indicating his/her affiliation, which is printed below the author's name, and before the abstract. It is obligatory to mark the corresponding author with superscript *) and provide his/her e-mail address. The affiliation should contain the full name of the institution where the author performed the research and its address.

Abstract

Abstract should contain 150-200 words. Motivation and objective of the conducted research should be presented; main results and conclusions should be briefly stated as well. References and abbreviations should be avoided.

Keywords

Keywords (up to 10) should be listed immediately after the abstract; abbreviations should be used only if they are generally accepted and well-known in the field of research.

Division into chapters

The manuscript should be divided into chapters and sub-chapters, which are hierarchically numbered with Arabic numbers. The headings of chapters and sub-chapters should appear on their own separate lines.

At the end of the manuscript, and before the references, it is obligatory to list the following statements:

CRediT authorship contribution statement

For transparency, we require corresponding authors to provide co-author contributions to the manuscript using the relevant CRediT roles. The CRediT taxonomy includes 14 different roles describing each contributor's specific contribution to the research output. The roles are: Conceptualization; Data curation; Formal analysis; Funding acquisition; Investigation; Methodology; Project administration; Resources; Software; Supervision; Validation; Visualization; Roles/Writing - original draft; and Writing - review & editing. Note that not all roles may apply to every manuscript, and authors may have contributed through multiple roles.

Declaration of competing interest

Corresponding authors, on behalf of all the authors of a submission, must disclose any financial and personal relationships with other people or organizations that could inappropriately influence their work. Examples of potential conflicts of interest include employment, consultancies, stock ownership, honoraria, paid expert testimony, patent applications/registrations, and grants or other funding. All authors, including those *without* competing interests to declare, should provide the relevant information to the corresponding author (which, where relevant, may specify they have nothing to declare).

Declaration of generative AI in scientific writing

This guidance only refers to the writing process, and not to the use of AI tools to analyze and draw insights from data as part of the research process. Where authors use generative artificial intelligence (AI) and AI-assisted technologies in the writing process, authors should only use these technologies to improve readability and language. Applying the technology should be done with human oversight and control, and authors should carefully review and edit the result, as AI can generate authoritative-sounding output that can be incorrect, incomplete or biased. AI and AI-assisted technologies should not be listed as an author or co-author, or be cited as an author. Authorship implies responsibilities and tasks that can only be attributed to and performed by humans. Authors should disclose in their manuscript the use of AI and AI-assisted technologies in the writing process by following the instructions below. A statement will appear in the published work. Please note that authors are ultimately responsible and accountable for the contents of the work.

Disclosure instructions

Authors must disclose the use of generative AI and AI-assisted technologies in the writing process by adding a statement at the end of their manuscript in the core manuscript file, before the References list. The statement should be placed in a new section entitled 'Declaration of Generative AI and AI-assisted technologies in the writing process'.

Statement: During the preparation of this work the author(s) used [NAME TOOL / SERVICE] in order to [REASON]. After using this tool/service, the author(s) reviewed and edited the content as needed and take(s) full responsibility for the content of the publication.
This declaration does not apply to the use of basic tools for checking grammar, spelling, references etc. If there is nothing to disclose, there is no need to add a statement.

Acknowledgments

State the institutions and persons who financially or in some other way helped the presented research. If the research was not supported by others, it should also be stated in this part of the manuscript.

Appendices

The manuscript may have appendices. If there is more than one appendix, they are denoted by A, B, etc. Labels of figures, tables and formulas in appendices should contain the label of the appendix, for example Table A.1, Figure A.1, etc.

ABBREVIATIONS

All abbreviations should be defined where they first appear. Consistency of abbreviations used throughout the text should be ensured.

MATH FORMULAE

Formulae should be in the form of editable text (not in the format of figures) and marked with numbers, in the order in which they appear in the text. The formulae and equations should be written carefully taking into account the indices and exponents. Symbols in formulae should be defined in the order they appear, right below the formulae.

FIGURES

- figures should be made so that they are as uniform in size as possible and of appropriate quality for reproduction;
- the dimensions of the figures should correspond to the format of the journal: figures with a width approximately equal to the width of 1 column (± 80 mm width), width of 2 columns (± 170 mm width) or width of 1.5 columns (± 130 mm width);
- figures should be designed so that their size is not disproportionately large in relation to the content;
- the text on the figures should be minimal and the font used should be the same on all figures (Arial, Times New Roman, Symbol);
- figures should be placed next to the appropriate text in the manuscript and marked with numbers in the order in which they appear in the text;
- each figure should have a caption that is placed below the figure - the caption should not be on the figure itself.

In cases of inadequate quality of reproduction, the author should be required to submit figures as separate files. In this case, the figure should be saved in TIFF (or JPG) format with a minimum resolution of 500 dpi.

TABLES

- tables should be in the form of editable text (not in the format of figures);
- tables should be placed next to the appropriate text in the manuscript and marked with numbers in the order in which they appear in the text;
- each table should have a caption that is placed below the table;
- the tables should not show the results that are already presented elsewhere in the manuscript - duplicating the presentation of results should be avoided;
- tables are without vertical lines as boundaries between cells and shading cells.

REFERENCES

Citation in the text

Each reference cited in the text should be in the reference list (and vice versa). It is not recommended to list unpublished results or personal communications in the reference list, but they can be listed in the text. If they are still listed in the reference list, the journal style references are used, with 'Unpublished results' or 'Personal communication' instead of the date of publication. Citing a reference as ‘in press’ means that it is accepted for publication.

Web references

Web references are minimally listed with the full URL and the date when the site was last accessed. These references can be included in the reference list, but can also be given in a separate list after the reference list.

Reference style

In text: References are given in the text by a number in square brackets in the order in which they appear in the text. Authors may also be referred to directly, but the reference number should always be given.

In reference list: References marked with a number in square brackets are sorted by numbers in the list.

Examples

Reference to a journal publication:

[1] V.W.Y. Tam, M. Soomro, A.C.J. Evangelista, A review of recycled aggregate in concrete applications (2000-2017), Constr. Build. Mater. 172 (2018) 272-292. https://doi.org/10.1016/j.conbuildmat.2018.03.240

Reference to a book:

[3] A.H. Nilson, D. Darwin, C.W. Dolan, Design of Concrete Structures, thirteenth ed., Mc Graw Hill, New York, 2004.

Reference to a chapter in an edited book:

[4] J.R. Jimenez, Recycled aggregates (RAs) for roads, in: F Pacheco-Torgal, V.W.Y. Tam, J.A. Labrincha, Y. Ding, J. de Brito (Eds.), Handbook of recycled concrete and demolition waste, Woodhead Publishing Limited, Cambridge, UK, 2013, pp. 351–377.

Reference to a website:

[5] WBCSD, The Cement Sustainability Initiative, World. Bus. Counc. Sustain. Dev. http://www.wbcsdcement.org.pdf/CSIRecyclingConcrete-FullReport.pdf, 2017 (accessed 7 July 2016).

SUPPLEMENTARY MATERIAL

Supplementary material such as databases, detailed calculations and the like can be published separately to reduce the workload. This material is published 'as received' (Excel or PowerPoint files will appear as such online) and submitted together with the manuscript. Each supplementary file should be given a short descriptive title.

ETHICS IN PUBLISHING

Authors are expected to respect intellectual and scientific integrity in presentation of their work. The journal publishes manuscripts that have not been previously published and are not in the process of being considered for publication elsewhere. All co-authors as well as the institution in which the research was performed should agree to the publication in the journal.
Authors are expected to submit completely original research; if the research of other researchers is used, it should be adequately cited. Authors who wish to include in their manuscript images, tables or parts of text that have already been published somewhere, should obtain permission from the Copyright owner and provide a proof in the process of submitting the manuscript. All material for which there is no such evidence will be considered the original work of the author. To determine the originality of the manuscript, it can be checked using the Crossref Similarity Check service. For more information, please see our Ethics and Malpractice Statement.

The Journal and Publishers imply that all authors, as well as responsible persons of the institute where the research was performed, agreed with the content of the submitted manuscript before submitting it. The Publishers will not be held legally responsible should there be any claims for compensation.

PEER REVIEW

This journal uses a single blind review process, which means that the authors do not know the names of the reviewers, but the reviewers know who the authors are. In the review process, the Editor-in-Chief first assesses whether the contents of the manuscript comply with the scope of the journal. If this is the case, the paper is sent to at least two independent experts in the field, with the aim of assessing its scientific quality and making recommendation regarding publication. If the manuscript needs to be revised, the authors are provided with the reviewers' remarks. The authors are obliged to correct the manuscript in accordance with the remarks, submit the revised manuscript and a special file with the answers to the reviewers within the given deadline. The final decision, whether the paper will be published in journal or not, is made by the Editor-in-Chief.

AFTER ACCEPTANCE

Once accepted for publication, the manuscript is set in the journal format. Complex manuscript is sent to the authors in the form of proof, for proof reading. Then, authors should check for typesetting errors, and whether the text, images, and tables are complete and accurate. Authors are asked to do this carefully, as subsequent corrections will not be considered. In addition, significant changes to the text and authorship at this stage are not allowed without the consent of the Editor-in-Chief.

After online publication, changes are only possible in the form of Erratum which will be hyperlinked to manuscript.

COPYRIGHT

Authors retain copyright of the published papers and grant to the publisher the non-exclusive right to publish the article, to be cited as its original publisher in case of reuse, and to distribute it in all forms and media.

The published articles will be distributed under the Creative Commons Attribution ShareAlike 4.0 International license (CC BY-SA). It is allowed to copy and redistribute the material in any medium or format, and remix, transform, and build upon it for any purpose, even commercially, as long as appropriate credit is given to the original author(s), a link to the license is provided, it is indicated if changes were made and the new work is distributed under the same license as the original.

Users are required to provide full bibliographic description of the original publication (authors, article title, journal title, volume, issue, pages), as well as its DOI code. In electronic publishing, users are also required to link the content with both the original article published in *Building Materials and Structures* and the license used.

Authors are able to enter into separate, additional contractual arrangements for the non-exclusive distribution of the journal's published version of the work (e.g., post it to an institutional repository or publish it in a book), with an acknowledgement of its initial publication in this journal.

OPEN ACCESS POLICY

Journal *Building Materials and Structures* is published under an Open Access license. All its content is available free of charge. Users can read, download, copy, distribute, print, search the full text of articles, as well as to establish HTML links to them, without having to seek the consent of the author or publisher.
The right to use content without consent does not release the users from the obligation to give the credit to the journal and its content in a manner described under *Copyright*.

Archiving digital version

In accordance with law, digital copies of all published volumes are archived in the legal deposit library of the National Library of Serbia in the Repository of SCIndeks - The Serbian Citation Index as the primary full text database.

Cost collection to authors

Journal Building Materials and Structures does not charge authors or any third party for publication. Both manuscript submission and processing services, and article publishing services are free of charge. There are no hidden costs whatsoever.

DISCLAIMER

The views expressed in the published works do not express the views of the Editors and the Editorial Staff. The authors take legal and moral responsibility for the ideas expressed in the articles. Publisher shall have no liability in the event of issuance of any claims for damages. The Publisher will not be held legally responsible should there be any claims for compensation.

Financial support

MINISTRY OF EDUCATION, SCIENCE AND TECHNOLOGICAL DEVELOPMENT OF REPUBLIC OF SERBIA

SERBIAN CHAMBER OF ENGINEERS

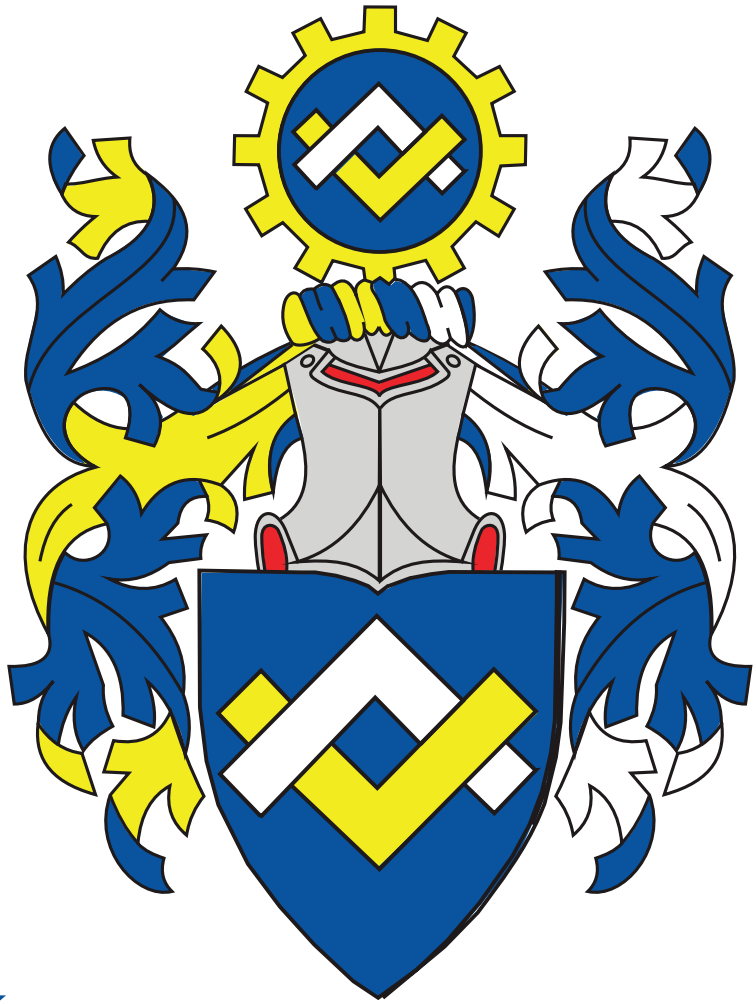

INŽENJERSKA KOMORA SRBIJE

Efikasno postavljanje oplate. Prilagođeno nameni.

DokaFit Handset

Doka Serb d.o.o. | Svetogorska 4 | 22310 Šimanovci | Srbija
T +381 22 400 100 | serb@doka.com | **www.doka.com**

Formwork & Scaffolding.
We make it work.

ADING
sastojak svake građevine

ZAŠTITNI PREMAZI

(MORAVSKI KORIDOR)

Nehruova 82, 11070 Novi Beograd; + 381 11 616 05 76; ading@ading.rs
www.ading.rs

CONSTRUCTION CHEMICALS SINCE 1969

ACO. The future of drainage.

ACO

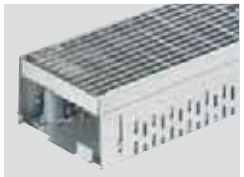

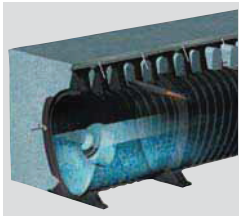

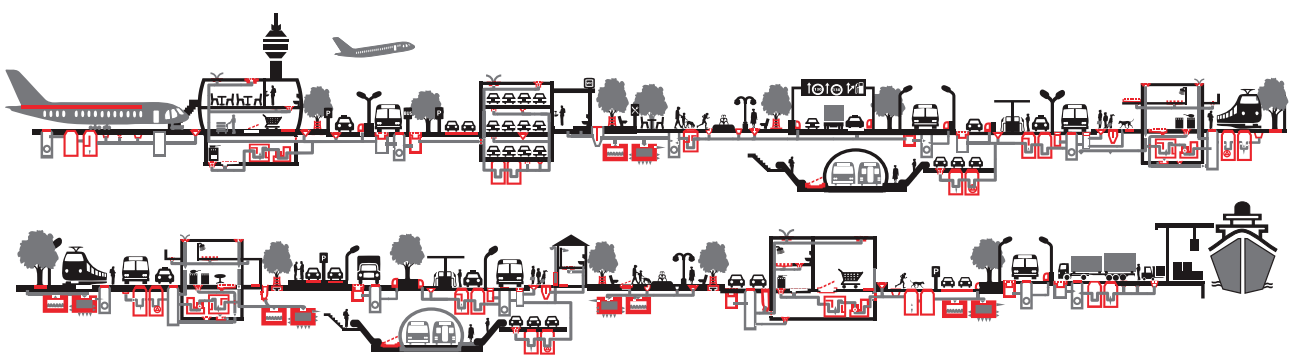

aco.rs

ИМС IMS INSTITUT IMS AD BEOGRAD

CENTAR ZA PUTEVE I GEOTEHNIKU

U okviru centra posluju odeljenja za geotehniku, nadzor i terenska ispitivanja, projektovanje saobraćajnica, laboratorija za puteve i geotehniku. Značajna aktivnost centra usmerena je ka terenskim i laboratorijskim geološko - geotehničkim istraživanjima i ispitivanjima terena za potrebe izrade projekno - tehničke dokumentacije, za različite faze i nivoe projektovanja objekata visokogradnje, niskogradnje, saobraćaja i hidrogradnje, kao i za potrebe prostornog planiranja i zaštite životne sredine. Stručni nadzor, kontrola kvaliteta tokom građenja, rekonstrukcije i sanacije objekata različite namene, izrada studija, ekspertiza, konsultantske usluge, kompletan konsalting u oblasti geotehničkog inženjeringa, neke su od delatnosti centra.

Ispitivanje šipova

- **SLT metoda (Static load test)**
- **DLT metoda (Dynamic load test)**
- **PDA metoda (Pile driving analysis)**
- **PIT (SIT) metoda (Pile (Sonic) integrity testing)**
- **CSL - Crosshole Sonic Logging**

- **Ispitivanje šipova**
  - **Geotehnička istraživanja i ispitivanja – in situ**
    - **Laboratorija za puteve i geotehniku**
      - **Projektovanje puteva i sanacija klizišta**
        - **Nadzor**

INNOVATIVE CONSTRUCTION TECHNOLOGIES

NOVKOL

Samarska 6
(bivši Surčinski put 1k),
11077, Novi Beograd, Srbija

+381117129180
+381117129194
+381117129324
+381112607979
+381112607981

Fax:
+381117129183

office@novkol.co.rs
priprema@novkol.co.rs

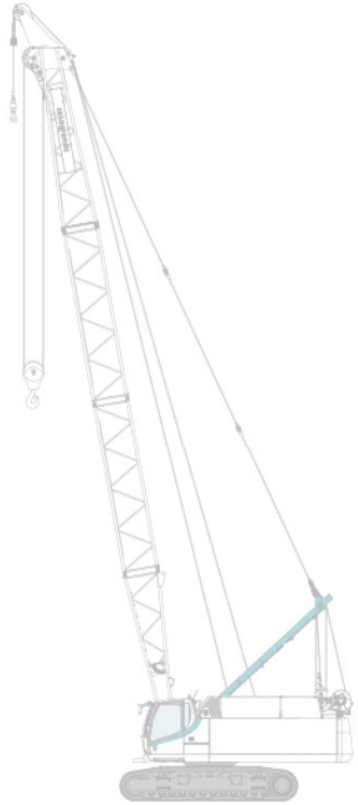

PUT INŽENJERING

Put inženjering d.o.o punih 25 godina radi kao specijalizovano preduzeće za izgradnju infrastrukture u niskogradnji i visokogradnji, kao i proizvodnjom kamenog agregata i betona. Preduzeće se bavi i transportom, uslugama građevinske mehanizacije i specijalne opreme.

Za spravljanje betona koristimo drobljeni krečnjački agregat sa našeg kamenoloma, deklarisanih frakcija, kontrolisane vlažnosti. Kompletan proces proizvodnje i kontrole kvaliteta vršimo prema važećim standardima.

Kao generalni izvođač radova, vršimo koordinaciju svih učesnika na projektu, planiranje, praćenje i nabavku materijala, kontrolu kvaliteta izvedenih radova, poštujući zadate vremenske rokove i finansijski okvir investitora.

Obradu armature vršimo brzo, stručno i kvalitetno, sa kompjuterskom preciznošću i dimenzijama po projektu.

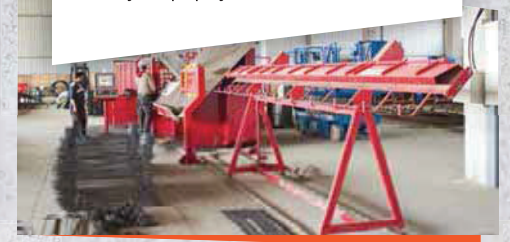

Osnovi princip našeg poslovanja zasniva se na individualnom pristupu svakom klijentu i pronalaženje najoptimalnijeg rešenja za njegove transportne i logističke potrebe.

Koristeći inovativne tehnike i kvalitetan građevinski materijal iz sopstvenih resursa, spremni smo da odgovorimo na mnoge zahteve naših klijenata iz oblasti niskogradnje.

Naša kompanija u oblasti visokogradnje primenjuje sistem prefabrikovnih betonskih elemenata koji u odnosu na klasičnu gradnju ima brojne prednosti.

Usluge građevinskom mehanizacijom vršimo tehnički ispravnim mašinama, sa potrebnim sertifikatima kako za rukovaoce građevinskim mašinama tako i za same mašine.

Osnovna prednost prefabrikovane konstrukcije jeste brzina kojom konstrukcija može biti projektovana, proizvedena, transportovana i namontirana.

Prednapregnute šuplje ploče su konstruktivni elementi visokog kvaliteta, proizvedeni u fabrički kontrolisanim uslovima.

Raspolažemo opremom i mašinama za sve zemljane radove, kipere i dampere za rad u teškim terenskim uslovima, automiksere i pumpe za beton, autodizalice, podizne platforme.

Izvodimo hidrograđevinske radove u izgradnji kanalizacionih mreža za odvođenje atmosferskih, otpadnih i upotrebljenih voda, izvođenjem hidrograđevinskih radova u okviru regulacije rečnih tokova, kao i izvođenjem hidrotehničkih objekata.

Izrađujemo betonske "New Jersey profile" koji se u svetu koriste za preusmeravanje saobraćaja i zaštitu pešaka u toku izgradnje puta, kao i Betonblock sistem betonskih blokova.

Sakupljanje i privremeno skladištenje otpada vršimo našim specijalizovanim vozilima i deponujemo na našu lokaciju sa odgovarajućom dozvolom. Kapacitet mašine je 250 t/h građevinskog neopasnog otpada.

Površinski kop udaljen je 35 km od Niša. Savremene drobilice, postrojenje za separaciju i sejalica efikasno usitnjavaju i razdvajaju kamene agregate po veličinama. Tehnički kapacitet trenutne primarne drobilice je 300 t/h.

Uslugu transporta vršimo automikserima, kapaciteta bubnja od 7 m³ do 10 m³ betonske mase. Za ugradnju betona posedujemo auto-pumpu za beton, radnog učinka 150 m³/h, sa dužinom strele od 36 m.

NIŠ
Knjaževačka bb, 18000 Niš - Srbija
+381 18 215 355
office@putinzenjering.com

BEOGRAD
Jugoslovenska 2a, 11250 Beograd – Železnik
+381 11 25 81 111
beograd@putinzenjering.com

MOBECO

www.putinzenjering.com

GRADIMO SADAŠNJOST ZA ODRŽIVU **BUDUĆNOST**

Strastvenost, timski duh i vizija budućnosti. Mapei aktivno doprinosi najvažnijim svetskim projektima u oblasti arhitekture, infrastrukture i stanovanja, kao i obnovi kulturno-istorijskih građevina. S predanošću radimo svakog dana, kako bismo oblikovali održivu budućnost građevinske industrije.

MAPEI®

Više na: **www.mapei.rs** i **www.mapei.com**

MATEST
YOUR PARTNER IN TESTING

iT TECH

INELAS ERECO d.o.o

MATEST "iT TECH" KONTROLNA JEDINICA

JEDNA TEHNOLOGIJA MNOGO REŠENJA

IT Touch Techlogy je Matestov najnoviji koncept koji ima za cilj da ponudi inovativna i user-friendly tehnologiju za kontrolu i upravljanje najmodernijom opremom u domenu testiranja građevinskih materijala

Ova tehnologija je srž Matestove kontrolne jedinice, software baziran na Windows platformi i touch screen sistem koji je modularan, fleksibilan i obavlja mnoge opcije

iT TECH pokriva

- INOVATIVNOST
- INTERNET KONEKCIJA
- INTERFEJS SA IKONICAMA
- INDUSTRIJALNA TEHNOLOGIJA

SISTEM JEDNOG RAZMIŠLJANJA JEDNOM SHVATIŠ - SVE TESTIRAŠ

NAPREDNA TEHNOLOGIJA ISPITIVANJA ASFALTA

- GYROTRONIC - Gyratory Compactor
- ARC - Electromechanical Asphalt Roller Compactor
- ASC - Asphalt Shear Box Compactor
- SMARTRACKER[tm] - Multiwheels Hamburg Wheel Tracker, DRY + WET test environment
- SOFTMATIC - Automatic Digital Ring & Ball Apparatus
- Ductilometers with data acquisition system

MULTIFUNKCIONALNI RAMOVI ZA TESTIRANJE

- CBR/Marshall digital machines
- Universal multispeed load frames
- UNITRONIC 50kN or 200kN Universal multipurpose compression/flexural and tensile frames

OPREMA ZA GEOMEHANIČKO ISPITIVANJE

- EDOTRONIC - Automatic Consolidation Apparatus
- SHEARLAB - AUTOSHEARLAB - SHEARTRONIC Direct / Residual shear testing systems
- Triaxial Load Frame 50kN

MIXMATIC - Automatic Programmable Mortar Mixer

INELAS ERECO D.O.O
Tošin bunar 274a, 11070 , Novi Beograd tel. +381 11 2284 574 email. info@inelasereco.rs